Pions réels et virtuels dans les noyaux

Noël Giraud

No d'ordre 8406   Année 1984

thèse

présentée

devant l'UNIVERSITE CLAUDE BERNARD   LYON - 1

pour obtenir

le grade de DOCTEUR D'ETAT   ES-SCIENCES

par

Noël   GIRAUD

* * *

PIONS REELS ET VIRTUELS DANS LES NOYAUX

Soutenue le   24   Février   1984

devant la Commission   d' Examen

JURY:

Mme   M. ERICSON   Président

MM   J. DELORME
      C. FAYARD
      G.H. LAMOT   Examinateurs
      P. QUENTIN

Université Claude Bernard Lyon-1

* * * * * * * * * *

Président Honoraire : M. le Professeur J. BOIDIN

Administrateur Provisoire	: M. le Professeur C. DUPUY
Administrateurs Provisoires Adjoints	: M. le Professeur J. CHANEL
	M. le Professeur R. MORNEX
Secrétaire Général de l'Université	: M. F. MARIANI

U.E.R. de Médecine Grange-Blanche	M. le Professeur P. ZECH
U.E.R. de Médecine Alexis-Carrel	M. le Professeur R. MORNEX
U.E.R. de Médecine Lyon-Nord	Mme le Professeur PINET
U.E.R. de Médecine Lyon-Sud	M. le Professeur J. NORMAND
U.E.R. Faculté de Pharmacie	M. le Professeur C.A. BIZOLLON
U.E.R. des Techniques de Réadaptation	M. le Professeur BRION
U.E.R. de Biologie Humaine	M. J.P. REVILLARD, M.C.A.
U.E.R. d'E.P.S.	M. A. MILLON, Professeur d'E.P.S.
U.E.R. Faculté d'Odontologie	M. le Professeur J. LABE
U.E.R. de Mathématiques	M. R. REDON, M.A.
U.E.R. de Physique	M. le Professeur R. UZAN
U.E.R. de Chimie et Biochimie	Mme A. VARAGNAT, M.A.
U.E.R. des Sciences de la Nature	M. le Professeur ELMI
U.E.R. des Sciences Physiologiques	Mme le Professeur J.F. WORBE
U.E.R. de Physique Nucléaire	M. le Professeur E. ELBAZ
I.U.T. - I	M. le Professeur J. GIELLY
I.U.T. - II	M. le Professeur P. MICHEL
Observatoire de Lyon	M. le Professeur MONNET
U.E.R. de Mécanique	M. le Professeur BATAILLE

Université Claude Bernard Lyon-1

43, Bd du 11 Novembre 1918
69622 VILLEURBANNE Cedex

* * * * *
* * *
*

PROFESSEURS de l'U.E.R. de PHYSIQUE NUCLEAIRE

* * * * * * * * * * * * *

M.   BERKES Istvan

M.   BURQ Jean-Pierre

M.   CHERY Roland

M.   DEMEYER Albert

M.   ELBAZ Edgard

Mme   ERICSON Magda

M.   GAILLARD Michel-Jean

M.   GIFFON Maurice

M.   GUSAKOW Mark

M.   LAMBERT Michel

M.   MAREST Gilbert

M.   PHILBERT Georges

M.   REMILLIEUX Joseph

M.   RUHLA Charles

RESUME

        La première partie de la thèse porte sur l'interaction des pions physiques avec le deuton étudié dans le cadre d'une théorie à trois corps. Nous avons déduit la section efficace élastique dans le domaine d'énergie au voisinage de la résonance (3-3), en tenant compte de l'absorption virtuelle du pion.

        La deuxième partie concerne les pions virtuels dans les noyaux. En particulier nous avons étudié le nuage de pions virtuels autour du noyau et déduit la constante de couplage effective pion noyau. Celle-ci est fortement réduite par les effets de polarisation du milieu nucléaire (essentiellement par excitation virtuelle de l'isobare Δ) par rapport à sa valeur pour une collection de nucléons libres. Nous avons également étudié dans le cadre du même modèle de polarisation le champ pionique à l'intérieur du noyau. A petit transfert de moment ce champ est diminué. A grand moment il est augmenté. Ce dernier phénomène correspond aux effets d'opalescence critique liés à la transition de phase de la condensation du pion. Nous avons effectué une étude détaillée de ce phénomène pour les facteurs de forme magnétiques dans les isotopes du carbone.

REMERCIEMENTS

INTRODUCTION

Une avancée des plus remarquables de la physique nucléaire pendant la décennie écoulée a été permise par le développement extraordinaire du domaine dit des énergies intermédiaires. Ce succès est attribuable à la fois à l'effort expérimental dans la construction de machines et de systèmes de détection de plus en plus performants et à l'application intensive de méthodes et concepts empruntés à la physique des particules par des théoriciens soucieux de maintenir un pont entre les deux disciplines. Un domaine qui a été et est toujours particulièrement fructueux est la physique du méson π qui apparaît sous un aspect dual. Soit le pion est étudié en tant que particule réelle, sonde du noyau au travers de diverses réactions, soit on s'intéresse à son rôle de particule virtuelle, vecteur privilégié de l'interaction entre nucléons.

Ce sont ces deux faces de la physique du méson π dans le noyau que notre travail abordera successivement. La première partie est consacrée à une étude du problème à trois corps posé par l'interaction πNN, cependant que la deuxième partie considère les renormalisations apportées à diverses observables de spin par le nuage pionique virtuel présent dans le noyau.

lère PARTIE

ETUDE DE LA DIFFUSION PION-DEUTON.

I - FORMALISME A TROIS CORPS POUR LE SYSTEME $\pi - N - N$:

1) Introduction :

Pour la physique des énergies intermédiaires, le pion constitue un sujet de choix. On dispose en effet avec cette particule d'une sonde :
- Qui interagit peu à basse énergie, ce qui facilite d'autant les calculs.
- Qui se couple ensuite fortement au nucléon pour former la plus célèbre des résonnances hadroniques la "delta-trois-trois", dont le caractère dominant permet une modélisation simple de l'interaction.
- Qui en tant que boson, peut être absorbé par un nucléon, plaçant ainsi le noyau cible, mis hors couche de quelques 140 MeV, dans une situation tout à fait exotique.
- Qui par sa faible masse, est justifiable d'un traitement en "pion mou" permettant à l'aide de méthodes inspirées de l'électromagnétisme, de modéliser son interaction à basse énergie d'une manière satisfaisante.
- Qui est disponible en abondance auprès des "usines à pions", avec une moisson de résultats expérimentaux.

Toutes ces raisons ont motivé un intérêt exceptionnel pour l'étude des systèmes pion-noyau, malgré la difficulté du sujet. On se trouve en effet placé devant un problème à N+1 corps, parmi lesquels les N premiers posent déjà de sérieuses difficultés.

Parmi ces systèmes pion-noyau, le système pion-deuton tient une place très particulière. Tout d'abord le petit nombre de nucléons mis en jeu permet de se "débarasser" des difficultés liées à la structure d'un noyau plus complexe. Ensuite, avec une cible peu liée et une sonde ayant une faible interaction avec ses constituants, on peut espérer que les effets d'ordre élevé seront modérés. Enfin, partant d'une approximation d'ordre zéro ("l'impulse approximation" que l'on pourrait traduire par l'approximation d'additivité) petite (nulle à la limite des pions mous à cause du caractère isoscalaire du deuton), on est dans de bonnes conditions pour observer les corrections à y apporter. A cela, on peut ajouter que l'absorption étant un phénomène essentiellement à deux nucléons, la compréhension de la réaction $\pi-d \rightarrow NN$ est une première étape nécessaire.

Les physiciens disposent ainsi d'un "laboratoire théorique" où tester leur compréhension de l'interaction pion-noyau.

En effet, un système de trois particules comme π-n-p obéit classiquement à un système d'équations intégrales couplées, dites "de Faddeev" [1] que l'on sait en principe résoudre, pourvu que l'interaction deux à deux des particules soit connue. A ce niveau, pour que l'étude puisse avoir le caractère extensif voulu, il est nécessaire que ces interactions puissent être approximées de manière raisonnable par des interactions non locales séparables, ou si l'on préfère, que chaque voie soit dominée par la formation d'un ou plusieurs isobares. De ce point de vue, le

caractère dominant de la Δ_{33} dans la voie π-N permet de travailler dans des condi-
tions quasi idéales, puisque l'approximation faite sur les autres voies ne sera fai-
te que sur des termes en général correctifs. Il reste toutefois un problème : un
pion a une masse de quelques 140 MeV/C^2 et vers la résonance une énergie cinétique
d'environ 180 MeV. Or, les équations de Faddeev supposent le système invariant sous
les transformations du groupe de Galilée, ce qui n'est certainement pas le cas ici.
En d'autres termes, il est nécessaire de disposer d'un équivalent relativiste des
équations "à trois corps". Mais, le nombre de particules d'un système relativiste
étant essentiellement variable, il y a là une contradiction qui va amener nécessai-
rement à des approximations. Le guide en ce domaine réside dans la relation d'uni-
tarité auquel doit obéir la matrice S représentant l'évolution du système :

$$(S^{+} \cdot S)_{fi} = \sum_{n} \left(\int d\Omega_{n} \cdot S_{fn}^{+} \cdot S_{ni} = \delta_{fi} \right.$$

où
- i et f sont les états initial et final
- n les états intermédiaires à n particules sur lesquels on somme.
On choisit donc de tronquer cette sommation aux états de trois particules au plus.
Le prix de cette approximation est la perte de la symétrie de croisement qui, fai-
sant intervenir des états d'anti-particules, est exclue du modèle choisi.

2) Equations à 3 corps :

Même dans ces conditions, la construction d'équations à trois corps
"relativistes" s'avère une tâche redoutable : de l'aveu de Freedman, Lovelace et
Namyslowski[2], auteurs de l'article de base en ce domaine 60 pages de Nuovo Cimento
"en omettant toutes les étapes nécessitant moins d'une semaine de travail"... Le
point de départ réside dans l'équation de Bethe-Salpeter[3], décrivant un système
de deux particules à l'aide d'une équation intégrale quadri-dimensionnelle. La pre-
mière étape consiste à éliminer l'intégration sur l'énergie relative des particules
de manière à se ramener à des intégrales spatiales. Cette étape a pu être franchie
grâce à la méthode de Blankenbecler et Sugar[4]. Le principe consiste à trouver un
propagateur qui possède la même singularité que la fonction de Green des deux par-
ticules à l'aide d'une relation de dispersion dans le plan s, la discontinuité du
propagateur étant exprimée à l'aide de la relation d'unitarité tronquée à deux par-
ticules. Ce travail a été repris sous une forme "intuitive" par Aaron, Amado et
Young[5] en supposant au départ, par analogie avec les équations non relativistes,
que les amplitudes de diffusion X(p,p';s) obéissent a une équation intégrale de la
forme :

$$X(p,p';s) = V(p,p') + \frac{1}{(2\pi)^4} \int d^4k \cdot V(p,k) \cdot G(k;s) \cdot X(k,p';s)$$

où
. V(p,p') est le potentiel
. G(k;s) est la fonction de Green des deux particules
On obtient alors la discontinuité de G(k;s) sur la coupure d'unitarité dans le
plan s :

$$G(k;s^{+}) - G(k;s^{-}) = i \cdot (2\pi)^2 \cdot \delta^{+}(k_1^2 - m_1^2) \cdot \delta^{+}(k_2^2 - m_2^2)$$

On construit alors par une relation de dispersion une fonction présentant la même singularité, et celle-là seulement :

$$G(k;s) = \frac{\pi}{\varepsilon_1 \varepsilon_2} \cdot \delta\left(k^0 - \frac{1}{2}\varepsilon_1 - \frac{1}{2}\varepsilon_2\right) \cdot \frac{\varepsilon_1 + \varepsilon_2}{(\varepsilon_1 + \varepsilon_2)^2 - s}$$

où ε_i est l'énergie de la particule i, m_i sa masse et k_i son impulsion. Il ne reste plus qu'à reporter dans l'équation pour éliminer l'intégration sur l'énergie relative des particules k^0 :

$$X(p,p';s) = V(p,p') + \frac{1}{(2\pi)^3} \cdot \int \frac{d^3k}{2\varepsilon_1\varepsilon_2} \cdot V(p,k) \cdot \frac{\varepsilon_1 + \varepsilon_2}{(\varepsilon_1 + \varepsilon_2)^2 - s} \cdot X(k,p';s)$$

On obtient ainsi une équation très similaire à l'équation de Lippman-Schwinger. Freedman et al. ont eu le mérite d'étudier la séparabilité de l'équation de Bethe-Salpeter en présence d'états liés ou de résonance entre les deux particules. Ce travail fondamental a permis d'utiliser la méthode des potentiels non locaux séparables de la même manière que dans le cas non relativiste : on introduit un potentiel de la forme :

$$V(p,p') = g(p^2)\lambda \, g(p'^2)$$

où $g(p^2)$ représente une fonction de vertex gouvernant la dissociation de l'isobare en la paire et $\lambda = \pm 1$.

Alors l'équation se résoud analytiquement pour donner :

$$X(p,p';s) = g(p^2) \, D^{-1}(s) \, g(p'^2)$$

avec
$$D(s) = \frac{1}{\lambda} - \frac{1}{(2\pi)^3} \cdot \int \frac{d^3k}{2\varepsilon_1\varepsilon_2} \cdot g^2(k^2) \cdot \frac{\varepsilon_1 + \varepsilon_2}{(\varepsilon_1 + \varepsilon_2)^2 - s}$$

où $D^{-1}(s)$ est le propagageur "habillé" de l'isobare.

Pour bien comprendre l'utilité de cette approximation dans les équations à trois corps, il est utile de s'appuyer sur la forme qu'en ont donné Alt, Grassberger et Sandhas[6] dans le cas non relativiste :

$$U_{ij} = -(1-\delta_{ij}) \cdot G_0^{-1} + \sum_{k \neq i} t_k \cdot G_0 \cdot U_{kj}$$

avec
i,j,k = n° des 3 particules

U_{ij} = opérateur de transition à 2 corps faisant passer de i(jk) à j(ik)

t_k = amplitude de diffusion à deux corps

G_0 = fonction de Green libre

Il est commode de représenter ces équations par un graphique :

où un rectangle représente un opérateur de transition U et un cercle une amplitude de diffusion t.

L'intégration sur les lignes "internes" fait apparaître une intégration sur trois moments qui se réduisent à deux avec la conservation de l'impulsion.
Le fait que l'amplitude de diffusion à deux corps soit séparable se traduit par :

$$t_{k} = \overbrace{}^{i}_{i} = \quad = \quad q_{k}(\rho^{2}) \cdot D_{r}^{-1}(s) \cdot q_{k}(\rho'^{2})$$

où les ½ cercles représentent les fonctions de vertex et $D_{r}^{-1}(s)$ le propagateur de l'isobare .
En remplaçant dans l'équation et en multipliant à gauche par $< in| \; G_{0}$ et à droite par $G_{0} |jm >$ pour faire apparaître l'amplitude de diffusion

$$X_{in,jm} = < in \mid G_{0} \quad U_{ij} G_{0} | jm >$$

de la particule i sur la paire m menant à la particule j en présence de la paire n on obtient :

$$X_{in,jm} = Z_{in,jm} + \sum_{k \neq i} Z_{in,kr} \cdot D_{r}^{-1}(s) \cdot X_{kr,jm}$$

Et l'intégration intermédiaire ne se fait plus que sur un seul moment, ce qui, après utilisation de l'invariance par rotation, conduira à un système d'équations intégrales unidimensionnelles [7]. En contrepartie, il faut noter que le nombre d'équations augmente du nombre d'isobares introduits.
La dominance d'isobares et d'états liés ayant, comme l'ont montré Freedman et al., les mêmes conséquences pour l'équation de Bethe-Sapeter que dans le cas non relativiste, il est légitime de penser qu'un système d'équations intégrales quadri-dimensionnelles similaires au cas non relativiste reste valable ici.

$$X(q,q';s) = B(q,q';s) + \frac{1}{(2_{\pi})^{4}} \int d^{4}k \; B(q,k;s) \; R(\sigma_{k}) \; X(k,q';s)$$

$$P = 4\text{-moment total}$$
$$\sigma_k = (P-k)^2$$

où on a supposé les particules identiques et interagissant par formation d'un seul
état lié pour alléger les notations. On se trouve alors devant le même problème que
pour l'équation à deux corps : l'élimination de l'intégration sur l'énergie relative.
Bien que les calculs soient nettement plus complexes ici, la méthode de Blanckenbecler
et Sugar permet encore de construire des fonctions Z et D^{-1} présentant les mêmes
singularités que celles imposées à B et R par l'unitarité à deux et trois corps. Il
est cependant à noter qu'Aaron, Amado et Young doivent, dans leur méthode, supposer
à priori une relation reliant le propagateur de l'isobare en présence de la 3ème
particule R, au propagateur de l'isobare : D^{-1}

$$R = 2 \pi \delta^+ (k^2 - m^2) \, D^{-1}$$

Finalement, on obtient des équations intégrales tridimentionnelles :

$$X(q,q';s) = Z(q,q';s) + \frac{1}{(2\pi)^3} \int \frac{d^3k}{2\varepsilon_k} \cdot Z(q,k;s) \cdot D^{-1}(\sigma_k) \cdot X(k,q';s)$$

avec

$$Z(q,q';s) = g\left(\frac{1}{4}(P-q-2q')^2\right) \cdot \frac{\varepsilon_q + \varepsilon_{q'} + \varepsilon_{q+q'}}{s - (\varepsilon_q + \varepsilon_{q'} + \varepsilon_{q+q'})^2} \cdot g\left(\frac{1}{4}(P-2q-q')^2\right)$$

$$\varepsilon_k = \sqrt{k^2 + m^2}$$

$$s = \text{invariant de P}$$

Après avoir exprimé les moments relatifs (arguments des fonctions de vertex g)de
manière à ce qu'ils soient du genre espace dans le référentiel du centre de masse
à deux corps par l'utilisation de moments de Wightman-Garding, on peut utiliser
l'invariance par rotation. On obtient donc, après développement en ondes partielles,
une série convergente de systèmes d'équations intégrales couplées solubles par les
méthodes habituelles.

3) Le système π-d :

Avant de décrire la forme particulière des équations dans le cas du
système π-d, il convient d'étudier tout d'abord le type d'interaction des particu-
les en présence.

En ce qui concerne nucléon-nucléon, des études préliminaires[8] ont
montré que seule la description de la voie du deuton, $^3S_1$-$^3D_1$ présentait de l'impor-
tance. Si l'on veut obtenir une description détaillée, la simple approximation de
la dominance de l'état lié ne saurait suffire ici dès que l'on s'éloigne du seuil.
On peut alors envisager l'utilisation de potentiels non locaux séparables plus com-
pliqués, visant à une description plus précise des caractéristiques sur couche de
la voie. La solution retenue ici consiste en l'utilisation de développements en
fractions continues dans les facteurs de forme dont les bonnes caractéristiques vis

à vis de l'extrapolation doivent conduire à un comportement hors couche raisonnable.
On peut ainsi construire une série d'interactions visant à une reproduction de
plus en plus affinée des caractéristiques de la voie, isolant ainsi les effets sur
la diffusion π-d.

Dans l'interaction pion-nucléon, la situation se présente d'une maniè-
re plus simple. L'importance de la résonance delta rend très plausible l'utilisa-
tion d'interactions séparables, les autres voies jouant alors un rôle correctif,
une description simplifiée doit suffire. La principale difficulté réside en fait
dans le choix des caractéristiques que l'on cherche à reproduire puisqu'à basse
énergie, la connaissance expérimentale de l'interaction pion-nucléon ayant sensible-
ment évolué, les résultats trois-corps des calculs suivent les mêmes variations.
Quant au choix des voies introduites dans le calcul, on se limitera toujours aux
ondes S et P, ce qui semble justifié au moins jusque vers 250 MeV. Il reste enfin
à signaler que la voie P_{11}, en tant que voie d'absorption, subit un traitement
particulier sur lequel nous reviendrons plus loin.

Dans ces conditions, le système d'équations peut s'écrire :

$$X_{dd} = \sum_{\Delta'} Z_{d\Delta'} D_{\Delta'}^{-1} X_{\Delta'd}$$

$$X_{\Delta d} = Z_{\Delta d} + Z_{\Delta d} D_d^{-1} X_{dd} + \sum_{\Delta'} Z_{\Delta\Delta'} D_{\Delta'}^{-1} X_{\Delta'd}$$

où $\begin{cases} d \text{ désigne la voie du deuton} \\ \Delta' \text{ désigne une des voies pion-nucléon (par exemple } P_{33}) \end{cases}$

Un dessin étant sans doute plus "parlant", cela donne :
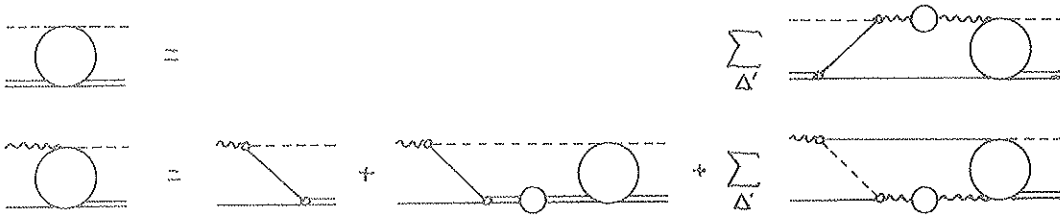
avec ------- = pion ———— = nucléon ===== = deuton ⟿⟿⟿ = isobare π-N

Notons que si l'on reporte la deuxième équation dans la première, on obtient :
- le premier graphe qui représente la simple diffusion du pion sur un des nucléons
du deuton.
- le deuxième qui initie la série de rediffusion des nucléons
- le troisième qui initie la série de rediffusion du pion.

On voit de la sorte en quel sens les équations "trois-corps" repré-
sentent une sommation des termes de la série de diffusion multiple à tous les
ordres. Il faut cependant se garder d'une identification terme à terme assimilant
le premier graphe à l'"impulse approximation". En effet, le comportement hors

couche des propagateurs imposé par l'unitarité rend vaine ce genre de comparaison
et le résultat final peut seul être confronté à l'"impulse approximation" en vue
d'une estimation des effets de diffusion multiple.

Pour terminer, il convient de remarquer que si aux énergies considérées
le pion est nettement relativiste, ce n'est pas le cas des nucléons. On peut donc
concevoir un moyen terme qui consiste à modifier les équations 3-corps non relati-
vistes en adoptant simplement une cinématique relativiste pour le pion. C'est ce qui
a été utilisé par Thomas[9] en premier lieu sous le non d'approximation R.P.K (Re-
lativistic Pion Kinematics) et sera utilisé ici dans les premiers calculs.

4) La prise en compte de l'absorption et le système π-N-N :

Afnan et Thomas[10] ont les premiers essayé d'introduire l'effet de
l'absorption vraie du pion en imposant un pole à $-m_\pi$ dans la voie P_{11} qui possède
les nombres quantiques du nucléon. Ce faisant, on impose que l'interaction dans
cette voie soit dominée par la formation d'un isobare N' ayant toutes les caracté-
ristiques du nucléon, y compris la masse. Le terme de Born correspondant :

$$Z_{dN'} = \begin{array}{c} \pi \text{----}\!\circ\ N' \\ \diagup \\ d \text{====}\!\circ\ N \end{array}$$

représente bien l'absorption du pion et on dispose ainsi d'une manière simple
d'étendre le modèle au processus $\pi d \to NN$.

Malheureusement, cette approche se heurte à deux difficultés liées
au fait que les deux nucléons N et N' ne sont pas identiques, l'un étant un "vrai"
nucléon, l'autre un isobare. Tout d'abord, n'étant pas identiques, ils n'obéissent
pas au principe de Pauli, ce qui leur permet d'être dans un état relatif avec $l+S$
pair alors que l'isospin total du système est égal à 1. On se trouve ainsi avec
des nucléons ayant $(-)^{l+S+T} = -1$. Ce défaut, d'abord noté par Thomas[11] sous le
nom de "blocage de Pauli" est facilement corrigé en interdisant la voie P_{11} quand
$l+S$ est pair. Il est à noter que cette mesure n'est valable que si le pole du nu-
cléon domine toute la voie P_{11} et est excessive dans le cas où cette voie reçoit
une autre contribution dont l'isobare est différent du nucléon.
La deuxième difficulté vient du fait que l'isobare N' est "privilégié" par rapport
au "vrai" nucléon dans la mesure où il est le seul a pouvoir réemettre un pion
dans un modèle trois corps. En d'autres termes, parmi les deux graphes :

On néglige le deuxième, ce qui conduit à un "sous-comptage". Une solution simple consiste alors a ajouter le second graphe partout où il est nécessaire dans les équations. Pratiquement, cela revient à doubler le terme de Born $Z_{N'N}$.

De cette manière, il reste encore une dissymétrie au niveau des propagateurs. Une solution radicale, consiste a prendre le propagateur de 2 nucléons libres, en supposant encore que le pôle du nucléon représente la seule contribution à la voie. Un des calculs présentés ici (article I.1) a été fait en utilisant simplement ces remèdes empiriques aux équations trois corps : blocage de Pauli sur les états (N,N'), terme de Born $Z_{N'N'}$ modifié et propagateurs de nucléons libres.

La solution rigoureuse de ces problèmes a demandé un travail théorique considérable de plusieurs équipes : Mizutani et Koltun[12], Rinat[13], Mizutani et Avishaï [14], Afnan et Blankleider[15] en particulier, ce qui a abouti à une bien meilleure compréhension du système π-N-N. Un point important réside ici dans la compréhension de la structure complexe de la voie P_{11}[16]. Dans un modèle lagrangien simple[17], on constate en effet que le pôle de nucléon dans la voie s subit une forte compensation de la part des pôles du ρ et du σ dans la voie t. Pour la longueur de diffusion par exemple, on aurait :

$$a_{pôle} \simeq -0.18 \; m_\pi^{-1} \qquad a_\rho \simeq 0.04 \; m_\pi^{-1} \qquad a_\sigma \simeq 0.04 \; m_\pi^{-1} \qquad a_{total} \simeq -.10 \; m_\pi^{-1}$$

Ceci amène naturellement à séparer dans la voie P_{11} une contribution venant du pôle de nucléon, et une contribution "non-pôle", avec, pour l'amplitude de diffusion :

$$t_{P_{11}} = t_{pôle} + t_{non \; pôle}$$

Avec

$$t_{pôle} = g(p^2) \; D^{-1}(s) \; g(p'^2) \quad =$$

$$t_{non \; pôle} \qquad =$$

$g(p^2)$ = vertex πNN

$D^{-1}(s)$ = propagateur du nucléon.

En explicitant cette séparation, les équations A.G.S. habituelles sont représentées par

où l'amplitude π-N :   comprend les voies autres que P_{11} et la partie non pôle de la P_{11} . Sous cette forme, on peut imposer le blocage de Pauli au propagateur N-N puisque dans la partie pôle, on a effectivement deux "vrais" nucléons. De la même manière, on peut ajouter le terme :

qui rétablit la symétrie des deux nucléons. Il reste alors a dériver les équations auxquelles obéissent les propagateurs $D^{-1}(s)$ et vertex $g(p^2)$. Une fois de plus, on utilise la réduction de Blankenbecler et Sugar de manière à éliminer les intégrations sur les énergies relatives tout en assurant le respect de l'unitarité. Partant de vertex nus $g_0(p^2)$ et du propagateur libre $D_0^{-1}(s)$, on trouve pour le vertex renormalisé

$$g(p^2) = g_0(p^2) + t_{non\ pôle}\ G_0(s)\ g_0(p^2)$$

et pour le propagateur renormalisé, l'équation :

$$D^{-1}(s) = D_0^{-1}(s) + D_0^{-1}(s)\ g_0(p^2)\ G_0(s)\ g(p^2)\ D^{-1}(s)$$

où $G_0(s)$ est le propagateur pion-nucléon libre. Ces équations correspondent aux graphes :

pour $g(p^2)$

pour $D^{-1}(s)$
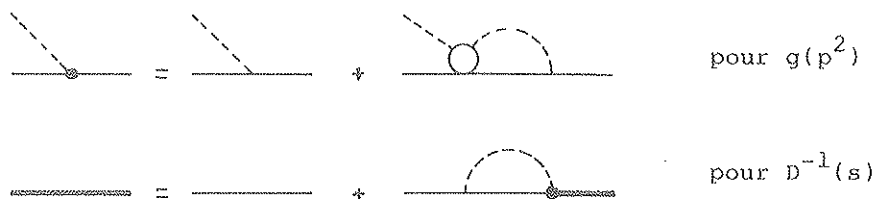
De la dernière équation, on tire l'équation à laquelle obéit le propagateur renormalisé pour deux nucléons $R(s)$:

$$R(s) = R_0(s) + 2\ R_0(s)\ g_0(p^2)\ \overline{G}_0(s)g(p^2)\ R(s)$$
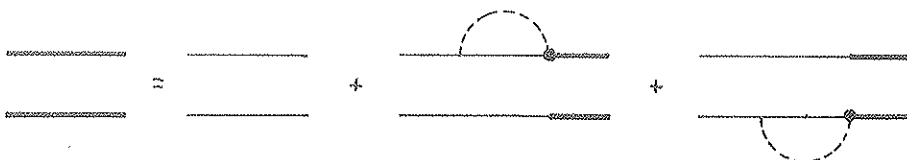
où $\overline{G}_0(s)$ est le propagateur π-N-N libre.

Finalement, en supposant que $t_{non\ pôle}$ est séparable et en multipliant comme précédemment par les propagateurs et les vertex appropriés, on aboutit au système d'équations fournissant les amplitudes de diffusion. Après antisymétrisation des deux nucléons on obtient :

$$\tilde{X}_{\alpha\beta} = \tilde{Z}_{\alpha\beta} + \sum_{\gamma} \tilde{Z}_{\alpha\gamma} \cdot \tau_{\gamma} \cdot \tilde{X}_{\gamma\beta}$$

Avec $\alpha = d$, Δ' ou N

$$\tau_d = D_d^{-1} \quad ; \quad \tau_{\Delta'} = D_{\Delta'}^{-1} \quad ; \quad \tau_N = \frac{R(s)}{2}$$

et les termes de Born antisymétrisés $\tilde{Z}_{\alpha\rho}$ sont reliés aux $Z_{\alpha\beta}$ par :

$$\tilde{Z}_{\alpha\beta} = C_{\alpha\beta} \cdot Z_{\alpha\beta}$$

$$C = \begin{array}{c} d \\ \Delta' \\ N \end{array} \begin{pmatrix} d & \Delta' & N \\ 0 & \sqrt{2} & 2\sqrt{2} \\ \sqrt{2} & 1 & 2 \\ 2\sqrt{2} & 2 & 4 \end{pmatrix}$$

Ces coefficients peuvent d'ailleurs être obtenus facilement par un développement perturbatif en "comptant" les graphes. Par exemple, les contributions de d et N au premier ordre donnent

$$\text{(graphes)} = 4\, Z_{dN}\, R_N\, Z_{Nd}$$
$$= \left(2\sqrt{2}\, Z_{dN}\right)\left(\frac{R_N}{2}\right)\left(2\sqrt{2}\, Z_{Nd}\right)$$

A l'ordre suivant, on a 8 graphes :

$$8 Z_{dN} \cdot R_N \cdot Z_{NN} \cdot R_N Z_{Nd} = \left(2\sqrt{2} \cdot Z_{dN}\right)\left(\frac{R_N}{2}\right)\left(4 Z_{NN}\right)\left(\frac{R_N}{2}\right)\left(2\sqrt{2} \cdot Z_{Nd}\right) \quad \text{etc} \ldots$$

Le principal intérêt de ce système d'équations réside dans le couplage obtenu entre les processus $\pi d \to \pi d$; $\pi d \to NN$ et $NN \to NN$. Alors que les travaux de Rinat par exemple se heurtaient à l'introduction de la force nucléon-nucléon dans les équations, le problème est résolu ici radicalement en générant cette force par l'échange de pions. Le pion ne constituant qu'une partie de cette force, l'étape suivante est naturellement d'introduire les échanges de mésons plus lourds. On peut en effet ajouter au terme de Born Z_{NN} , qui représente l'échange d'un pion, les processus d'échange des divers mésons introduits dans les potentiels OBEP. On arrive ainsi à un modèle qui, avec comme données les couplages des divers mésons au nucléon et l'interaction N-N dans la voie $^3S_1 - ^3D_1$ du deuton, peut décrire d'une manière cohérente l'ensemble des trois processus $\pi - d \to \pi - d$; $\pi - d \to NN$; $NN \to NN$

dans le domaine des énergies intermédiaires[18].

II - RESULTATS : DIFFUSION ELASTIQUE PION-DEUTON :

Les résultats expérimentaux obtenus en diffusion pion-deuton se classent na-
turellement en trois catégories :

- les données au seuil obtenues avec les atomes mésiques

- les expériences a basse énergie jusqu'à une centaine de MeV. Ces expé-
riences sont rendues très délicates par la faible durée de vie du pion. Même avec
une ligne de faisceau très courte, il est difficilement envisageable de descendre
en dessous de 25 MeV. Les données sont donc assez rares, et leur interprétation com-
pliquée par l'influence de la force coulombienne difficile à prendre en compte dans
les calculs basés sur les équations à trois corps. Nous n'aborderons donc pas ce
domaine ici.

- les expériences de 100 à 300 MeV qui encadrent la région de la résonance
. C'est dans cette zone d'énergie que les "usines à pions" (SIN, LAMPF, TRIUMF)
produisent leur meilleure intensité. On dispose donc de nombreux résultats, tant
pour les distributions angulaires que pour les observables de polarisations.

1) Longueur de diffusion π-d :

La partie réelle de cette quantité est reliée au décalage du niveau d'éner-
gie des atomes mésiques par la relation de Treiman :

$$R_e(a_{\pi d}) = \frac{r_0}{4} \left(\frac{\Delta E_{1s}}{E_{1s}}\right) \quad \text{avec} \quad r_0 = \text{rayon de l'orbite de Bohr } (\approx 194 \text{ fm}$$

pour le deuton)

$$\frac{\Delta E_{1s}}{E_{1s}} = \text{décalage relatif du niveau 1s.}$$

La partie imaginaire (non nulle à cause de l'absorption π d → NN) est obtenue à par-
tir de la section efficace de la réaction inverse au seuil, par la balance détaillée

$$\sigma_{NN \to \pi d} = \alpha k + \beta k^3 + \ldots \text{ avec } k = \text{impulsion du pion}$$

$$\alpha = \frac{6\pi}{m_N} \text{ Im } (a_{\pi d}) = \text{"coefficient de production s"}$$

Ces quantités sont connues avec une précision très limitée et on retient actuelle-
ment :

$$R_e(a_{\pi d}) \approx -0.052(^{+.022}_{-.017}) \, m_\pi^{-1} \quad [19]$$

$$\alpha \approx 200 \text{ à } 300 \, \mu b \quad [20]$$

Du point de vue théorique, le point de départ pour le calcul de cette quantité est
"l'approximation d'impulsion" qui exprime la longueur de diffusion π-d en fonction
de la combinaison isoscalaire $(a_1 + 2a_3)$ des longueurs de diffusion π-N :

$$a_{\pi d}^{(o)} = \frac{4}{3} \cdot \frac{m_N + m_\pi}{2 \cdot m_N + m_\pi} \cdot (a_1 + 2a_3)$$

Une première difficulté apparait dans le fait que les estimations expérimentales de $a_1 + 2a_3$ sont très dispersées. Ainsi, les calculs présentés ici ont utilisé :

1. $a_1 + 2a_3 = -0.12 \ m_\pi^{-1}$ → $a_{\pi d}^{(o)} = -.008 \ m_\pi^{-1}$ basé sur les analyses de Salomon[21] et Bugg[22].

2. $a_1 + 2a_3 = -.025 \ m_\pi^{-1}$ $a_{\pi d}^{(o)} = -.018 \ m_\pi^{-1}$ basé sur les analyses de Salomon[21] et Saclay[23].

3. $a_1 + 2a_3 = -.029 \ m_\pi^{-1}$ $a_{\pi d}^{(o)} = -.021 \ m_\pi^{-1}$ basé sur l'analyse de Koch-Pietarinen[24].

parmi lesquelles la troisième valeur semble être la mieux établie actuellement. Les deux calculs présentés ici diffèrent sur trois points : 1) le premier fait appel au formalisme R.P.K. alors que le second (article I.2) utilise des équations relativistes. 2) L'absorption est traitée dans le premier d'une manière simplifiée tel que décrit page 8 avec une P_{11} comportant simplement une partie "pôle". 3) Les potentiels utilisés sont différents, avec en particulier $a_1 + 2a_3 = -025 m_\pi^{-1}$ pour le premier, et $-.012 \ m_\pi^{-1}$ pour le second.

La correction apportée par le calcul complet donne : $a_{\pi d}^{(R+A)} = -.024 \ m_\pi^{-1}$ dans le premier cas et $-.023 \ m_\pi^{-1}$ dans le second. Cette correction se répartit en une correction de rediffusion : $a^{(R)} = -.018 \ m_\pi^{-1} (-.020 \ m_\pi^{-1})$ et une d'absorption : $a^{(A)} = -.006 \ m_\pi^{-1} (-.003 \ m_\pi^{-1})$. On constate que les corrections de rediffusion sont comparables tandis que l'effet de l'absorption est très différent. Ceci s'explique par la présence de la partie "non pôle" de la P_{11} dans le deuxième calcul. En effet, on constate dans le deuxième calcul que $a^{(A)}$ se décompose en $a_{\text{non pôle}} = +.003 \ m_\pi^{-1}$ et $a_{\text{pôle}} = -.006 \ m_\pi^{-1}$ (qui représente la véritable contribution de l'absorption) alors que dans le premier, on a simplement $a_{\text{pôle}} = -.006 \ m_\pi^{-1}$.

En ce qui concerne les corrections de rediffusion, on peut, dans le deuxième calcul, les décomposer en : une contribution dominante des ondes S : $a^{(R.s)} = -.023 \ m_\pi^{-1}$, une contribution de la voie P_{33} : $a^{(R.\Delta)} = +.004 \ m_\pi^{-1}$ et une contribution de "petites" ondes P : $a^{(R.P)} = -.001 \ m_\pi^{-1}$. D'où, en utilisant $a_1 + 2a_3 = -.021 \ m_\pi^{-1}$ pour le calcul de $a_{\pi d}^{(0)}$, un bilan pour $a_{\pi d}$:

	$a^{(0)}$	$= -.021$	m_π^{-1}	"approximation d'impulsion"
+	$a^{(R.s)}$	$= -.023$	m_π^{-1}	rediffusion s
+	$a^{(R.\Delta)}$	$= +.004$	m_π^{-1}	rediffusion P_{33}
+	$a^{(R.P)} + a^{(A)}_{\text{non pôle}}$	$= +.002$	m_π^{-1}	rediffusion petites ondes p + partie non pôle de P_{11}
+	$a^{(a)}_{\text{pôle}}$	$= -.006$	m_π^{-1}	absorption
	$R_e(a_{\pi d})$	$= -.044$	m_π^{-1}	

Ce résultat est bien sûr compatible avec la valeur expérimentale mais de ce point de vue, la balle est dans le camp des expérimentateurs car seules des mesures plus précises de $a_1 + 2a_3$ d'une part et de $a_{\pi d}$ d'autre part permettraient de conclure.

Les résultats concernant le coefficient de production s : $\alpha = 258 \mu b$ (140 μb) sont très différents entre les deux calculs. Là encore, la décomposition de la voie P_{11} en une partie "pôle" et une "non pôle" est sans doute responsable de la différence constatée. Cette quantité présente en effet une grande sensibilité envers les données du calcul comme on peut le constater à la lecture du tableau (I, article II.2) où l'on voit en particulier que la description retenue pour le deuton ($P_D = 4$ ou 6.7 %) n'est pas sans effet sur le résultat, contrairement au cas de la partie réelle de a $_{\pi d}$. D'autre part, cette quantité étant directement liée à l'absorption de pion, il est probable que la rediffusion N-N doit y jouer un rôle important. Un traitement avec Z_{NN} contenant les échanges de mésons lourds modifiereait donc sans doute la valeur obtenue. Il reste que le résultat final $\alpha \simeq 140$ μb est assez faible au vu des estimations expérimentales et là encore des mesures plus précises seraient les bienvenues.

2) Région de la résonance Δ :

On dispose dans cette gamme d'énergie, en plus de nombreux résultats sur les distributions angulaires de section efficace (T_π =38, 116, 142, 180, 217, 230, 256, et 292 MeV),de quelques résultats concernant les polarisations (voir la référence 18 pour une revue). Deux observables ont été étudiées la polarisation vectorielle it_{11} et une polarisation tensorielle t_{20}, la seule non nulle à 180°. La polarisation vectorielle, ou plutôt le pouvoir d'analyse vectoriel iT_{11} est mesuré dans la réaction $\vec{d}(\pi^+, \pi^+)d$ sur une cible contenant des deutons polarisés vectoriellement, à partir de l'assymétrie des sections efficaces suivant la direction de polarisation.

$$iT_{11} = \frac{\sqrt{3}}{2} \cdot \frac{1}{P} \left(\frac{\sigma_\uparrow - \sigma_\downarrow}{\sigma_\uparrow + \sigma_\downarrow} \right) \qquad \text{avec } P = \text{polarisation des deutons}$$

Pour la polarisation tensorielle t_{20}, on mesure la polarisation du deuton de recul à l'aide d'un réaction (^{3}He$(\vec{d},p)^4$He en général) dont le pouvoir d'analyse T_{20} est connu. On obtient alors t_{20} à partir du rapport r des sections efficaces polarisées et non polarisées dans cette réaction :

$$r = 1 + t_{20}T_{20}$$

(dans la pratique, ceci est quelque peu compliqué par des problèmes de changement de référentiel).

Une première étude[25] faite dans le cadre de l'approximation R.P.K nous avait permis de mettre en évidence la sensibilité de la section efficace envers les "petites" ondes pion-nucléon d'une part, et à la description de la fonction d'onde du deuton d'autre part. Nous avons donc été amenés à utiliser différents types d'interaction :
- Pour les voies pion-nucléon, à l'exception de la P_{11}, nous avons utilisé les potentiels construits par Rinat et al.[26] (notés R par la suite)   d'une part et Schwarz et al.[27] (notés S par la suite)d'autre part. Dans les deux cas, les paramètres sont obtenus en ajustant les longueurs (ou volumes) de diffusion et les

déphasages jusque vers quelques centaines de MeV, les différences résident essen-
tiellement dans le choix du jeu de déphasages choisi (plus récent dans le cas de
Rinat et al.).

- Pour la voie P_{11}, on impose dans la partie pôle, le pôle du nucléon, avec comme
résidu la constante de couplage π-N-N. On contraint alors l'amplitude totale à re-
produire le volume de diffusion et les déphasages.

- Pour la voie du deuton, nous avons construit 3 types de potentiels, notés YL, S
et SF visant à reproduire de mieux en mieux les caractéristiques de la voie. Pour
YL, on utilise des facteurs de forme de Yamaguchi et seules les caractéristiques
statiques du deuton (énergie de liaison, longueur de diffusion, moment quadripo-
laire, pourcentage d'état D et rapport asymptotique des fonctions d'ondes dans
l'état D et S) sont contraintes. Pour S, on utilise des rapports de polynomes plus
complexes, et on ajoute,en plus des caractéristiques statiques, le déphasage $^3S_1$
jusque vers 200 MeV. Enfin, pour SF, on ajoute comme contrainte le facteur de for-
me monopolaire (fig.1 article I.5) du deuton. Dans les trois cas, nous avons cons-
truit deux jeux de paramètres donnant respectivement une probabilité d'état D de
4 ou 6.7 %. Nous avons d'autre part utilisé les potentiels de Hammel et al [28], noté
QT, qui sont ajustés pour reproduire le déphasage $^3S_1$, le facteur de forme du deuton
avec différentes possibilités, mais qui reproduisent mal certaines données stati-
ques du deuton (voir la table 1 -article I.5-). Il est à noter que tous ces poten-
tiels sont de rang 1 et donnent de ce fait un déphasage $^3D_1$ avec le mauvais signe
(attractif), mais des calculs en approximation RPK ont montré que ceci n'a que
peu d'influence ici.

Au vu des résultats obtenus pour la section efficace (articles I-4,5,6)
on constate tout d'abord (article I.4) que les "petites ondes" pion-nucléon jouent
sauf à 180 MeV, un rôle assez important dans tout le domaine angulaire, et en
particulier à l'avant. La seconde remarque concerne le peu d'effet de l'absorption
à 142 et 180 MeV (fig.2.3, article I.6). Par contre, à 256 MeV, on a un effet très
important à l'arrière, où sa prise en compte remonte la section efficace d'un fac-
teur 2,5 environ. Enfin, on peut constater fig.2, article I.5, le rôle important
joué au-delà de 90° par la description du deuton puisque entre les potentiels YL4
et QT4-1, on obtient une variation d'un facteur 2,5. Pour trouver la caractéristique
de la voie $^3S_1$-$^3D_1$ à laquelle la section efficace π-d est sensible, on peut se
guider sur l'approximation d'impulsion dans laquelle $(d\sigma/d\Omega)$ devrait être propor-
tionnelle au facteur de forme monopolaire du deuton au transfert considéré. La
figure 3, article I-5, montre que cette propriété est conservée dans le calcul
"3 corps" puisque avec les divers potentiels YL, S, SF et QT, la seule caractéris-
tique importante pour $(d\sigma/d\Omega)(180°)$ est la valeur du facteur de forme, indépen-
demment de P_D (YL et YL 6.7 par exemple), des autres caractéristiques statiques
(QT 6.7 et SF 6.7 par exemple) ou du déphasage $^3S_1$ (YL 6.7 et S 6.7 par exemple).

Si l'on compare maintenant le résultat"final" aux mesures expérimentales
(fig.2-3, article I.6) deux conclusions s'imposent :

- Dans l'hémisphère avant (0° à 90°) l'accord est tout à fait satisfai-

sant, sauf à 230 MeV où la seule explication raisonnable est un problème de norma-
lisation expérimentale.

— Dans l'hémisphère arrière (90° à 180°), on reproduit bien les valeurs
expérimentales jusqu'à 142 MeV puis, à partir de 180 MeV, l'accord se dégrade pour
devenir vraiment mauvais à 256 MeV. A cette énergie, il est à remarquer que l'in-
clusion de l'absorption améliore la forme de la distribution angulaire, mais avec
une valeur absolue surestimée d'un facteur 2 à 3. Il est actuellement difficile
de trouver une explication à ce désaccord, mais il est à noter que, dans le cadre
d'un modèle unifié pour le système π-N-N, il est nécessaire, pour reproduire la
voie π-d $\rightarrow$ NN, d'introduire une modification "hors-couche", des voies pion-nucléon[18].
Cette modification a des conséquences sur la diffusion pion-deuton et l'accord est
bien meilleur à 180 MeV mais reste mauvais au-delà.
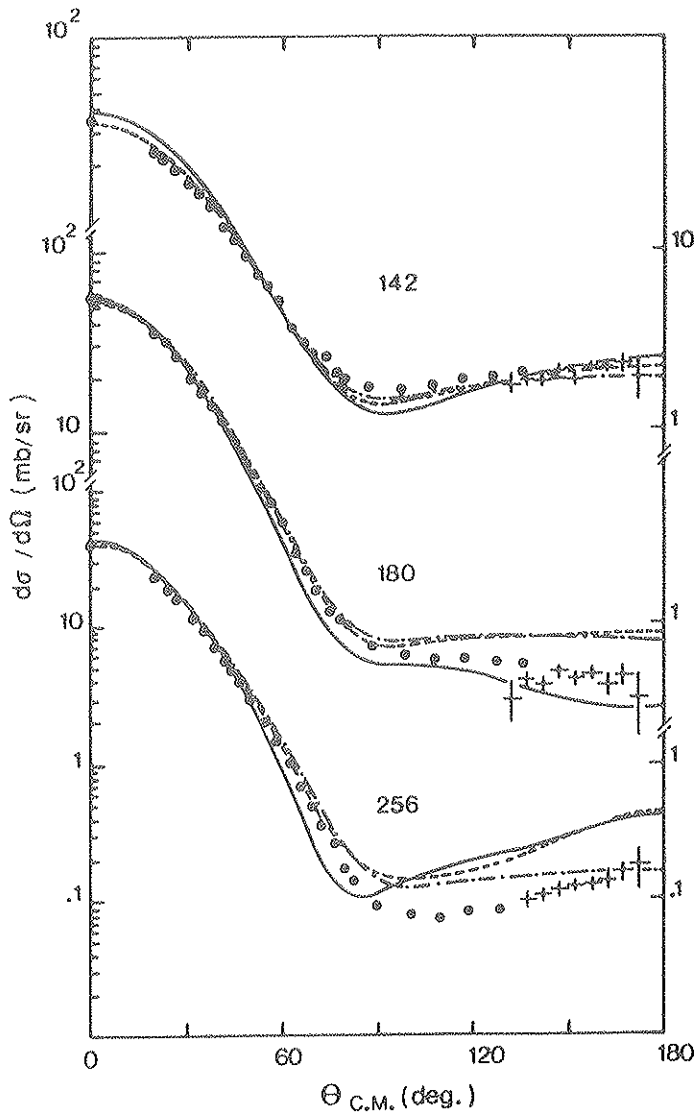
Fig.1 : Section efficace différentielle
πd : sans absorption (   ), avec
absorption, avec (   ) et sans (－－－)
modification hors-couche.
Tiré de la référence 18

Si l'on passe à l'étude des observables de polarisation, on peut s'atten-
dre à des effets plus marqués, puisque les interférences y jouent en général un
rôle plus important. En commençant par la polarisation vectorielle it_{11}, une pre-
mière étude en approximation R.P.K (article I.3) dégage immédiatement le trait mar-
quant de cette observable, à savoir l'importance qu'y jouent les "petites ondes"
pion-nucléon . Leur inclusion dans le calcul modifie profondément la distribution
angulaire pour donner un pic à peu près symétrique, centré vers 80°. La forme gé-
nérale ne varie pas avec l'énergie, seule la hauteur augmente légèrement pour at-
teindre un maximum vers l'énergie de la résonnance delta. Par contre, les autres
données du calcul influent peu sur cette observable et en particulier, le résultat
est pratiquement indépendant de la description du deuton utilisé. L'absorption
(article I.6) enfin joue aussi un rôle qui se limite à augmenter légèrement la hau-
teur du pic, ce qui aboutit a une croissance monotone de ce pic avec l'énergie.
Des résultats expérimentaux étant disponibles depuis ces calculs, on peut tenter
une comparaison avec l'expérience. A 142 MeV tout d'abord, l'agrément est satis-
faisant et confirme en particulier le rôle joué par les petites ondes π -N. A
256 MeV par contre, il apparaît une structure complexe sans rapport avec la forme
simple prévue par le calcul. Au vu de la faible sensibilité de cette observable par
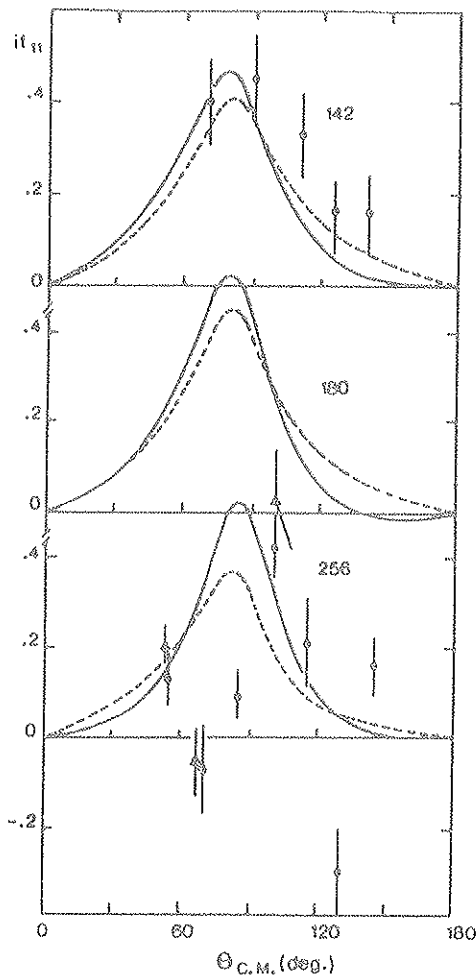
Fig.2 : Polarisation vectorielle
it_{11} dans la diffusion π-d, avec
(   ) et sans (---) absorption.
Le point expérimental négatif à
130° et 256 MeV n'a pas été con-
firmé par de nouvelles mesures
Tiré de la référence 18.

rapport aux données du calcul, il semble difficile d'expliquer cette structure dans le cadre du modèle trois corps et plusieurs auteurs [29] ont été amenés à coupler les amplitudes "trois corps" obtenues à des résonances dibaryoniques $(^{1}D_{2}, {}^{3}F_{3}, {}^{1}G_{2})$ paramétrisées par des formes de Breit et Wigner. Locher et Sainio par exemple arrivent ainsi a reproduire l'observable it_{11} sur tout le domaine d'énergie couvert. Malheureusement ce genre d'ajout au modèle trois corps n'est pas inoffensif pour les au-
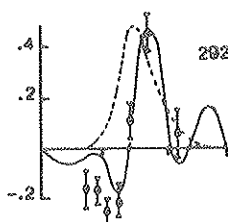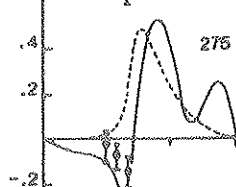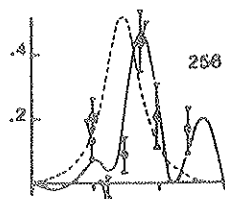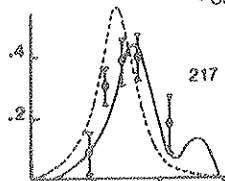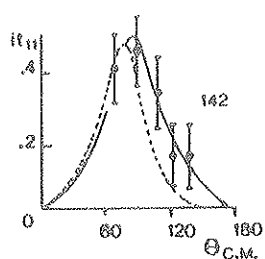
Fig.3 : Polarisation vectorielle it_{11} dans la diffusion π-d, obtenue en ajoutant aux amplitudes "trois corps" (courbes------) des résonnances dans les voies $^{1}G_{11}$ et $^{1}D_{2}$ (courbes)

D'après Locher et Sainio, réf.15

tres observables et la section efficace en particulier présente alors une structure à l'arrière non observée expérimentalement. Pour terminer, il est a noter que l'observable it_{11} est très sensible a des amplitudes $T^{J}_{LL'}$ non dominantes (celles pour lesquelles L = L' = J+1) et que l'on est ainsi sensible à de petits effets (par exemple les petites ondes π-N). Il reste donc a découvrir celui qui déclenche ces oscillations dans it_{11}.

Pour la polarisation tensorielle t_{20}, on peut résumer en disant que les effets sont à l'opposé de it_{11}. Ainsi l'étude préliminaire faite en approximation RPK (article I.3) montre peu d'effet aux petites ondes π-N mais un effet très important de la description du deuton, avec en particulier, comme l'avait déjà noté Gibbs [30], une variation importante à 180° suivant la valeur du pourcentage

d'état D retenue. Si cette dépendance a pu être envisagée comme moyen de mesurer P_D, la différence obtenue entre les potentiels Pieper rang $2(P_D)= 6.7 \%)$ et Yamaguchi $(P_D = 7 \%)$ (fig.2 article I.3) laisse supposer un effet plus complexe Comme dans le cas de la section efficace, on est amené à étudier une dépendance en fonction du facteur de forme du deuton et la figure 4 (article I.5) montre clairement cet effet : pour une valeur de P_D donnée, on a une dépendance linéaire entre t_{20} (180°) et $A(q_{Max}^2)$, indépendamment des autres données. La situation est de plus compliquée par le rôle joué par l'absorption . En effet, son introduction modifie peu t_{20}, sauf à l'arrière ou l'on note une diminution (en valeur absolue) très importante (article I.6) passant, à 142 MeV (180 MeV, 256 MeV) de - 0.73 (-1.08 ; 1.27) à -.08 (-55 ; -.44). On peut alors tenter de comparer le résultat "final" avec les données expérimentales disponibles depuis et on se heurte a deux problèmes :
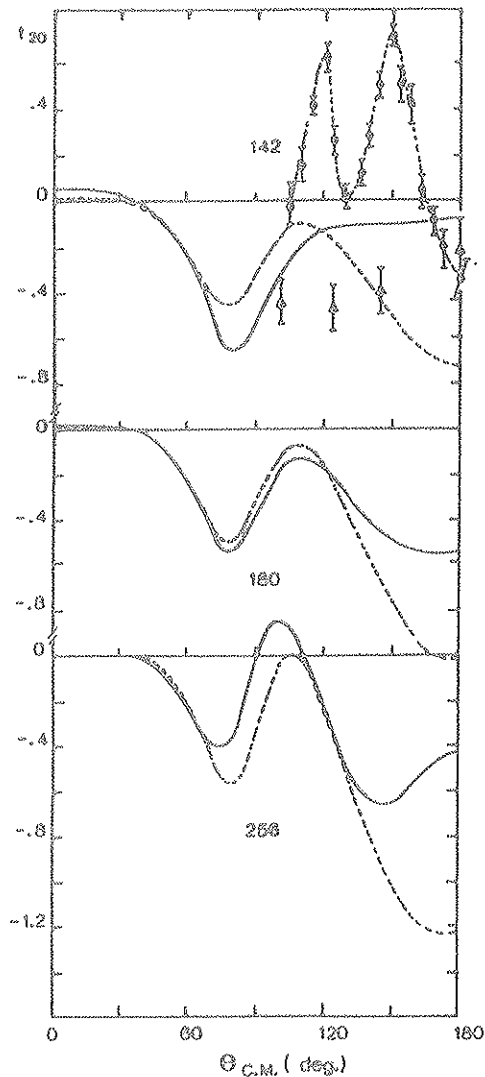
Fig.4 : Polarisation tensorielle t_{20} dans la diffusion —d avec ( ) et sans (---) absorption. Les tirets reliant les points expérimentaux à 142 MeV sont décoratifs.
Tiré de la référence 18.

— tout d'abord un problème expérimental puisque les résultats obtenus par deux équipes[31] ne sont pas compatibles.

— puis un problème théorique puisque de toute façon le résultat du calcul ne reproduit aucune des expériences, avec toutefois un désaccord moins flagrant dans le cas de Holt et al.

Il est dans ces conditions difficile d'apporter une conclusion. On peut simplement noter, que d'une part l'importance de l'effet de l'absorption sur cette

observable et les progrès possibles dans son traitement peuvent faire espérer une
amélioration, et que d'autre part la variation des petits termes d'interférence
$T_{L,L'}^{J}$ (L ≠ L') (fig.2a article I-3) peut ici encore induire des effets importants.

Pour conclure sur la description du système pion-deuton à l'aide d'équa-
tions à trois corps, on dispose : —pour la longueur de diffusion d'une prédiction
assez bien établie qui attend une mesure plus précise.

—pour les distributions angulaires d'un bon ac-
cord général avec les nombreuses données expérimentales, sur un domaine d'énergie
important.

Il reste cependant trois problèmes sérieux :

- Le comportement de (d σ /d Ω) à l'arrière au-dessus de 180 MeV
- Le comportement de it_{11} au dela de 180 MeV
- Le comportement de t_{20} en général.

Dans les trois cas, on a pu montrer que ces observables sont très sensibles aux détails
des données du calcul et de petites causes peuvent modifier sérieusement les résultats
obtenus. De ce point de vue, on peut attendre des progrès du côté d'un traitement
unifié du système π –N–N où le nombre d'observables(en particulier la diffusion
N–N pour laquelle les mesures sont nombreuses et précises) contraint considérable-
ment les données du calcul. L'exemple des modifications hors-couche apportées aux
potentiels π –N est ici significatif, mais on touche peut-être ici certaines limi-
tations des équations trois corps utilisées, à savoir l'approximation des interac-
tions séparables, et l'absence des termes de croisement.

REFERENCES :

1) A.W.Thomas et I.R.Afnan, Phys.Let. 45B (1973) 437

2) D.Freedman, C. Lovelace et J.Namyslowski, Nuovo Cimento 43 (1966) 248

3) E.E.Salpeter et H.Bethe, Phys.Rev. 84 (1951) 1232

4) R.Blankenbecker et R.Sugar, Phys.Rev. 142 (1966) 1051

5) R.Aaron, R.D.Amado et J.E.Young, Phys.Rev. 174 (1968) 2022

6) E.O.Alt, P.Grassberger et W.Sandhas, Nucl.Phys. B2 (1967) 167

7) H.Stingl et A.S.Rinat, Nucl.Phys. A 154 (1970) 613

8) N.Giraud, Y.Avishai, C.Fayard et G.H.Lamot, Phys.Rev. C19 (1979) 465

9) A.W.Thomas, Nucl.Phys. A 258 (1976) 417

10) A.W.Thomas et I.R.Afnan, Phys.Rev. C10 (1974) 109

11) A.W.Thomas in "Few problems in Nuclear and Particle Physics"
    (R.J.Slobodrian, B.Cujec et K.Ramavataram Eds ; University of Laval Press,
    Quebec, 1975) p.287.

12) T.Mizutani et D.S.Koltun. Ann. Phys. 109 (1977) 1.

13) A.S.Rinat Nucl.Phys. A287 (1977) 399

14) Y.Avishai et T.Mizutani. Nucl.Phys. A 326 (1979) 352, A338(1980) 377, A352
    (1981)399 .

15) I.R.Afnan et B.Blankleider, Phys.Rev. C22 (1980) 1638

16) T.Mizutani, C.Fayard, G.H.Lamot et S.Nahabetian, Phys.Rev. C24(1981)2633

17) M.Chemtob, Saclay Lecture Notes, Report D.Ph.T 75/114 (1975) p.276

18) C.Fayard, G.H.Lamot et J.L.Perrot, 7ème Session d'Etudes Biennale de Physique
    Nucléaire. Aussois 14-18 Mars 1983, p. C5

19) J.Bailey et al. Phys.Lett. 50B (1974) 403

20) J.Spuller et D.F.Measday, Phys.Rev. D12 (1975) 3550

21) M.Salomon, TRIUMPH Report TRI-74-2(1974)

22) P.V.Bugg et al. Phys. Lett. 44B (1973) 278.

23) P.Y.Bertin et al. Nucl.Phys. B106(1976) 341.

24) R.Koch et E.Pietarinen. Nucl.Phys. A 336(1980)331.

25) N.Giraud, C.Fayard et G.H.Lamot, Phys.Rev.Lett.40 (1978) 438

26) A.S.Rinat, Y.Starkand, E.Hammel et A.W.Thomas, Nucl.Phys.A329 (1979)285

27) K.Schwartz, H.Zingl et L.Mathelitsch, Phys.Lett. 83B (1979) 297

28) E.Hammel, H.Baier et A.S.Rinat, Phys.Lett. B85 (1979) 193

29) K.Kubodera et al. J.Phys. G6 (1980) 171
    W.Grein et M.P.Locher, J.Phys. G7 (1981) 1355

30) W.R.Gibbs , Phys.Rev.C3 (1971) 1127

31) R.J.Holt et al, Phys.Rev.Lett. 47 (1981) 472
    J.Ulbricht et al. Phys.Rev.Lett. 48 (1982) 311.

Article I-1

PRACTICAL SCHEME FOR LOW π-d SCATTERING [+]

Y. Avishai[*], N. Giraud, C. Fayard and G.H. Lamot
Institut de Physique Nucléaire de Lyon and IN2P3
Université Claude Bernard Lyon-I
43, Bd du 11 Novembre 1918, 69621 Villeurbanne, France

Recently, it became clear that the solution of the π-d scattering problem in the presence of pion absorption rests outside the Faddeev theory. The most one can expect from this theory is the N-N' model of Afnan-Thomas[1], in which the Pauli principle is violated. In the present work, we impose the exclusion principle on the Afnan-Thomas model as an ad-hoc assumption, and get a modified set of equations in which the two nucleons are identical through all intermediate states, and non-Faddeev terms with two successive pion emissions are included (but states of more than one pion are eliminated).

We also make the approximation (tested and justified to within 2%[2]) that the N-N interaction in three-body states is allowed strictly in the $^3S_1$-$^3D_1$ quantum numbers. At the expense of imposing "external" assumption on a self consistent model we arrive at a compact set of equations, which couples the amplitudes for the reactions $\pi + d \longrightarrow \pi + d$, $N + \Delta \longrightarrow \pi + d$ and $N + N \longrightarrow \pi + d$.

The fact that the two nucleon amplitudes in $T = i$ states are generated (as by-products) do not lead to bootstrap since these states are not used in advance, and there is no input-output overlap. In addition, these amplitudes are not used as input for the production process, since all the unknown amplitudes are generated by multiple scattering. Therefore, our equations are free of overcounting.

From a numerical point of view, our equations are relatively simple and no extra work is needed beyond the use of three-body codes. Exact solution has recently been reported[3]. Here we give the following results : 1) Singlet scattering length $a_{\pi d}$ and triplet scattering volume $A_{\pi d}$. 2) The effect on the real part of the singlet πd scattering amplitude (at threshold) of including the coupling to the N-N channel, denoted by $\Delta a_{\pi d}$. 3) Production coefficients at threshold, α β defined by $\sigma (N + N \longrightarrow \pi + d)_{k \longrightarrow 0} \approx \alpha k + \beta k^3$ ($[k] = m_\pi^{-1}$) (β has contribution from the partial wave amplitudes $T_1^J{}_1$, $J = 0,1,2$.)

$$L = 0$$

	Theor.	Exp.
$a_d \, (m^{-1})$	$- 0.042$	$- 0.052 \pm \binom{0.022}{0.017}$ [4]
$a_d \, (m^{-1})$	$- 0.0057$	
(μb)	258	200 300 [5]

$$L = 1$$

	$J=0$	$J=1$	$J=2$	Exp.
$A_d \, (m^{-3})$	$- 0.29$	0.11	0.48	none
(μb)	small	$0.$	1.20	$1.(?)$ [5]

References

1. I.R.Afnan and A.W.Thomas, Phys. Rev. C10, 109 (1974)

2. N.Giraud, Thèse de troisième cycle, Université Lyon-1 (unpublished)

3. Y.Avishai, N.Giraud, C.Fayard and G.H.Lamot, Lyon preprint (1978)

4. J.Baily et al., Phys. Lett. B50, 403 (1974)

5. J.Spuller and D.F. Measday, Phys. Rev. D12, 3550 (1975)

* On leave of absence from Ben Gurion University, Beer-Sheva, Israël.

Article I-2

STUDY OF THE REACTION $N+N \longrightarrow \pi+d$ AT THRESHOLD

N. GIRAUD, C. FAYARD, and G. H. LAMOT
Institut de Physique Nucléaire (and IN2P3), Université Claude Bernard Lyon-I
43, Bd du 11 Novembre 1918, 69622 Villeurbanne Cedex, France

and

T. MIZUTANI
Division de Physique Théorique, Institut de Physique Nucléaire,
91406 Orsay Cedex, France

The $N+N \longrightarrow \pi+d$ reaction at threshold can give some information on the validity of the theory of pion absorption. We present here some preliminary results obtained with the Avishai-Mizutani (AM) equations [1] with fully relativistic kinematics. In our model the absorption phenomena occur via the P_{11} πN channel which contains a non-pole part in addition to the pole part. The parameters of the P_{11} channel are adjusted in order to give the π-N coupling constant, the P_{11} scattering volume and the phase shift up to 250 MeV. We have thus calculated the $\pi+d$ elastic scattering observables up to the resonance region [2]. Here, we present only some results at threshold, namely the scattering length (volume) and the production coefficients α and β in the $L=0$ and $L=1$ partial waves. In table I, we give the $L=0$ results, with and without absorption. In order to test the effect of P_D (D-state percentage value), two $^3S_1$-$^3D_1$ NN parametrizations are used [3] (denoted SF4 and SF 6.7). It is well-known that the main part of the scattering length is given by the S_{31} and S_{11} πN channels and also by the P_{33} channel, but also the " small " π-N partial waves (P_{13}, P_{31}) give noticeable contribution.

	Without absorption			Absorption		
	$S_{11}+S_{31}$	$+P_{33}$	all π-N	$S_{11}+S_{31}$	$+P_{33}$	all π-N
SF4	-.0310	-.0266	-.0278	-.0334	-.0296	-.0307
	-	-	-	116.	133.	142.
SF 6.7	-.0316	-.0266	-.0279	-.0340	-.0296	-.0310
	-	-	-	90.	112.	127.

Table I : $J = 1^-$, $L = 0$. The first number is the scattering length (m_π^{-1}), and the second the S-wave production coefficient (μb).

2.

One can note that α decreases with increasing P_D. We have also observed that α is very sensitive to the P_{11} parametrization and depends mainly on the range of the pole part. If we compare to experimental data[4]

$$a_{\pi d}^{exp} = -.052 \left({}^{+.017}_{-.022} \right) m_\pi^{-1}$$, our value $(-0.031 \ m_\pi^{-1})$ seems too large. One can write the real part of the calculated $a_{\pi d}$ as :

$$Re \ a_{\pi d} = a_{\pi d}^{(o)} + \Delta a_{\pi d}^{MS} + \Delta a_{\pi d}^{A}$$

where $\Delta a_{\pi d}^{MS}$ and $\Delta a_{\pi d}^{A}$ are respectively the corrections due to multiple scattering (MS) and absorption (A). $a_{\pi d}^{(o)}$ is obtained in the impulse approximation and is proportional to $(a_1 + 2a_3)$, where a_1 and a_3 are the S_{11} and S_{31} scattering lengths. Here, we use the parametrizations of Schwarz et al.[5] which give $a_1 + 2a_3 = -0.0116 \ m_\pi^{-1}$, while the recent analysis of Koch and Pietarinen[6] leads to $a_1 + 2a_3 = -0.029 \ m_\pi^{-1}$. Using this last value, we obtain the corrected value $Re \ a_{\pi d} \sim -0.043 \ m_\pi^{-1}$, in good agreement with experiment. The production coefficient $\alpha \sim 135 \ \mu b$ (mean value of the results obtained with all πN channels) has the correct order of magnitude compared with the analysis of Spuller and Measday[7] $(200 < \alpha < 300 \ \mu b)$.

	$a_{\pi d}$	$a_{\pi d}^{A}$	β
$J = 0^+$	-.042	-.241	.98
$J = 1^+$	.059	.127	0.
$J = 2^+$	.255	.253	.69

Table II : L = 1 scattering volumes (m_π^{-3}) $a_{\pi d}$ (without absorption), $a_{\pi d}^{A}$ (absorption included) and production coefficient β (mb). The tensor force is SF4, all S and P πN channels are taken into account.

In the L = 1 case, the effect of absorption on the scattering volume is large for J = 0 and 1, but negligible for J = 2 (Table II). For the present, none experimental data are available for the scattering volumes. For the total production coefficient β, we obtain 1.67 mb, in agreement with the value of Spuller and Measday $(\sim 1mb)$. In fact, we have $1.4 < \beta < 2 \ mb$, according to the choosen P_{11} and $^3S_1 - ^3D_1$ parametrizations.

1) Y. Avishai and T. Mizutani, Nucl. Phys. A326 (1979) 352 ; A338 (1980) 377, and this conference. 2) C. Fayard et al., to be published, and this conference. 3) N. Giraud et al., to appear in Phys. Rev. C. 4) J. Bailey et al., Phys. Lett. B50 (1974) 403. 5) K. Schwarz et al., Phys. Lett. 83B (1979) 297. 6) R. Koch and E. Pietarinen, Nucl. Phys. A336 (1980) 331. 7) J. Spuller and D. F. Measday, Phys. Rev. D12 (1975) 3550.

Article I-3

POLARIZATION OBSERVABLES IN π–d SCATTERING

N. GIRAUD, Y. AVISHAI [1], C. FAYARD and G.H. LAMOT
Institut de Physique Nucléaire (and IN2P3), Université Lyon-1, 69621 Villeurbanne, France

Received 16 March 1978
Revised manuscript received 6 June 1978

Exact calculations of vector and tensor polarizations are presented for the reaction $\pi + d \to \pi + \vec{d}$ at $T_\pi = 142$ MeV.
They are aimed at meeting the apparent demand raised by upcoming pertinent experiments. The effects of (i) deuteron D
state, (ii) participating π–N partial waves and (iii) coupling of different π–d orbital angular momenta are found to be very
important.

The purpose of the present work is to present theoretical calculations of deuteron polarization observables induced by elastic π–d scattering. It is our belief that with the advent of meson factories, the simplest experiment in this category namely

$$\pi + d \to \pi + \vec{d}, \tag{1}$$

is imminent [1]. Therefore, the presentation of some reliable theoretical data is indispensable.

Naturally, experiments that involve polarizations are much harder to perform than those who do not. Yet, the information that they can give on the nature of the forces among the particles involved, especially their spin dependence, encourage people to perform them. For the π–d system, the importance of which has been reiterated elsewhere [2], some additional interesting points arise in connection with polarization observables. The properties of the pion–deuteron optical potential, which is the central result of such analysis, will shed some light on the interaction between pion and more complex nuclei.

It will be helpful to point toward a few directions of investigation that relate the π–d optical potential to polarization observables. Those which are given below are by no means complete. One might start by studying either the hermiticity of the optical potential

or the adequacy of the Born approximation. According to a well-known theorem [3] the Born approximation gives zero polarization for interactions which are hermitian, and therefore the amount of polarization will check these properties.

Another point in connection with the π–d interaction is its ability to couple different orbital angular momenta. In recent calculations of the elastic cross section [4] this coupling has been neglected due mainly to computational difficulties. Yet, in a more recent calculation [5], some of us have shown that even in cross-section calculations this coupling cannot be discarded. However, as we shall see later on, the effect of the coupling on the polarization is so dramatic that one cannot even think about its omission.

The spin dependence of the pion–deuteron interaction arises from both spin–orbit and tensor forces. If the main contribution to the tensor polarization is assigned to the tensor part of the optical potential [6], the amount of tensor polarization is a direct indication of this kind of interaction. In general, however, the tensor polarization arises also from higher order spin–orbit interaction.

Polarization observables in π–d reaction can be used to test the validity of the frequently used folding model interaction defined by

$$\langle \nu | V_{\pi-d}(r) | \nu' \rangle = \langle \Phi_\nu | V_n(r - \tfrac{1}{2}\rho) + V_p(r + \tfrac{1}{2}\rho) | \Phi_{\nu'} \rangle, \tag{2}$$

where $\Phi_\nu(\rho)$ is the deuteron wave function with spin

---

[1] On leave of absence from Ben Gurion University, Beer-Sheva, Israel.

projection ν and V_n, V_p are the π–n and π–p potentials. In this model, the central and spin–orbit parts of $V_{\pi-d}$ are related to those components in V_p and V_n, while the tensor part of $V_{\pi-d}$ arises because the deuteron is not spherically symmetric. If one now performs an "exact" three-body calculation and sets the D-state probability (P_D) of the deuteron equal to zero, the amount of tensor polarization indicates whether the assumption (2) is correct. For example, in three-body calculations of $\vec{d} + \alpha \to d + \alpha$, it is found that setting $P_D = 0$ has very little effect on the tensor polarization [7] and therefore, the folding potential cannot be accepted there.

Beside these and other interesting points, there are the usual peculiarities of the pi–nucleus interaction which are related to the pion–nucleon force namely, the existence of the P_{33} resonance and the possibility of pion absorption. Concerning the P_{33} resonance, the obvious question is whether other π–N partial waves are also important, and at what energy. Our present calculations have been performed at pion lab energy $T_\pi = 142$ MeV. The answer we give to this question is identical to that given regarding the coupling of different orbital angular momenta, namely: the inclusion of all S and P π–N partial waves has an important effect in cross-section calculations [5] and a dramatic effect on the polarization. The ever popular assumption of P_{33} dominance should be taken with care even at energies which are "covered" by this resonance.

As for the property of pion absorption, it will not be discussed here mainly because of the lack of a tractable theory at medium energies [8]. It has been neglected in almost all the calculations performed up till now, and is expected to be important mainly near threshold.

Finally, the comparison of theory with experiment can give information about the N–N force, especially the value of P_D and the importance of N–N scattering states.

We shall now briefly discuss the calculations. They are based on Faddeev three-body theory for the π–d system with relativistic pion kinematics (RPK). The π–N and N–N interactions are assumed to be separable and are chosen in the usual way to fit the two-body scattering data. The resulting set of one dimensional coupled integral equations has a rather complicated structure [9] and its precise form will be published elsewhere [10]. The solution is obtained by the Padé

approximant method and its reliability has been guaranteed by comparing it to Thomas calculations using his parameters and his zero coupling (between different orbital angular momenta) approximation.

By far, the present calculations seem to be the most complete ones with regard to the following three fundamental points, namely (i) the inclusion in an exact way of all S and P π–N channels, (ii) the use of either Yamaguchi or Pieper–Reid [11] parametrizations for the $^3S_1 - ^3D_1$ N–N channel and (iii) the retaining of coupling between different orbital angular momenta. The resulting partial wave elastic π–d amplitudes $T^J_{L'L}(E)$ (J = total angular momentum, L, L' = initial and final orbital angular momenta and E = total three-body c.m. energy) are used to construct the M matrix through

$$M_{\nu'\nu} = \sum_{\substack{LmL'm' \\ JM}} \langle L'm'|\nu'|JM\rangle\langle JM|Lm|\nu\rangle$$

$$\times Y_{L'm'}(\hat{k}')Y^*_{Lm}(\hat{k})T^J_{L'L}(E), \tag{3}$$

where ν and ν' are the initial and final spin projections of the deuteron whereas k and k' refer to the initial and final momenta of the pion. From the M matrix the final density matrix ρ_f is constructed by

$$\rho_f = MM^+, \tag{4}$$

from which polarization observables are computed according to the Madison convention [12].

We shall now describe the N–N and π–N forces which have been used as an input to the three-body equations. These are summarized in table 1. Since these forces are extensively used elsewhere we just give their title and the reference in which the actual form as well as the value of the parameters could be found. We note that the Pieper parametrization gives a better description of the $^3S_1 - ^3D_1$ channel than the simple Yamaguchi, namely it has the same deuteron wave function as the Reid soft-core potential. The reason that we have used also Yamaguchi tensor force rests in our intention to check the sensitivity of the results to P_D, since the Pieper interaction is restricted to $P_D = 6.5\%$.

Let us now present our results. The pion kinetic energy in the laboratory frame is 142 MeV. We have chosen this energy because it is not too far from the P_{33} resonance on the one hand, but it is still far

Table 1
Details of the two-body forces used throughout. The following combinations have been applied: P2-SP, Y7-SP in fig. 1. P2-SP, P2-P33 in figs. 2a, b, and Y0-SP, Y4-SP, Y7-SP in fig. 2c.

N—N forces

Title	P_D	Ref.	Notation
Yamaguchi	0%	15	Y0
Yamaguchi	4%	16	Y4
Yamaguchi	7%	16	Y7
Pieper rank-2	6.5%	11	P2

π—N forces

Partial waves		Ref.	Notation
all S and P		9	SP
P_{33} alone		9	P33

enough to demonstrate the importance of other partial waves on the other hand. Besides, this energy is low enough so that relativistic effects of the nucleons could be neglected.

First, we show the advantage of the Pieper tensor force over Yamaguchi in π—d cross-section calculations. In fig. 1, we give the differential cross sections obtained with the P2-SP and Y7-SP interactions. Clearly the P2 tensor force leads to a better agreement with experimental data at backward angles than Y7. It is worth mentioning that the effect of P_D was found to
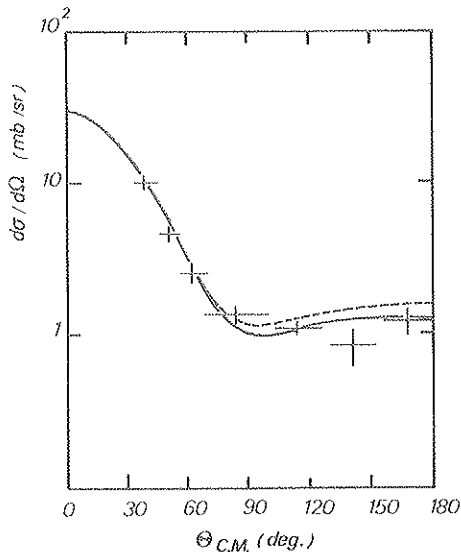
Fig. 1. Elastic differential cross section. Solid line, P2-SP. Dashed line, Y7-SP. Experimental data are from ref. [17].

be very small when using Yamaguchi tensor forces [5].

In order to avoid piling of data we present here the vector polarization it_{11} and one tensor polarization, namely t_{20}, the only tensor observable which is non zero at $180°$. The first experiments will apparently start at this angular region. Yet, we point out that any other observables at energies below $T_\pi = 200$ MeV could be calculated upon request.

The angular distributions of it_{11} and t_{20} are shown in fig. 2. As a rule, the most reliable results are those in which Pieper rank 2 interaction has been assumed for the two nucleon system, while all S and P π—N partial waves are retained. These results are drawn in solid lines.

The message of our results is self contained and can be stated briefly as follows: (1) In the quantity it_{11}, fig. 2a, the effect of using all S and P π—N partial waves and not the P_{33} alone is so profound that any thought about retaining only P_{33} in this context should be discouraged. This result is universal in the sense that it is persistent also if Yamaguchi type forces are assumed among the nucleons. (2) In the quantity t_{20}, fig. 2b, the effect of coupling different angular momenta has a dramatic effect on the angular distribution at large angles. On the other hand, in contrast with it_{11}, the assumption of P_{33} dominance affects slightly t_{20} as shown in fig. 2b. (3) The quantity t_{20} is sensitive at large angles to the value of P_D, as is seen from fig. 2c. For a Yamaguchi tensor force, $t_{20}(180°)$ decreases with increasing P_D, its values for $P_D = 0\%$, 4% and 7% being respectively 0.04, —0.56 and —0.67. The fact that t_{20} is quite large for $P_D = 0$ indicates that the use of the folding potential should be done with some care. From the comparison between P2-SP and Y7-SP results, one can see that t_{20} is rather model dependent, mainly in the backward region: for the P2 and Y7 interaction which have similar P_D, $t_{20}(180°)$ takes respectively the values —0.73 and —0.67. These differences must be attributed to the fact that the P2 and Y7 potentials give different description of the $^3S_1$ —$^3D_1$ channel.

Our results for t_{20} are in close agreement with those of Gibbs [13], namely the dependence of $t_{20}(180°)$ as a function of P_D is similar. However, as can be seen from fig. 1a, and contrary to his statement, it_{11} is by no means small. We also point out that our results for it_{11} assuming the P_{33} dominance resemble in shape to those of Händel et al. [14] who used a D^*
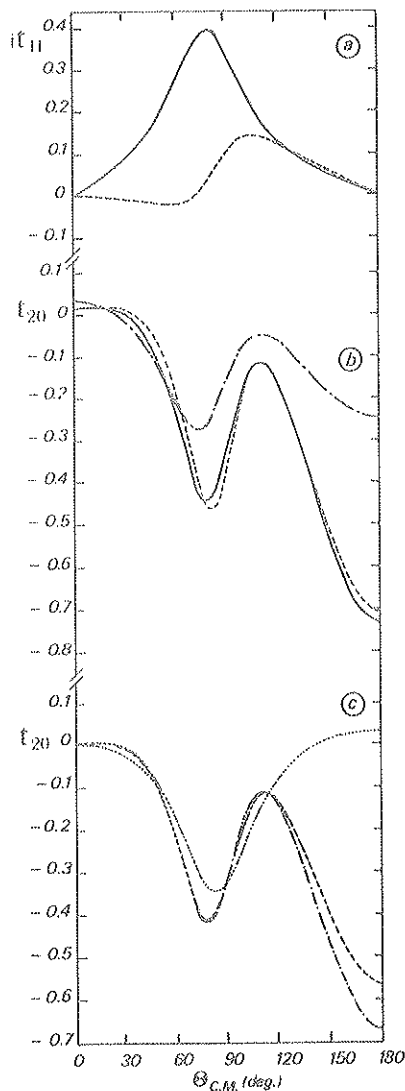
Fig. 2 (a) Vector polarization. Solid line, all S and P π–N partial waves (P2-SP). Dashed line, only P_{33} (P2-P33). (b) Tensor polarization with P2. Solid line (P2-SP) and dashed line (P2-P33), coupling between different π–d angular momenta is retained. Dash–dot line (P2-SP), coupling is neglected. (c) Sensitivity of t_{20} to P_D. Dot line, P_D = 0% (Y0-SP). Dashed line, P_D = 4% (Y4-SP). Dash–dot line, P_D = 7% (Y7-SP).

model for the π–d scattering. Without the use of all S and P π–N partial waves this model seems to be inadequate with regard to vector polarizations.

In conclusion, we have presented here a reliable calculation of deuteron polarization observables induced by elastic π–d scattering. These calculations seem to be quite complete since they are based on a three-body formulation of the problem which is then solved exactly. The results obtained thereby might serve as a bona-fide comparison test for near future experiments.

We would like to thank Professor E. Elbaz for very helpful discussions during the course of the present work.

References

[1] W. Grüebler, SIN proposal and private communication.
[2] A.W. Thomas, Invited talk at the 7th Intern. Conf. on High energy physics and nuclear structure (Zürich, 1977).
[3] M.L. Goldberger and K.M. Watson, Collision theory (Wiley) p. 415.
[4] A.S. Rinat and A.W. Thomas, Nucl. Phys. A282 (1977) 365.
[5] N. Giraud, C. Fayard and G.H. Lamot, Phys. Rev. Lett. 40 (1978) 438;
N. Giraud, Thèse de Troisième Cycle, Université Lyon-I, unpublished, Report no. LYCEN 78 05.
[6] L.D. Knutson and W. Haeberli, Phys. Rev. C12 (1975) 1469.
[7] B. Charnomordic, C. Fayard and G.H. Lamot, Phys. Rev. C15 (1977) 864.
[8] T. Mizutani and D. Koltun, Ann. Phys. 109 (1977) 1;
A.S. Rinat, Nucl. Phys. A287 (1977) 399.
[9] A.W. Thomas, Nucl. Phys. A258 (1976) 417.
[10] N. Giraud, C. Fayard, G.H. Lamot and Y. Avishai, to be published.
[11] S.C. Pieper, Phys. Rev. C9 (1973) 883.
[12] Polarization phenomena in nuclei, eds. H.H. Barschall and W. Haeberli (Madison, 1970).
[13] W.R. Gibbs, Phys. Rev. C3 (1971) 1127.
[14] R. Händel et al., Phys. Lett. 73B (1978) 4.
[15] Y. Yamaguchi and Y. Yamaguchi, Phys. Rev. 95 (1954) 1628.
[16] A.C. Phillips, Nucl. Phys. A107 (1968) 209.
[17] E.G. Pewitt, T.H. Fields, G.B. Yodh, J.G. Fetkovitch and M. Derrick, Phys. Rev. 131 (1963) 1826.

Relativistic description of πd elastic scattering in the (3,3) resonance region

N. Giraud, C. Fayard, and G. H. Lamot

Institut de Physique Nucléaire (et IN2P3), Université Claude Bernard Lyon-I, 43, Bd du 11 Novembre 1918 - 69622 Villeurbanne, Cedex, France

(Received 28 December 1979)

The πd elastic scattering observables are calculated in the 142 to 256 MeV energy range within a relativistic three-body theory without π absorption. The nonresonant πN partial waves are included perturbatively to an excellent degree of accuracy. Various NN tensor forces are elaborated at different levels of quality. The sensitivity of elastic differential cross sections and polarization parameters to the description of the NN and πN channels is investigated. The importance of using a realistic deuteron wave function is demonstrated.

I. INTRODUCTION

Recently,[1] we have performed detailed calculations of πd elastic scattering at 142 and 180 MeV, based on the nonrelativistic three-body theory of Thomas,[2] with relativistic kinematics for the pion only (RPK theory). Various NN tensor forces were used, and we have considered either the P_{33} scheme, where only the P_{33} πN channel was retained, or the case where the "small" S and P πN partial waves were included in an exact manner, denoted as the SP scheme. The main conclusions we have drawn are the following:

(i) The SP scheme lowers the differential cross section $d\sigma/d\Omega$ at backward angles, thus improving the agreement with experimental data, and changes completely the structure of the vector polarization it_{11}, while the tensor polarization t_{20} is only slightly affected.

(ii) The use of a $^3S_1$-$^3D_1$ parametrization giving a "realistic" deuteron wave function leads to a better agreement of $d\sigma/d\Omega$ with experimental data at backward angles. On the other hand, changing the value of P_D (D-state probability of the deuteron) has little influence on $d\sigma/d\Omega$ and it_{11}, but produces an appreciable decrease of the backward part of t_{20}.

At the same time, Rinat et al.[3] have reported on calculations of πd elastic scattering in the energy range 142 to 256 MeV, based on a fully relativistic (FR) three-body theory including the effects of genuine pion absorption and emission. These calculations, where the interference effects from the small πN waves are treated perturbatively, constitute an extension of the FR approach of Rinat and Thomas[4] limited to the P_{33} scheme. The changes in the observables due to the small πN waves

are similar to those we have observed in the RPK approach, and the absorptive corrections are found to be important both in the backward part of $d\sigma/d\Omega$ and in the polarization parameters.

The following aspects provided the motivation for the present work. At first, we extend our RPK calculations on the basis of the FR theory, in order to ensure a correct treatment of the relativistic effects when energy increases. Next, we want to produce πd calculations which can serve as reference for further calculations including the genuine effects of π absorption. Indeed, we think it is more reasonable to investigate such effects insofar as the situation without π absorption is completely clear, namely with regard to the sensitivity of the πd observables to the description of the NN and πN channels. To this end, the $P_{11}\pi N$ channel being completely omitted, two sets of parametrizations for the S and P πN channels are used, and various sets of NN tensor forces are elaborated in order to improve the usual Yamaguchi-type interactions.

Of course, the various experiments which are in progress are also strongly motivating. At SIN, Gabathuler et al.[5] are analyzing the elastic differential cross-section data at seven energies from 80 to 300 MeV in the angular range 0° to 140°, and Grüebler et al.[6] plan to measure $t_{20}(180°)$ at 140 MeV; the LAMPF group[7] has recently observed $d\sigma/d\Omega$ (180°) and t_{20} (180°) at 140 MeV and has proposed measuring t_{20} as a function of angle, and the CERN group[8] has given preliminary results for the cross section at backward angles between 130° and 175° in the energy range 140 to 260 MeV.

The paper is organized as follows. In Sec. II, we describe the practical calculation, namely the numerical procedure and the perturbation scheme

used to include the small πN channels. Section III is devoted to the description of the πN and NN interactions used as input. Our results are presented and discussed in Sec. IV, and we conclude the paper in Sec. V.

II. PRACTICAL CALCULATION

A. Basic equations

We use the three-body equations described by Rinat and Thomas[4] which satisfy two and three-body unitarity and covariance. In operator form, the equations read, with the notation of Ref. 1:

$$X_{nm} = \sum_{\alpha} Z_{n\alpha} R_{\alpha} X_{\alpha m},$$

$$X_{\alpha m} = Z_{\alpha m} + \sum_{\beta} Z_{\alpha\beta} R_{\beta} X_{\beta m} + \sum_{n} Z_{\alpha n} R_n X_{nm}, \qquad (1)$$

where the α, β and n, m labels refer respectively to $N(\pi N)$ and $\pi(NN)$ three-body channels. In our case, the α, β labels do not contain the $N-P_{11}$ channel. The driving terms Z and the propagators R are defined in terms of the form factors of the separable interactions, and for the relative momenta of the interacting pairs, we take the choice (a) of Ref. 4 corresponding to the exchanged particle on its mass shell.

The scattering amplitudes $2X_{dd}$ are obtained by solving the system of coupled one-dimensional integral equations which result from angular momentum reduction of Eq. (1). The singularities of the kernel are treated by contour rotation and the system is solved by the Padé approximant technique. The coupling of πd channels with l, $l' = J \pm 1$ orbital angular momentum is included exactly.

Compared with the RPK case, the FR calculation is much more time consuming because of the intricate coefficients which appear in the relative momenta [see Eqs. (2.20) and (2.21a) in Ref. 4]. In order to save computing time, we have (i) reduced the number of mesh points in the $[0, +\infty]$ domain, and (ii) treated perturbatively the small πN channels.

B. Numerical integration

In order to preserve the numerical accuracy when energy goes up to 300 MeV, without increasing too much the number of mesh points, we split the $[0, +\infty]$ domain of integration for the integral equation into two intervals $[0, k_c]$, $[k_c, +\infty]$. The energy-dependent parameter k_c is chosen to be in the middle of the interval delimited by the pole of the propagator and the extreme position of the logarithmic singularity in the driving term. In each interval, we use Gaussian quadratures mapped onto $[0, k_c]$ and $[k_c, +\infty]$ with, respectively,

N_1 and N_2 mesh points. Because of the structure of the kernel, the convergence in the $[k_c, +\infty]$ domain is faster than in the $[0, k_c]$ region, and we take usually $N_2 = N_1/2$. The two main advantages of the method are (i) the number of mesh points is large in the region around k_c where the kernel is rapidly varying, and (ii) we have observed that the convergence of the scattering amplitudes is monotonic when N_1 and N_2 increases. Therefore, the stability of the results can be obtained with a total number of mesh points appreciably lower than in the case where the Gaussian quadrature mapped directly onto $[0, +\infty]$ is used. We estimate the accuracy to be within 2% with $N_1 = 16$ and $N_2 = 8$ at 256 MeV, while 32 points are necessary if the interval is not split.

C. Perturbation scheme

In order to treat the small πN channels, we choose the first order Alt-Grassberger-Sandhas (AGS) approximation which was applied successfully in the $n-d$ elastic scattering problem some years ago.[9] In this method, the kernel is split into a dominant part which is treated exactly and a weak part treated approximately. In Ref. 9, it is shown that the convergence condition for the AGS perturbation theory can be formulated entirely in terms of the weak part of the kernel. From a practical point of view, the first order AGS approximation is obtained when the weak part of the kernel is taken to be zero.

In our case, the dominant part corresponds to the $\pi-d$ and $N-\Delta$ channels, and the weak part involves all the $N-(\pi N)$ channels with the πN pair in the S or P states (except P_{11}) other than Δ. We therefore set equal to zero all the overlapping terms between these weak channels in the three-body kernel, i.e., we set $Z_{\alpha\beta} = 0$ for α and β not equal to d or Δ. So, a large amount of computing time (~ 30%) is saved compared with the exact calculation.

Of course, the full advantage of this method can be exploited only in the case where the system of equations is solved by means of the Padé approximant technique. We give in Table I the comparison between the exact and AGS results for two dominant scattering amplitudes T_{11}^J calculated at 142, 180, and 256 MeV with the $SF(6.7)-SP(S)$ interactions described hereafter in Sec. III. Clearly the AGS approximation is very good, the accuracy being of about 2%.

A different approximation is used in Ref. 3 where the small πN channels are introduced one at a time after the dominant part has been solved exactly. The choice of this method is imposed by the fact that the system of equations is solved by

TABLE I. Comparison of the first order AGS approximation with the exact calculation (in brackets) for two dominant scattering amplitudes. The T are dimensionless.

T_π (MeV)	T^{2+}_{33}	T^{2+}_{11}
142	$-12.976 - i28.190$	$-865.39 - i1138.4$
	$(-12.999 - i28.172)$	$(-856.72 - i1142.7)$
180	$5.657 - i56.747$	$-275.36 - i1421.0$
	$(5.630 - i56.733)$	$(-268.42 - i1420.4)$
256	$56.251 - i52.286$	$459.17 - i869.80$
	$(56.245 - i52.261)$	$(460.53 - i869.32)$

matrix inversion, so that the storage problems are crucial. The accuracy was determined to be at the 5% level for the dominant scattering amplitudes.

In what follows, all the calculations including the small πN channels (SP scheme) are done with the AGS approximation.

III. TWO-BODY INTERACTIONS

We describe in this section the relativistic πN and NN separable interactions used as input in our calculations.

A. Pion-nucleon interactions

For the S_{11}, S_{31}, P_{13}, P_{31}, and P_{33} πN channels, we use two sets of parametrizations constructed by Rinat et al.[3] (denoted hereafter R) and by Schwarz et al.[10] (denoted S).

In the R case, the parameters are fitted in each channel to the experimental phase shifts taken from the recent analysis of Rowe et al.[11] which provides a smooth "best" fit to all modern πN phase shifts determined by various groups for energies below 400 MeV.

In the S case, the parameters are fitted to the "experimental" phase shifts and scattering lengths. These values are rather old and correspond to the data chosen by Thomas[2] for fitting the πN inter-

actions in the RPK calculations. We note that in the P_{33} channel, the position of the resonance is imposed as an additional constraint in the fitting procedure.

The fits to the data are excellent as one can see in Fig. 3 of Ref. 3, and in Figs. 1 and 2 and Tables I–III of Ref. 10. We have recalculated the phase shifts and the scattering lengths for each set. The results are quite similar, the most apparent differences occurring in the P_{33} channel. This is illustrated in Table II where we give the scattering lengths for the two sets compared with the experimental values.

B. Nucleon-nucleon tensor forces

The simplest ${}^3S_1 - {}^3D_1$ parametrizations are the relativistic generalizations of Yamaguchi-type interactions described in Ref. 3, with P_D values 4 and 6.7% (denoted hereafter $Y4$ and $Y6.7$). The parameters are fitted to the ${}^3S_1$ phase shift only, without any constraint on the low energy parameters a_t (scattering length) and Q (quadrupole moment). We have calculated these quantities, which are found to be far from the correct values. For $Y4$ and $Y7$ we get, respectively, $a_t = 5.63$ and 5.79 fm (accepted value 5.40 fm), and $Q = 0.37$ and 0.40 fm^2 (accepted value 0.280 to 0.286 fm^2).

In order to improve the situation, we have constructed three sets of rank-1 interactions (denoted YL, S, and SF), using more elaborate form factors, and introducing in the fitting procedure more and more constraints.

For the YL potentials, we take the usual Yamaguchi form factors:

$$g_L(p) = C_L p^L / (p^2 + \beta_L^2)^{(L+2)/2}. \tag{2}$$

For the S and SF potentials we define the form factors as a ratio of polynomials:

$$g_L(p) = C_L p^L (1 + \gamma_L p^2) \bigg/ \prod_{i=0}^{L+2} (1 + \beta_{Li} p^2). \tag{3}$$

The parameters are adjusted to fit the following

TABLE II. πN scattering lengths (in m_π^{-1} for S waves) and scattering volumes (in m_π^{-3} for P waves) for the Rinat (Ref. 4) and Schwarz (Ref. 10) parametrizations. The "new" experimental data are from Ref. 11, and the "old" are given in Refs. 9–11 of the Schwarz paper.

Parametrizations	Scattering length or volume				
	S_{11}	S_{31}	P_{13}	P_{31}	P_{33}
R	0.172	−0.092	−0.013	−0.039	0.170
S	0.170	−0.091	−0.016	−0.036	0.211
Exp. (old)	0.174	−0.092	−0.016	−0.037	0.220
Exp. (new)	0.185	−0.098	−0.013	−0.029	0.205
	±0.008	±0.003	±0.002	±0.002	±0.050

quantities

(i) For the YL potentials, we impose only the static parameters, namely the deuteron binding energy $E_D = 2.2245$ MeV, the triplet scattering length $a_t = 5.40$ fm, the quadrupole moment $Q = 0.285$ fm^2, the D-state probability P_D, and the ratio of the D to S asymptotic deuteron wave functions $\eta = 0.026$.

(ii) For the S parametrizations, the $^3S_1$ phase shift up to 200 MeV is added to the foregoing constraints.

(iii) For the SF interactions, we impose one more constraint, namely the monopole form factor of the deuteron $F_0(q^2)$ up to $q \sim 6$ fm^{-1}. We choose to fit the Reid soft-core (RSC) form factor which has a minimum at $q \sim 4.5$ fm^{-1}.

In each set, two parametrizations are constructed with $P_D = 4$ and 6.7%. The parameters for the S and SF interactions are given in Table III. For the YL potentials, the values of $(C_0, \beta_0; C_2, \beta_2)$ are (124.707, 1.329; 220.795, 1.559) for $YL4$, and (98.941, 1.261; 446.940, 1.970) for $YL7$ (the C are in fm^{-2} and β in fm^{-1}).

We show in Fig. 1 the $^3S_1$ phase shift for the various interactions with $P_D = 6.7$%, and in Table IV we give the monopole form factors compared with the Reid soft-core values. The phase shift for the SF interaction is not as good as for the S interaction above 100 MeV, but the form factor is much better for $q > 2$ fm^{-1}. We think that the SF interactions are therefore more "realistic" in the sense that the fitting procedure to $F_0(q)$ ensures the correct behavior of the deuteron wave function. Let us point out that the $SF6.7$ potential is the relativistic equivalent to the Pieper rank-1 potential used in our RPK calculations.[1]

IV. RESULTS AND DISCUSSIONS

We have performed detailed calculations at 142, 180, 230, and 256 MeV in order to investigate the

FIG. 1. Theoretical $^3S_1$ phase shifts given by the Y ($—\cdot—$), YL ($—$ $—$ $—$), S (identical to YL), and SF ($—$) parametrizations for $P_D = 6.7$%. The experimental data are from Ref. 12.

sensitivity of πd observables to the NN and πN input. There are three subsections devoted, respectively, to the differential cross sections (A), the total cross sections (B), and the polarization parameters (C).

In what follows, each calculation is specified by two labels: The first one denotes the NN tensor force, and the second one refers to the πN channels which are retained (P_{33} or SP) and to the parametrization.

A. Differential cross sections

1. Effect of the small πN partial waves

The SP scheme consists in introducing with the AGS perturbation method the small πN channels S_{11}, S_{31}, P_{13}, and P_{31} in addition to P_{33}. As stated

TABLE III. Parameters for the S and SF tensor forces. The C_L are in fm^L and the β are in fm^2.

	$S4$	$S6.7$	$SF4$	$SF6.7$
C_0	76.832	64.530	66.508	58.659
γ_0	−0.0404	−0.0381	−0.231	−0.240
β_{01}	0.227	0.351	0.121	0.0494
β_{02}	0.252	0.190	0.118	0.241
C_2	37.038	31.362	33.057	27.562
γ_2	1.299	0.340	0.813	0.688
β_{21}	0.364	0.0217	0.216	0.0268
β_{22}	0.503	0.428	0.414	0.580
β_{23}	0.468	0.384	0.301	0.254
β_{24}	0.271	0.0794	0.424	0.262

TABLE IV. Monopole charge form factor of the deuteron $F_0(q)$ for the new tensor forces SF, S, and YL with $P_D = 6.7$%, compared with the Reid soft-core values.

q (fm^{-1})	RSC	SF	S	YL
0.2	0.975	0.975	0.975	0.975
1	0.616	0.614	0.618	0.623
2	0.257	0.254	0.269	0.283
3	0.0875	0.0877	0.112	0.129
4	0.0151	0.0190	0.0453	0.0614
5	−0.0120	−0.0600	0.0177	0.0308
6	−0.0188	−0.0127	0.0064	0.0163

37.

in the Introduction, we omit completely the P_{11}
channel. The reason is that the formalism we use
here does not include the effect of pion absorption,
so that the nucleon pole part which is the domi-
nant part cannot be introduced. On the other hand,
the P_{11} phase shift is very small up to 150 MeV,
and it seems reasonable to neglect its background
contribution. The latter assumption was checked
at 142 and 256 MeV. Using a separable paramet-
rization adjusted only to the P_{11} phase shift, the
πd observables calculated in the SP scheme with
and without the nonpole P_{11} contribution were found
to be almost identical.

We compare in Fig. 2 the differential cross
sections calculated at 142, 180, 230, and 256 MeV
in the SP and P_{33} schemes, with the $SF6.7$ tensor
force and the S parametrizations of the πN chan-
nels. The forward part of $d\sigma/d\Omega$ is lowered by
the SP scheme at energies below the resonance,
and is enhanced above the resonance, while the
backward part is systematically lowered. The
effect is very small at 180 MeV which is close
to the resonance. At all energies the SP scheme
improves significantly the agreement with experi-
mental data[13-16] throughout the angular range, ex-
cept at forward angles for $T_\pi = 230$ MeV. Never-
theless, the situation at 230 and 256 MeV is not
satisfactory, especially for $\theta_{c.m.} > 80°$, where the
broad minimum observed in the experiments is
not reproduced by the theory, which remains too
high. However, we do not understand the dis-
crepancy at forward angles with the experiment
of Cole et al.[15] at 230 MeV, since our theory de-
scribes correctly, in this angular range, the "old"
data at 142, 180, and 256 MeV as well as the pre-
liminary data of Gabathuler et al.[5] for $T_\pi = 140$ to
300 MeV. We can thus consider the possibility of
an incorrect normalization. In fact, if we enhance
Cole's results by a factor of 1.4, the theory be-
comes quite good. On the other hand, the recent
experiments of Ref. 5 seem to indicate that the
minimum at 256 MeV is not so deep, but the the-
ory still remains higher than experiment.

Let us briefly compare these results with the
RPK calculations using the Pieper tensor force
at 142 and 180 MeV [see Figs. 3(b) and 4(b) of
Ref. 1]. The FR and RPK differential cross sec-
tions look quite similar, demonstrating that rela-
tivistic effects are moderate at these energies.
We also note that the interference effects from
the small πN channels are smaller in the FR the-
ory than in RPK.

2. Sensitivity to the πN parametrizations

We compare in Table V the values of $d\sigma/d\Omega$ ob-
tained in the SP scheme with the S and R para-
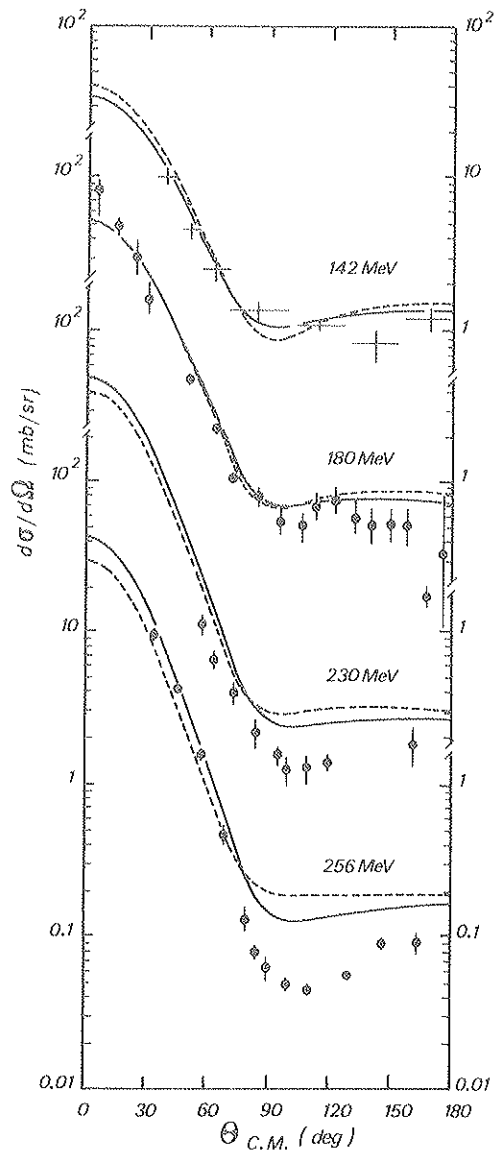
FIG. 2. πd elastic differential cross section at T_π
$= 142$ (Ref. 13), 180 (Ref. 14), 230 (Ref. 15), and 256
(Ref. 16) MeV calculated with the SF 6.7 tensor force
and the S parametrizations of the πN channels. $- - -$
only P_{33}, $——$ P_{33} : small πN waves, except P_{11}.

metrizations of the πN channels and the $SF6.7$ ten-
sor force, at $T_\pi = 180$ and 256 MeV. The R values
are slightly higher than the S results throughout
the angular range. However, the maximum varia-
tion does not exceed 13% at backward angles, re-
flecting that the two sets are nearly equivalent as
shown in Sec. III A.

3. Sensitivity to the NN tensor force

Now, the calculations are done in the SP scheme
with the S parametrizations of the πN channels.

TABLE V. Sensitivity of the differential cross section to the πN parametrizations. The numbers in each case are the values of $d\sigma/d\Omega$ in mb/sr, at $\theta_{c.m.}$ $=0°$, 90°, and 180°.

T_π (MeV)	S	R
	53.6	53.9
180	0.74	0.77
	0.73	0.77
	41.9	44.7
256	0.15	0.17
	0.16	0.18

First, we consider the influence of D-state probability. In order to study a genuine effect of P_D, we use our parametrizations which, in a given set (YL, S, or SF), differ only by their P_D values as explained in Sec. III B. The differential cross sections calculated at 180 and 256 MeV with the $SF4$ and $SF6.7$ interactions are given in Table VI. When P_D goes from 4 to 6.7%, the forward part of $d\sigma/d\Omega$ decreases by about 3%, and the backward part increases by 4% at 180 MeV and by 14% at 256 MeV. Similar conclusions hold with the $S4$ and $S6.7$ interactions, and also with the $YL4$ and $YL6.7$ potentials. These results show that the overall effect of P_D is rather small, while the large variation at backward angles found in Ref. 4 is not a genuine effect, but is due to the fact that the $Y4$ and $Y6.7$ interactions give different values for the low energy parameters as mentioned in Sec. III B.

Next, we investigate the sensitivity to the description of the deuteron wave function for a fixed P_D value. We use the YL, S, and SF interactions with $P_D = 6.7\%$. The variation of $d\sigma/d\Omega$ at forward angles is very small ($\sim 2\%$), but the backward part exhibits large variations (up to 25%). For example, the values of $d\sigma/d\Omega$ (180°) at 180 MeV are 0.97, 0.86, and 0.73 mb/sr for the YL, S, and SF tensor forces, respectively. Similar effects are observed at the other energies. If we remember

TABLE VI. Sensitivity of the differential cross section to the D-state probability. The numbers are ordered as in Table V.

T_π (MeV)	$SF4$	$SF6.7$
	54.9	53.60
180	0.78	0.74
	0.70	0.73
	43.3	41.9
256	0.16	0.15
	0.14	0.16

how we have constructed the YL, S, and SF interactions in Sec. III B, we see that the agreement of theory with experimental data at backward angles becomes better as we improve the description of the $^3S_1$-$^3D_1$ channel, namely with regard to the deuteron wave function. These considerations justify the systematic use throughout this paper of the SF interactions, even if they fail to reproduce the minimum for $T_\pi = 230$ and 256 MeV.

B. Elastic, reaction, and total cross sections

We have calculated the elastic (σ_{el}), reaction (σ_R), and total ($\sigma_T = \sigma_{el} + \sigma_R$) cross sections in the energy range 70 to 320 MeV with the $SF6.7$-$SP(S)$ interactions. In Fig. 3 we show our results and we compare the total cross section with the recent experimental data of Pedroni et al.[17] The agreement is fairly good, especially in the resonance region 140 MeV $< T_\pi < 260$ MeV where the theoretical curve goes through experiment. Outside this domain, the theoretical values are lower than experimental data, and the deviation increases when energy decreases from $T_\pi = 120$ MeV or increases from $T_\pi = 260$ MeV.

Compared with the RPK results (Fig. 5 or Ref. 1), the FR values of σ_T are better in a wider energy range. We also note a very good agreement with the calculations of Rinat et al.[3] without absorption. Our values for σ_T with the $SF6.7$-$SP(S)$ interactions at 142, 180, and 256 MeV are respectively 174, 230, and 135 mb, while the values of Rinat for $P_D = 6.7\%$ are 176, 239, and 146 mb. In fact, we have observed that the total cross section is rather insensitive to the two-body input.
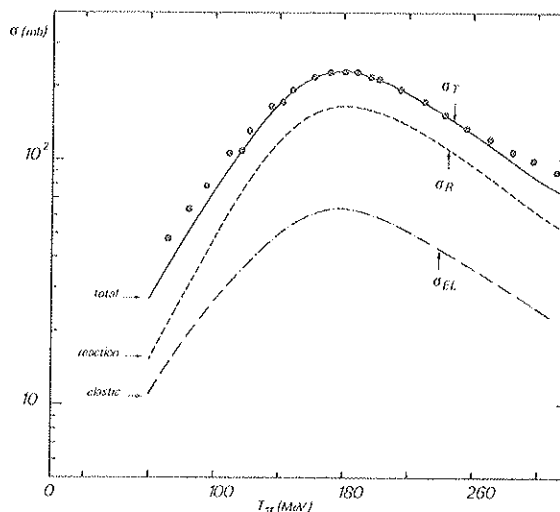

FIG. 3. Elastic (—·—), reaction (— — —), and total (——) cross sections calculated with the SF 6.7-$SP(S)$ interactions. The experimental results are from Pedroni et al. (Ref. 17).

C. Polarization parameters

The vector polarization it_{11} and the tensor polarizations t_{20}, t_{21}, and t_{22} for $\pi + d \to \pi + \tilde{d}$ elastic scattering are easily calculated from the scattering amplitudes. The qualitative effects noted in the RPK approach are also observed in the FR calculations, only the numbers change more or less. We limit thus the present discussion to the most important aspects.

The complete change in structure of it_{11} due to the inclusion of the small πN partial waves in addition to P_{33} is observed at all energies. The FR curves look similar to the RPK curves shown in Fig. 6 of Ref. 1. The vector polarizations calculated in the SP scheme have a pronounced maximum which has the following characteristics: (i) the position is nearly independent of energy and of the two-body input and corresponds to $\theta_{c.m.} = 80°$, and (ii) the magnitude is practically independent of the πN and NN input, but varies with energy; namely, it is maximum around $T_x = 180$ MeV. For example, the values of it_{11} $(80°)$ obtained with the SF6.7–SP(S) interactions at 142, 180, 230, and 256 MeV are respectively 0.43, 0.45, 0.40, and 0.36.

In contrast with it_{11}, the tensor polarizations are only slightly affected when we include the small πN channels (the difference between the SP and P_{33} results is less than 5%) or when we change the πN parametrizations from S to R (the effect is ~2%). Of course, the most important variations in the tensor polarizations are due to the NN tensor force. We discuss only the quantity t_{20} which presents an immediate interest. The angular distributions of t_{20} have the same aspect as in the RPK theory (see Fig. 7 of Ref. 1), and the values of t_{20} $(180°)$ calculated with the SF6.7–SP(S) interactions at 142, 180, 230, and 256 MeV are respectively –0.74, –1.08, –1.26, and –1.27. The polarization $t_{20}(180°)$ behaves as follows. (i) It decreases with increasing D–state probability; we give in Table VII the values obtained with the SF4 and SF6.7 tensor forces at 142, 180, and 256 MeV. (ii) It depends on the description of the deuteron wave function; for instance, the results at $T_x = 180$ MeV corresponding to the SF, S, and YL interactions with the same P_D value (6.7%) are

TABLE VII. Sensitivity of t_{20} (180°) to the D–state probability.

T_x (MeV)	SF 4	SF 6.7
142	–0.63	–0.74
180	–0.92	–1.08
256	–1.17	–1.27

respectively –1.08, –0.96, and –0.90. These variations are therefore of the same order as the variations coming from different P_D values. Recently, t_{20} (180°) was observed for the first time at $T_x = 140$ MeV by Holt et al.,[7] the value being –0.24±0.15. The theoretical values obtained with the most elaborate tensor forces, namely the SF interactions, still remain far from this result since we find –0.74 for $P_D = 6.7\%$ and –0.61 for $P_D = 4\%$.

V. CONCLUDING REMARKS

We have presented an extensive analysis of πd elastic scattering observables in the resonance region within a fully relativistic three-body theory. The small πN channels have been included to an excellent degree of accuracy through the AGS perturbation method, and the numerical integration has been refined in order to save computing time without losing accuracy. Since the theory we used did not include the effects of pion absorption, the P_{11} πN channel was completely omitted.

The great sensitivity of πd observables (namely the differential cross section and the t_{20} polarization at large angles) to the details of the two-body input that was demonstrated in previous RPK calculations[1] is still observed in the FR approach. The agreement between the theoretical and experimental differential cross sections is significantly improved when the small πN channels are included and when a tensor force giving a realistic deuteron wave function is used.

Let us note here that the differences between the present calculations and those of Rinat et al.,[3] without absorption, are moderate. Seeing that the two sets of πN interactions used in each calculation are nearly equivalent, it is clear that the differences must be attributed to the tensor forces. Figure 6 of Ref. 3 gives a spectacular illustration of the model dependence of $d\sigma/d\Omega$ at backward angles relative to the deuteron wave function. The variations corresponding to different tensor forces are found to be as important as the variations due to the inclusion of absorption effects. Our main effort in the present work was to produce pure three–body calculations based on a tensor force having the maximum degree of quality. So, we have now a sound reference for further theoretical investigations. We think that the SF parametrizations that we have constructed represent a real improvement compared with the tensor forces used up to now. Of course, they have some defects deriving from their structure: The SF interactions are of rank 1, and therefore the ${}^3S_1$ phase shift remains positive and the ${}^3D_1$ phase shift has the wrong sign. These difficulties

should be removed by considering rank 2 parametrizations. However, from our experience in the RPK approach with the Pieper rank-1 and rank-2 interactions (they have the same deuteron wave function but differ by their $^3D_1$ phase shifts, and they give nearly the same πd observables), we think that this step is not essential.

None of our calculations do reproduce the minimum in the differential cross sections which is observed in the experiments at 230 and 256 MeV, and it seems now clear that the two-body input is not responsible for this discrepancy. Besides the apparent need to reconfirm the experimental data, we have now to consider further theoretical investigations. At first, we must include the effects of absorption. Detailed calculations have been recently performed in this direction by Rinat et al.[3] within a field-theoretical formulation including genuine pion absorption and ρ-meson exchange. The effects of absorption induce significant changes in the large angle differential cross section, but they do not produce the deep minimum at 256 MeV. On the other hand, absorption has a tremendous influence on all polarization parameters; for example, t_{20} $(180°)$ becomes small positive at 142 MeV. An independent calculation of πd elastic scattering including π absorption is now in progress in our group, based on the approach to the theory of coupled πNN-NN systems recently developed by Avishai and Mizutani.[18] Also the effects of inelasticity in the πN partial waves may be important[19] (mainly in the P_{11} channel) in accounting for the minimum in the cross section at 256 MeV. Another direction concerns the inclusion of dibaryon resonances, but here the situation is not clear. For some people,[20] the resonant amplitude (the $^3F_3$ NN for instance) must be added to the πd elastic scattering amplitude, while for others[21] the πNN system itself is resonant and the inclusion of the NN $(^3P_2)$ and πN $(P_{11}$ and $P_{33})$ leads to a resonant $^3F_3$ wave.

Finally, we think that the new experimental data which ought to appear in the near future will be decisive for further theoretical work.

ACKNOWLEDGMENTS

[1] N. Giraud, Y. Avishai, C. Fayard, and G. H. Lamot, Phys. Rev. C 19, 465 (1979); Phys. Lett. 77B, 141 (1978); N. Giraud, G. H. Lamot, and C. Fayard, Phys. Rev. Lett. 40, 438 (1978).

[2] A. W. Thomas, Nucl. Phys. A258, 417 (1976).

[3] A. S. Rinat, Y. Starkand, E. Hammel, and A. W. Thomas, Phys. Lett. 80B, 166 (1979); Nucl. Phys. A329, 285 (1979).

[4] A. S. Rinat and A. W. Thomas, Nucl. Phys. A282, 365 (1977).

[5] K. Gabathuler et al. (private communication).

[6] W. Grüebler et al., SIN proposal R-73-01.1.

[7] R. J. Holt, J. R. Specht, E. J. Stephenson, B. Zeidman, R. L. Burman, J. S. Frank, M. J. Leitch, J. D. Moses, M. A. Yates-Williams, R. M. Laszewski, and R. P. Redwine, LAMPF report, 1979.

[8] A. Stanovnik et al., in Proceedings of the 2nd Conference on Meson-Nuclear Physics, Houston, 1979.

[9] G. Bencze and P. Doleschall, Phys. Lett. 44B, 235 (1973).

[10] K. Schwarz, H. Zingl, and L. Mathelitsch, Phys. Lett. 83B, 297 (1979).

[11] G. Rowe, M. Salomon, and R. H. Landau, Phys. Rev. C 18, 584 (1978).

[12] M. H. MacGregor, R. A. Arndt, and R. M. Wright, Phys. Rev. 182, 1714 (1969).

[13] E. G. Pewitt, T. H. Fields, G. B. Yodth, J. G. Fetkovich, and M. Derrick, Phys. Rev. 131, 1826 (1963).

[14] J. H. Norem, Nucl. Phys. B33, 512 (1971).

[15] R. H. Cole, J. S. MacCarthy, R. C. Minehardt, and E. A. Wadlinger, Phys. Rev. C 17, 681 (1978).

[16] K. Gabathuler, C. R. Cox, J. J. Domingo, J. Rohlin, N. W. Tanner, and C. Wilkin, Nucl. Phys. B55, 397 (1973).

[17] E. Pedroni, K. Gabathuler, J. J. Domingo, W. Hirt, P. Schwaller, J. Arvieux, C. H. Q. Ingram, P. Gretillat, J. Piffaretti, N. W. Tanner, and C. Wilkin, Nucl. Phys. A300, 321 (1978).

[18] Y. Avishai and T. Mizutani, Nucl. Phys. A326, 352 (1979), and Saclay report, 1979.

[19] J. T. Londergan, K. W. McVoy, and E. J. Moniz, Ann. Phys. (N.Y.) 86, 147 (1974).

[20] K. Kubodera, M. P. Locher, F. Myhrer, and A. W. Thomas, in Proceedings of the 8th International Conference on High Energy Physics and Nuclear Structure, Vancouver, 1979.

[21] M. Araki, Y. Koike, and T. Ueda, Osaka University Report No. 79-9-6 (unpublished).

Article I-5

Correlation between Backward πd Elastic Scattering and Deuteron Form Factor.

G. H. Lamot, N. Giraud and C. Fayard

Institut de Physique Nucléaire (et IN2P3), Université Claude Bernard Lyon-1
43, Bd. du 11 Novembre 1918, 69622 Villeurbanne Cedex, France

Summary. — We show the great sensitivity of the πd elastic-scattering observables to the details of the deuteron wave function. At 142 MeV and 256 MeV we find that the differential cross-section at $\theta_{c.m.} = 180°$ depends linearly upon the quantity $A(q^2)$, which is the most important part of the deuteron electromagnetic form factor. A similar behaviour appears for the tensor polarization $t_{20}(180°)$ at 142 MeV. Our results are compared with existing experimental data at backward angles.

1. – Introduction.

In the past few years the three-body equations appear to be a very useful tool in the understanding of the experimental data relative to πd elastic scattering. Various calculations have been performed at different levels of sophistication with respect to the treatment of relativistic effects and to the two-body input. We will restrict there the discussion to the resonance region ($T_{\pi\,lab}$ from 140 to 260 MeV). The first fully relativistic (FR) calculations [1] included only the $P_{33}(\Delta)$ πN channel and the $^3S-^3D_1$ NN channel, the parametrization of the latter being of simple Yamaguchi type. Next, the model has been refined in many aspects.

---

[1] A. S. Rinat and A. W. Thomas: *Nucl. Phys. A*, **282**, 365 (1977).

i) The small S and P πN channels were introduced in addition to the dominant P_{33}, exactly or within a perturbation scheme. This was done at first in the semi-relativistic approach ([2]) using relativistic kinematics for the pion only (RPK), and next in the FR approach ([3,4]).

ii) The Yamaguchi tensor forces being very poor, more elaborated parametrizations giving a realistic deuteron wave function were used, both in the RPK ([2]) and FR ([3,4]) calculations.

iii) The genuine effects of π absorption and emission were recently taken into account in the FR approach ([3]) by introducing only the nucleon pole part of the P_{11} channel.

The corresponding theoretical results have been compared with the available experimental data, namely the elastic differential cross-sections $d\sigma/d\Omega$ at 142 MeV ([5]), 180 MeV ([6]), 230 MeV ([7]) and 256 MeV ([8]). Moreover, the polarization parameters were predicted.

The general conclusion is that the πd observables are strongly dependent on the details of the two-body input, namely the effect of the small πN channels is noticeable throughout the angular range, and the backward part of $d\sigma/d\Omega$ is very sensitive to the description of the deuteron wave function. The best agreement with experiments is obtained when conditions i) and ii) above are fulfilled. However, significant differences between theory and experiments at backward angles appear beyond 180 MeV, and the discrepancy increases with increasing energy. The most striking fact is that the minimum in $d\sigma/d\Omega$ (near $\theta_{c.m.} = 100°$) at 256 MeV is not reproduced by the theory, even if a realistic tensor force is used or if absorption is included.

In this paper, we want to investigate the strong dependence of the backward parts of $d\sigma/d\Omega$ and t_{20} on the details of the tensor force. If we consider the πd elastic scattering at $T_\pi = 142$ MeV, the incident pion transfers to the deuteron a momentum with maximum value $q_{max} \sim 2$ fm^{-1}. Thus the pion can probe the deuteron wave function at rather large momenta, i.e. at short distances. It is thus clear that the πd observables must depend on the behaviour

([2]) N. GIRAUD, Y. AVISHAI, C. FAYARD and G. H. LAMOT: Phys. Rev. C, 19, 465 (1979).

([3]) A. S. RINAT, Y. STARKAND, E. HAMMEL and A. W. THOMAS: Nucl. Phys. A, 329, 285 (1979).

([4]) N. GIRAUD, C. FAYARD and G. H. LAMOT: Phys. Rev. C (to appear).

([5]) E. G. PEWITT, T. H. FIELDS, G. B. YODH, J. G. FETKOVICH and M. DERRICK: Phys. Rev., 131, 1826 (1963).

([6]) J. H. NOREM: Nucl. Phys. B, 33, 512 (1971).

([7]) R. H. COLE, J. S. MACCARTHY, R. C. MINEHARDT and E. A. WADLINGER: Phys. Rev. C, 17, 681 (1978).

([8]) K. GABATHULER, C. R. COX, J. J. DOMINGO, J. ROHLIN, N. W. TANNER and C. WILKIN: Nucl. Phys. B, 55, 397 (1973).

of the deuteron wave function. In order to study this dependence, we consider various types of tensor forces. As the information on the deuteron wave function is not directly tractable, we refer to the deuteron electromagnetic form factor $A(q^2)$, and we demonstrate the existence of a strong correlation between this quantity and the πd observables at backward angles.

In sect. 2 we describe the relativistic NN parametrizations we have used. Some of them are extracted from the literature [9], while we have constructed the others in order to improve the description of the $^3S_1$-$^3D_1$ channel. The main characteristics of these interactions are given, namely the static properties, phase shifts and electromagnetic form factors. Section 3 is devoted to the πd observables calculated in the FR approach at 142 and 256 MeV with the various tensor forces. We take into account only the P_{33} πN channel and we neglect the « small » S and P πN partial waves. We have shown recently [4] that the backward part of $d\sigma/d\Omega$ is lowered up to 20 % when these channels (except P_{11}) are introduced in addition to P_{33}. We can thus consider that the results obtained with P_{33} alone should be purely translated if the other πN channels are introduced. The problem of including the P_{11} channel is more complicated, since it contains the process of pion absorption and emission, and we devote it for a further investigation. Finally, we give our conclusions in sect. 4.

2. – Parametrization of the tensor force.

We use rank-one separable $^3S_1$-$^3D_1$ interactions which satisfy the relativistic Blankenbecler-Sugar integral equation. These interactions cannot reproduce the change of sign in the $\delta(^3S_1)$ phase shift at ~ 300 MeV, and they give a $\delta(^3D_1)$ phase shift with the wrong sign. However, these defects are not really important in the case of πd scattering at energies around the (3, 3) resonance. Indeed, the corresponding maximum relative energy of the two nucleons (on shell) is less than 100 MeV and $\delta(^3S_1) \gg \delta(^3D_1)$ in this domain. Let us note that these considerations are supported by numerical results: we have shown in the RPK approach [2] that the Pieper rank-1 and rank-2 tensor forces [10] (they have the same static properties and the same deuteron wave functions, but the rank-2 interaction gives a correct $\delta(^3D_1)$) lead to nearly equivalent πd observables at 142 and 180 MeV, the differences being at most 3 %.

We have used four sets of parametrizations denoted respectively YLx, Sx, QTx and SFx. Here x stands for the P_D value, and the order corresponds to an improved description of the $^3S_1$-$^3D_1$ channel. The QT parametrizations

[9] E. HAMMEL, H. BAIER and A. S. RINAT: *Phys. Lett. B*, **85**, 193 (1979); E. HAMMEL and H. BAIER: *Nuovo Cimento A*, **53**, 359 (1979).
[10] S. C. PIEPER: *Phys. Rev. C*, **9**, 883 (1973).

are from HAMMEL et al. ([9]), while we constructed the YL, S and SF potentials ([4]). Let us briefly describe their main characteristics.

i) For YL interactions, we use Yamaguchi form factors:

$$(1) \qquad g_L(p) = C_L p^L / (p^2 + \beta_L^2)^{(L+2)/2} .$$

The parameters are adjusted to fit the static properties, namely the deuteron binding energy E_D, the triplet scattering length a_t, the quadrupole moment Q, the D-state probability P_D and the ratio ϱ_D of the D to S asymptotic deuteron wave functions.

ii) For the S interactions, we take form factors which are ratio of polynomials:

$$(2) \qquad g_L(p) = C_L p^L (1 + Y_L p^2) / \prod_{i=1}^{L+1} (1 + \beta_{Li} p^2).$$

The parameters are fitted to the $^3S_1$ phase shift up to 200 MeV in addition to the static properties.

iii) For the SF potentials, we also use the above form factors given in eq. (2). Now, the parameters are adjusted as in the S case with one more constraint, namely the monopole (charge) form factors of the deuteron $G_C(q^2)$ up to $q \sim 6$ fm^{-1}. We choose to fit the Reid soft-core (RSC) form factor which as a minimum at $q \sim 4.5$ fm^{-1}.

iv) HAMMEL et al. ([9]) choose form factors of Tabakin type (denoted QT). For $L = 0$ and 2, they read, respectively,

$$(3) \qquad g_0(p) = (p^2 - p_c^2)/(p^2 + \beta_0^2)^2 ,$$

$$(4) \qquad g_2(p) = p^2/(p^2 + \beta_2^2)^2 .$$

These interactions were constructed to investigate the relativistic corrections on three-nucleon observables. The values of p_c were varied in order to change the position of the minimum in $G_C(q^2)$, but it appears that the other characteristics were not kept constant (see table I).

The parameters of the QT interactions are given in ref. ([9]) and those of YL, S and SF can be found in ref. ([4]). In each case, different parametrizations are available corresponding to P_D values around 4 and 6.5%.

We summarize in table I their properties. The upper part of the table gives the values of the static parameters, and the lower part shows the $\delta(^3S_1)$ phase shifts at 10, 50, 100 and 200 MeV laboratory energy. It is clear that the YL, S and SF potentials are equivalent with respect to the quantities a_t, Q and ϱ_D, while this is not the case for the QT interactions. Moreover, our S and SF

TABLE I. – Characteristics of the $^3S_1$-$^3D_1$ channel for the YL, S, SF and QT interactions (for the latter, the number in brackets refers to p_0, eq. (3) in the text). The upper part of the table gives the low-energy parameters and the lower part the $^3S_1$ phase shifts.

	YL 4	YL 6.7	S 4	S 6.7	SF 4	SF 6.7	QT 4.6 (0.372)	QT 6.4 (0.372)	QT 4.1 (0.343)	QT 6.1 (0.343)	QT 4.1 (0.306)	Experimental
P_D (%)	4.0	6.7	4.0	6.7	4.0	6.6	4.6	6.4	4.1	6.0	4.0	3÷7
a_t (fm)	5.40	5.40	5.41	5.41	5.39	5.40	5.41	5.34	5.48	5.50	5.68	5.39
Q (fm²)	0.282	0.281	0.286	0.286	0.285	0.287	0.349	0.447	0.352	0.455	0.367	0.286
$\varrho_D = A_D/A_S$	0.028	0.026	0.026	0.026	0.027	0.025	0.037	0.054	0.038	0.052	0.037	0.026
$T_{N \text{lab}}$ (MeV)												
10	103.2	103.3	102.8	102.9	102.9	102.9	102.5	104.3	101.2	101.1	97.2	102.1
50	65.1	67.4	62.8	64.5	61.4	62.9	59.2	60.8	56.0	54.7	47.9	60.7
100	45.6	49.1	40.0	43.6	36.3	38.3	32.5	31.8	28.5	24.8	19.2	40.9
200	25.2	22.5	17.3	16.1	10.0	7.7	6.4	6.3	3.1	2.2	0.0	17.0

parametrizations give better $\delta(^3S_1)$ than QT, especially at energies above 50 MeV. The best fit to experimental data [11] is given by the S potentials which are not constrained to reproduce $G_C(q^2)$.

Let us now comment on the characteristics linked to the electron-deuteron elastic scattering. As usual, the cross-section is written as [12]

$$(5) \qquad \left(\frac{d\sigma}{d\Omega}\right)_{lab} = \left(\frac{d\sigma}{d\Omega}\right)_{Mott} \left[A(q^2) + B(q^2)\, tg^2\frac{\theta}{2}\right],$$

where θ is the scattering angle, and

$$(6) \qquad A(q^2) = G_C^2(q^2) + \frac{8}{9}\,\eta^2\,G_Q^2(q^2) + \frac{3}{2}\,\eta(1+\eta)\,G_M^2(q^2)\,,$$

$$(7) \qquad B(q^2) = \frac{4}{3}\,\eta(1+\eta)^2\,G_M^2(q^2)\,.$$

The η-variable is expressed in terms of the momentum transfer q and the deuteron mass M_d as $\eta = q^2/4\,M_d^2$, and the functions G_C^2, G_Q^2 and G_M^2 are, respectively, the charge, quadrupole and magnetic form factors of the deuteron. In the range of momentum transfer we are interested in, we have $G_C^2 \gg G_Q^2 \gg G_M^2$. However, we keep the three terms in eq. (6) for evaluating $A(q^2)$. The quantity $A(q^2)$ has been measured in various experiments [13] in the q range $(0 \div 6)$ fm^{-1}. The theoretical results for the various interactions are found to be widely dispersed. As an example, we give in table II the values of $A(q^2)$ at $q = 2$ fm^{-1}, which is the region of interest for our further investigations. We note that the dispersion within a given set of interaction is smaller than the dispersion between the various sets. We also note that the QT results do not overlap with the others and are systematically lower (this behaviour is observed at any q value). Comparing with the experimental data (0.033) and with the RSC value (0.036), we conclude that the S and SF interactions are reliable in this region.

Another interesting quantity is the monopole form factor of the deuterons $F_0(q^2)$, which is linked to the charge form factor $G_C(q^2)$ through

$$(8) \qquad G_C(q^2) = F_0(q^2)\, G_{ES}(q^2)\,,$$

where $G_{ES}(q^2)$ is the nucleon form factor. We known that $|F_0(q^2)|$ has a minimum at an accepted value $q_+ \sim (4 \div 5)$ fm^{-1}, reflecting the fact that the $^3S_1$ $\mathcal{N}\mathcal{N}$

[11] M. H. MacGregor, R. A. Arndt and R. M. Wright: *Phys. Rev.*, **182**, 1714 (1969).
[12] M. Gourdin: *Diffusion des électrons de haute énergie* (Paris, 1966).
[13] S. Galster, H. Klein, J. Moritz, K. H. Schmidt, D. Wegener and J. Bleckwenn: *Nucl. Phys. B*, **32**, 221 (1971), and references therein.

TABLE II. – *Some two- and three-body characteristics for the various tensor forces. The upper part of the table gives the position q_+ of the minimum of $|F_0(q^2)|$ and $A(q^2)$ at $q = 2$ fm^{-1}. The middle and lower parts concern the πd observables at 142 MeV, namely the differential cross-section and tensor polarization t_{20} at $\theta_{c.m.} = 180°$, and the total and elastic cross-sections.*

	YL 4	YL 6.7	S 4	S 6.7	SF 4	SF 6.7	QT 4.6 (0.372)	QT 6.4 (0.372)	QT 4.1 (0.343)	QT 6.1 (0.343)	QT 4.1 (0.306)
q_+ (fm^{-1})	∞	∞	> 10	8.4	4.7	4.7	4.4	4.5	4.2	4.1	3.7
A ($q = 2$ fm^{-1})	0.039	0.040	0.035	0.036	0.032	0.033	0.030	0.030	0.026	0.024	0.019
$d\sigma/d\Omega$ (0°)	40.2	39.4	40.9	39.9	40.8	40.1	40.7	40.2	40.9	41.4	42.2
$d\sigma/d\Omega$ (180°)	1.88	1.84	1.71	1.68	1.50	1.46	1.31	1.34	1.09	1.05	0.74
t_{20} (180°)	-0.52	-0.63	-0.59	-0.66	-0.63	-0.74	-0.71	-0.81	-0.75	-0.91	-0.93
σ_{tot} (mb)	169.5	166.8	170.8	167.8	169.7	167.2	168.9	167.3	169.0	170.3	172.2
σ_{el} (mb)	61.4	59.5	61.4	59.3	60.4	58.5	58.8	58.2	57.4	57.0	55.3

47.

phase shift has a zero at laboratory energy ~ 300 MeV. This is a fundamental constraint, if one wants to construct a «realistic» interaction. In that sense, even if they give reasonable values for the other characteristics, the YL and S parametrizations are incorrect, since there is no zero in $F_0(q^2)$ for YL, and the zero is at $q > 8$ fm^{-1} for the S interactions. We give in table II the values
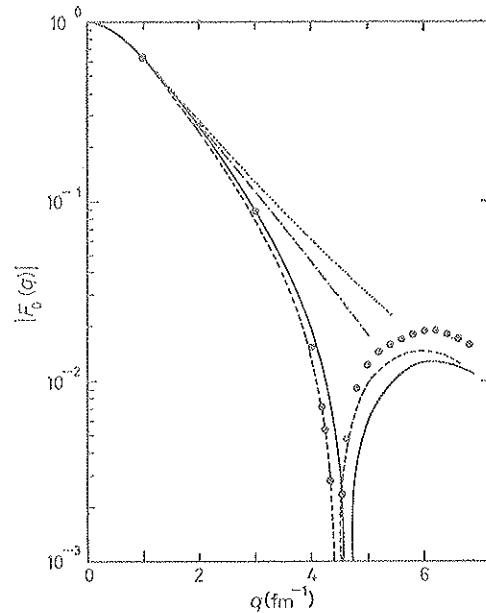
Fig. 1. – Monopole charge form factor of the deuteron $|F_0(q)|$ for the YL ($\cdots$), S (— · — · —), SF (———) and QT (— — —) interactions with $P_D = 6.7\%$. The points correspond to the Reid soft-core local interaction.

of q_+ where $F_0(q^2)$ changes sign for the various parametrizations. In fig. 1 we show some typical curves obtained with the YL, S, SF and QT parametrizations for $P_D = 6.7\%$, using the nucleon form factor of Galster et al. [13]:

$$G_{ES}(q^2) = (1 + q^2/18.234)^2 .$$

We also compare with the values given by the RSC interaction.

3. – πd observables at 142 MeV and 256 MeV.

In this section we investigate the connection between the πd observables and $A(q^2)$. We concentrate on quantities which are known to be very sensitive to the description of the NN tensor force, namely the backward parts of

$d\sigma/d\Omega$ and of the tensor polarization t_{20}. As explained in the introduction, all these calculations are performed within the fully relativistic approach, and we take into account only the $^3S_1$-$^3D_1$ NN channel and the P_{33} πN channel. For the latter, we use the parametrization of Schwarz et al. [14], which is fitted to the phase shifts and to the scattering volume $a_{P_{33}} = -0.21 m_\pi^{-3}$.

The differential cross-sections obtained at 142 MeV with the various interactions lie within the dashed area shown in fig. 2. The values of $d\sigma/d\Omega$ at
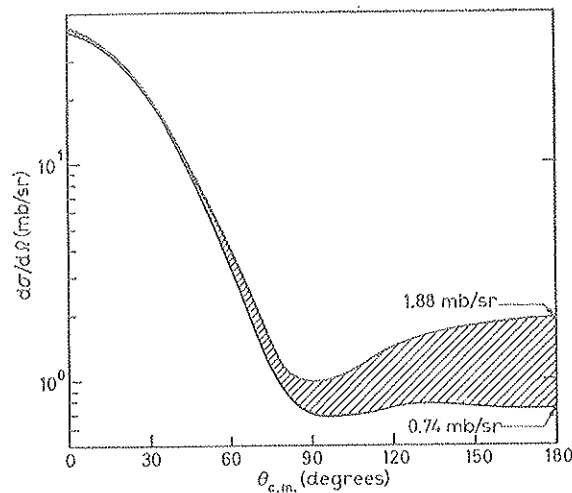

Fig. 2. — πd elastic differential cross-section at 142 MeV. All the angular distributions obtained with the interactions described in the text lie within the shaded area.

$\theta_{c.m.} = 0°$ and 180° are specified in table II. We notice the stability of the forward part of $d\sigma/d\Omega$ and the tremendous variations of the backward part.

From table II, the variations of $d\sigma/d\Omega$ (0°) do not exceed 6%, while the maximum and the minimum values of $d\sigma/d\Omega$ (180°) corresponding, respectively, to the QT 4.1 ($p_c = 0.306$) and YL 4 interactions are in the ratio of 2.5. The backward part of the tensor polarization t_{20} is also strongly dependent on the tensor force, and the variations of $t_{20}(180°)$ given in table II are of the same order as for $d\sigma/d\Omega$ (180°). On the other hand, the elastic and total cross-section are rather model independent, as shown in the last two rows of table II (the variations are within 3% for σ_{tot} and 10% for σ_{el}).

If we refer to sect. 2, we see that the various sets of interactions differ mainly in the description of the deuteron form factor. It appears also from table II that the change in $d\sigma/d\Omega$ (180°) due to P_D in a given set is much smaller than the variations observed when one uses different sets at fixed P_D.

[14] K. SCHWARZ, H. ZINGL and L. MATHELITSCH: Phys. Lett. B, 83, 297 (1979).

Therefore, it is clear that the variations of $d\sigma/d\Omega$ and t_{20} at backward angles are connected with the behaviour of the deuteron form factor. The quantity which is directly available from experiment is $A(q^2)$. Thus we have plotted $d\sigma/d\Omega$ ($180°$) at $T_\pi = 142$ MeV as a function of $A(q^2_{max})$ for $q_{max} = 2$ fm^{-1}, which is the maximum value of the momentum transfer as explained before.

We see in fig. 3 that $d\sigma/d\Omega$ ($180°$) increases linearly with $A(q^2_{max})$. The straight line results from least-square fit, and we note that the points are distributed in pairs along this line with a small dispersion. Each pair corresponds to a type of interaction (for the QT potential with $p_0 = 0.306$ we have only one parametrization with $P_D = 4.1\%$). The small dispersion shows that
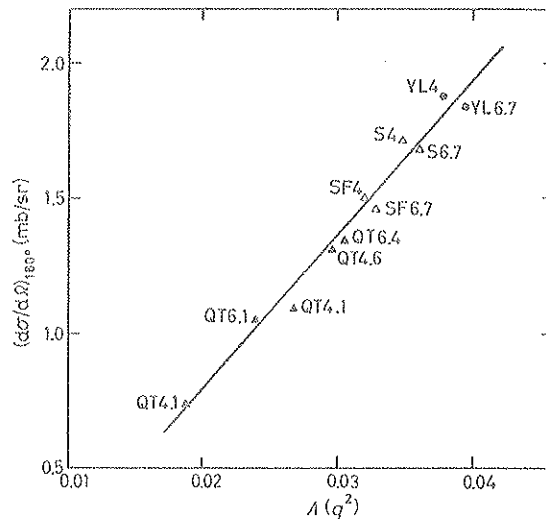

Fig. 3. − The backward differential cross-section $d\sigma/d\Omega$ ($180°$) at 142 MeV as a function of $A(q^2)$ ($q = 2$ fm^{-1}).
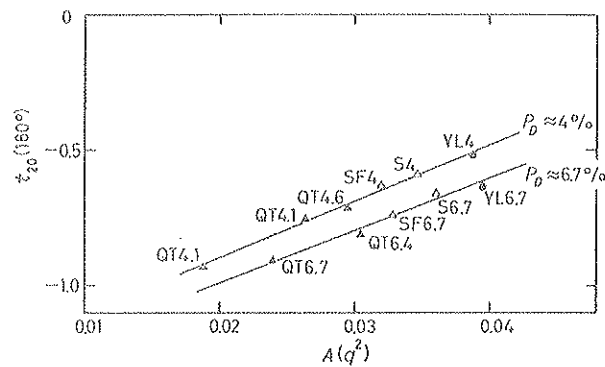

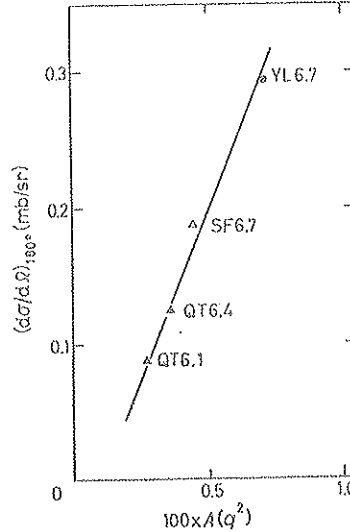Fig. 4. − The polarization t_{20} ($180°$) at 142 MeV as a function of $A(q^2)$ ($q = 2$ fm^{-1}).

Fig. 5. – The backward differential cross-section $d\sigma/d\Omega$ (180°) at 256 MeV as a function of $A(q^2)$ ($q = 2.8$ fm^{-1}).

$d\sigma/d\Omega$ (180°) is slightly sensitive to the D-state probability. Noticing that the value of $A(q^2_{max})$ induces the position of the minimum q_+ in the deuteron form factor (table II), we can also conclude that $d\sigma/d\Omega$ (180°) increases together with q_+, but the relation is not so simple as the above linear relation.

Likewise, the quantity $t_{20}(180°)$ at 142 MeV is a linear function of $A(q^2_{max})$ as shown in fig. 4. The points are distributed along two nearly parallel lines, each one corresponding to a given value of P_D. The two straight lines in fig. 4 represent least-square fits to the points corresponding, respectively, to $P_D \sim 4\%$ and $P_D \sim 6.7\%$. Their relative distance measures the sensitivity of $t_{20}(180°)$ to P_D.

A similar but less extensive analysis has been performed at $T_\pi = 256$ MeV, using the YL, QT and SF interactions with $P_D \sim 6.7\%$. Now the value q_{max} is ~ 2.8 fm^{-1}, and we show in fig. 5 $d\sigma/d\Omega$ (180°) as a function of $A(q^2_{max})$ for the chosen parametrization. The corresponding values are given in table III. As was the case at 142 MeV, $d\sigma/d\Omega$ (180°) increases linearly together with

TABLE III. – *Differential cross-section and polarization t_{20} at $\theta_{c.m.} = 180°$ calculated at 256 MeV with different tensor forces. The first row gives $A(q^2)$ at $q = 2.8$ fm^{-1}.*

	YL 6.7	SF 6.7	QT 6.4	QT 6.1
A ($q = 2.8$ fm^{-1})	7.01 (—3)	4.55 (—3)	3.7 (—3)	2.78 (—3)
$d\sigma/d\Omega$ (180°)	0.30	0.19	0.12	0.09
t_{20} (180°)	—1.07	—1.35	—1.36	—1.32

$A(q^2_{max})$, but the slope is smaller (~ 49 mb per unit of $A(q^2)$ at 256 MeV compared with ~ 57 mb at 142 MeV). The situation is not so clear for $t_{20}(180°)$. From table III we see that the three interactions which have a minimum in their deuteron form factor lead to identical values for $t_{20}(180°)$, while the YL 6.7 interaction gives a rather different result. Thus the linear variation noted at 142 MeV does not exist at 256 MeV. This may be understood by considering that at this energy there is a saturation effect in $t_{20}(180°)$, all interactions leading to values of $t_{20}(180°)$ close to the maximum value of this parameter, namely $|t_{20} \max| = \sqrt{2}$.

Now, a comparison of our results with experiment is in order. Let us consider at first the differential cross-section at 142 MeV. According to time ordering, there are four experiments by PEWITT et al. [5] ($40° < \theta_{c.m.} < 170°$), STANOVNIK et al. [15] ($130° < \theta_{c.m.} < 180°$), HOLT et al. [16] ($\theta_{c.m.} = 180°$) and GABATHULER et al. [17] ($0° < \theta_{c.m.} < 140°$). At forward angles ($0° < \theta_{c.m.} < 110°$), the agreement between the data of Pewitt and Gabathuler is good, but the various data do not overlap at backward angles. The results of Stanovnik do not match those of Gabathuler (at $\theta = (130 \div 135)°$ STANOVNIK gives (1.24 ± 0.16) mb, while GABATHULER gives (1.44 ± 0.07) mb at $\theta = 135°$), and they are appreciably higher than the old values of Pewitt. On the other hand, the results of Holt at 180° agree with the values of Stanovnik, provided that we omit in the latter the last point at $\theta = (170 \div 175)°$, which is outside the trend of data at smaller angles. The situation at $\theta_{c.m.} = 180°$ is summarized in table IV, where we have extrapolated «by hand» the data of Gabathuler. It seems reasonable to conclude that the experimental value of $d\sigma/d\Omega$ (180°) is somewhere in the range 1.4 to 1.7 mb/sr. If we now refer to table II and fig. 3, it appears that the results obtained with the S and SF parametrization lie within this experimental range. In fact, one must remember that our calculations do not include the interference effects from the small

TABLE IV. – *Differential cross-section at backward angles predicted by various experiments at 142 MeV.*

Experiment	$d\sigma/d\Omega$ (mb/sr)	$\theta_{c.m.}$ (degrees)
PEWITT [5]	1.2 ± 0.2	$165 \div 180$
STANOVNIK [15]	1.63 ± 0.18	$165 \div 170$
	1.37 ± 0.34	$170 \div 175$
HOLT [16]	1.58 ± 0.11	180
GABATHULER [17]	1.6 to 1.8	extrapolated

[15] A. STANOVNIK: private communication; K. Bos et al.: in *Proceedings of the II Conference on Meson Nuclear Physics* (Houston, Tex., 1979).

[16] R. J. HOLT et al.: LAMPF Report (1979).

[17] K. GABATHULER: private communication.

πN partial waves. We know from other works ([2,4]) that the small partial waves decrease the backward differential cross-section of about 10% at 142 MeV, so that the results in fig. 3 should be translated in this amount in the downward direction. With this correction, the S and SF results still remain within the experimental range. We know in addition the experimental value of $A(q^2_{max}) = 0.33$ for $q_{max} = 2$ fm^{-1}. We can thus conclude that only the SF parametrization does reproduce the experimental informationa bout $A(q^2_{max})$ and $d\sigma/d\Omega$ (180°).

At last, we consider the differential cross-section at 256 MeV. There are three experiments by GABATHULER et al. ([8]) ($0° < \theta_{c.m.} < 160°$), STANOVNIK et al. ([16]) ($130° < \theta_{c.m.} < 180°$) and again by GABATHULER et al. ([17]) ($0° < \theta_{c.m.} < 140°$) to confirm the first experiment. The results obtained by GABATHULER in the second experiment differ from the first ones only at backward angles ($\theta_{c.m.} > 90°$), where they are higher by nearly a factor 1.5, and the data of Stanovnik appear to match these data. For the latter, the value at $\theta = (135 \div 140)°$ is (0.099 ± 0.012) mb, while GABATHULER gives (0.105 ± 0.006) mb at the last point $\theta = 138°$. However, the data of Gabathuler exhibit a broad minimum around $\theta = 110°$, and it would be hazardous to extrapolate them at 180° (this was not the case at 142 MeV, where the minimum was not so well marked). Therefore, we will take as experimental datum for $d\sigma/d\Omega$ (180°) the value of Stanovnik at $\theta = (170 \div 175)°$, which bears a large error, namely 0.178 ± 0.059. The experimental value of $A(q^2_{max})$ at $q \sim 2.8$ fm^{-1} is 0.0035 and it appears from fig. 5 that no interaction does reproduce simultaneously the experimental information. The SF 6.7 interaction has a too large $A(q^2)$ and a correct $d\sigma/d\Omega$ (180°), while the situation is opposite for the QT 6.4 potential. Moreover, the small πN partial waves lead to a decrease of about 16% in the backward differential cross-section at 256 MeV as shown in ref. ([4]), so that the SF 6.7 results still remain within experiment, while the QT 6.4 results become too small. In fact, it is not very significant to restrict the discussion to the value of $d\sigma/d\Omega$ at 180°. The main problem at 256 MeV concerns the broad minimum observed in the angular range 80° to 140°, which is so far not reproduced by any theory.

4. – Conclusion.

We have demonstrated the existence of a strong correlation between the deuteron form factor and the πd observables $d\sigma/d\Omega$ and t_{20} at backward angles. The sensitivity of these quantities to the description of the NN tensor force was pointed out in ref. ([4]) in a qualitative manner, but now we have quantitative features relative to various interactions.

The model used here is very simple, since the effects of absorption are not included, and we omit the small πN partial waves. In order to compare with

458   G. H. LAMOT, N. GIRAUD and C. FAYARD

experiment, we have estimated the contribution of the small πN channels from our previous work ([4]). However, the experimental situation for the differential cross-section at backward angles is not completely clear, especially at 256 MeV, where other experiments would be highly appreciated in addition to those of Stanovnik et al. The interesting fact is that the best agreement between theory and experiment at 142 MeV and 256 MeV is obtained by using the SF potentials, which gives a better overall description of the NN channel than the other interactions. We point out that this conclusion is valid for the whole angular distributions, even if the experimental minimum at 256 MeV is not reproduced by the theory, which remains too high with respect to experiment (concerning this point, it appears that a better tensor force does not improve the situation).

The polarization parameter t_{20} has recently been measured for the first time at 142 MeV by Holt et al. ([16]), but no theoretical prediction does reproduce the value -0.24 ± 0.11 at $\theta_{c.m.} = 180°$. Of course, this quantity is strongly dependent on the tensor force, and further experimental investigations are awaited.

From the theoretical point of view, the effects of absorption are missing in our model. However, we think that absorption will affect in the same amount every result, so that the general features presented here will still remain valid.

To conclude, we think that one must be aware of the importance of choosing a « realistic » parametrization for the NN tensor force, before considering more refined effects in the calculation of πd elastic-scattering observables.

* * *

⊛ RIASSUNTO (*)

Si mostra la grande sensibilità delle osservabili dello scattering elastico πd ai particolari della funzione d'onda del deuterone. A 142 MeV e a 256 MeV si trova che la sezione d'urto differenziale per $\theta_{c.m.} = 180°$ dipende linearmente dalla quantità $A(q^2)$, che è la parte più importante del fattore di forma elettromagnetico del deuterone. Un comportamento simile si osserva per la polarizzazione del tensore t_{20} (180°) a 142 MeV. Si confrontano i risultati con i dati sperimentali osservati per gli angoli all'indietro.

(*) Traduzione a cura della Redazione.

Резюме не получено.

Article I-6

RELATIVISTIC APPROACH OF πd ELASTIC SCATTERING *

FAYARD C., LAMOT G.H., and GIRAUD N.

Institut de Physique Nucléaire (et IN2P3), Université Claude Bernard Lyon-1
43, Bd du 11 Novembre 1918 - 69622 Villeurbanne Cedex, France

I. INTRODUCTION

The recent progress in the understanding of πd scattering within the 3-body approach are noteworthy [1,2]. In the resonance region, the latest improvements concern :

i) the use of the fully relativistic (FR) treatment,

ii) the choice of a "relativistic" NN tensor force,

iii) the inclusion of the small πN channels in addition to P_{33}, and

iv) the effects of genuine pion absorption and emission.

Up to now, theory was compared with three old sets of experimental data for the differential cross section $d\sigma/d\Omega$ at 142, 180 and 256 MeV, but in the course of the past few months, the analysis of various $\pi^+ d$ elastic scattering experiments was achieved, providing "fresh" data for $d\sigma/d\Omega$ in a wide energy range. The situation is summarized in Table I.

Group	Energy range	Observables	Angular range (C.M.)
Gabathuler et al. [3] (SIN)	82-292 MeV	$d\sigma/d\Omega$	0° to 130°
Stanovnik et al. [4] (CERN)	141-260 MeV	$d\sigma/d\Omega$	130° to 175°
Frascaria et al. [5] (SIN)	130-280 MeV	$d\sigma/d\Omega$	180°
Holt et al. [6] (LAMPF)	140 MeV	$d\sigma/d\Omega$ t_{20}	180°

Table I

Status of the recent $\pi^+ d$ data

We present here a short review of the most refined 3-body calculations that we have done within the FR approach compared, with these recent data.

II. SENSITIVITY OF πd OBSERVABLES TO THE TWO-BODY INPUT

1/ NN tensor force : We have recently investigated [2] the strong dependence of the backward parts of $d\sigma/d\Omega$ and t_{20} on the description of the deuteron wave function. Various tensor forces were used which differ in the constraints imposed in the fitting procedure of the parameters as shown in Table II.

We have found that $d\sigma/d\Omega$ (180°) increases linearly with $A(q^2_{max})$, where $A(q^2)$ is the deuteron electric form factor and q_{max} the maximum value of the

Interaction	Low energy parameters	$\delta(^3S_1)$ up to 200 MeV	$F_0(q)$ up to 6 fm^{-1}
YL	yes	no	no
S	yes	yes	no
SF	yes	yes	yes
QT	no	no	yes

Table II. Constraints imposed to fit the parameters for various sets of tensor force. $F_0(q)$ is the deuteron charge form factor. In each set, different values of the D-state probability are considered.
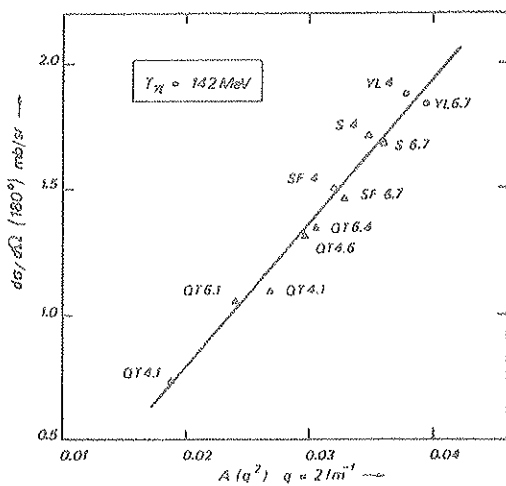

Fig. 1 - $d\sigma/d\Omega$ (180°) at 142 MeV as a function of $A(q^2)$ at $q = 2$ fm^{-1}, for various tensor forces (the number is the P_D value).

momentum transferred to the deuteron by the incident pion. This is illustrated in Fig. 1 at T_π = 142 MeV ($q_{max} \sim 2$ fm^{-1}). Let us mention that q_+, the position of the minimum in $|F_0(q)|$, increases when we go along the straight line in Fig. 1 in the upward direction.

2/ πN interaction : The effect of introducing the "small" πN channels in addition to P_{33} is noticeable : the forward part of $d\sigma/d\Omega$ is lowered at energies below the resonance, and is enhanced above the resonance, while the backward part ($\theta_{CM} > 90°$) is lowered at all energies (the variation is up to 20%). The smallest effect is observed at 180 MeV, and the general trend is to improve the agreement with experimental data.

III. SYSTEMATICS IN THE ENERGY RANGE 80 TO 300 MeV

We show in Fig. 2-3 $d\sigma/d\Omega$ calculated at eight energies with the SF tensor force (P_D = 6.7%), all πN channels (except P_{11}) being taken into account.

The agreement between theory and experiment is excellent at 82, 116 and 142 MeV, throughout the angular range. At 180 MeV and beyond, the agreement is good only at forward angles, but the backward part is not reproduced, neither in shape nor in magnitude.

IV. THE EFFECTS OF ABSORPTION

We have used the set of equations for the coupled πNN-NN systems recently derived by Avishaï and Mizutani [8]. The full P_{11} t-matrix is splitted into a pole and a non-pole part, and the parameters are fitted to the πN coupling constant, the P_{11} scattering volume and the phase shift up to 250 MeV.

The effect of absorption on $d\sigma/d\Omega$ is very small throughout the angular range at 142 MeV and 180 MeV (fig. 2-3). The only noticeable variation appears at backward angles where absorption increases $d\sigma/d\Omega$ of about 10% at 142 MeV, in agreement with the experimental trend . At 256 MeV, absorption lowers slightly the forward part of $d\sigma/d\Omega$ and enhances strongly the backward part. Compared
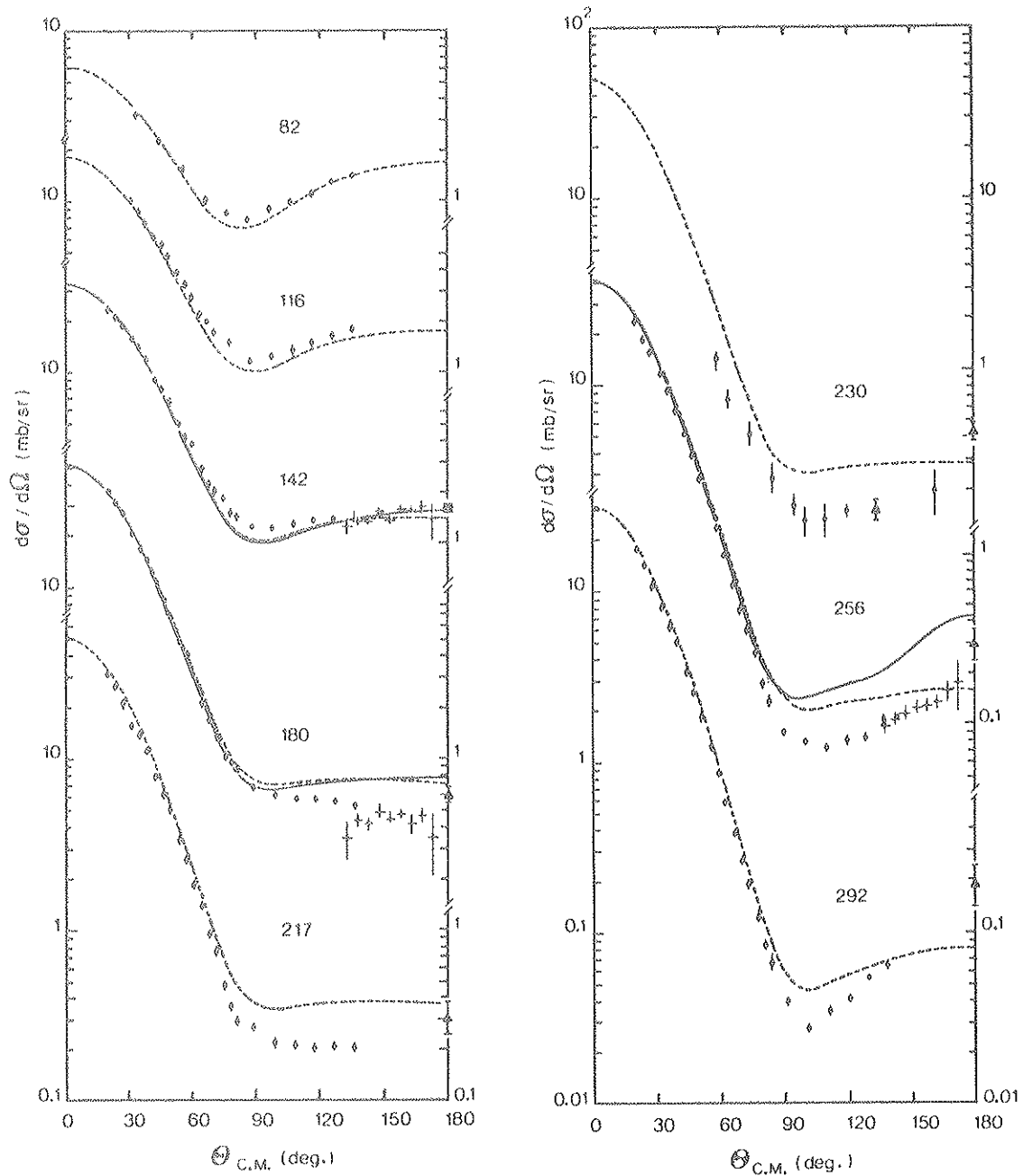
Fig. 2-3 – Differential cross sections in the energy range 82 to 292 MeV, calculated with the SF 6.7 tensor force. (– – – –) all ⁻N channels (except P_{11}), (———) absorption included. The experimental data are from Cabathuler (⌀), Stanovnik (+), Frascaria (⌀) and Holt (▩), and from Cole (⌀) at 230 MeV.

with experiment, the shape of the curve is better with absorption than without absorption, namely a broad minimum appears at $\theta_{CM} \sim 100°$, but the magnitude still remains incorrect.

The polarization parameters are not affected in shape by absorption, but only in magnitude. The most important variations concern the backward part of t_{20} : the values of $t_{20}(180°)$ at 142, 180 and 256 MeV are respectively -0.08, -0.55 and -0.44 with absorption, and -0.73, -1.08 and -1.27 without absorption.

V. FURTHER INVESTIGATIONS

1/ Theory - The ɔ meson exchange is incorporated in the absorption model of Avishai and Mizutani , and its inclusion in the practical calculation is under examination. The problem of dibaryonic resonances is also under investigation.

2/ Experiment - The matching of the various sets of data is not obvious. Now further experiments are awaited in the backward angle region which is very sensitive to the theoretical description.

References

1) A.S. Rinat and W. Thomas, Nucl. Phys., A 282, (1977), 365
2) N. Giraud et al., Phys. Rev., (to appear)
   G.H. Lamot et al., to be published
3) K. Gabathuler et al., SIN-Report, 1980
4) A. Stanovnik et al., Prof. of the Houston Conference, (1979)
5) R. Frascaria et al., Private communication
6) R.J. Holt et al., Phys. Rev., Lett., 43, (1979), 1229
7) R.H. Cole et al., Phys. Rev., C 17, (1978), 681
8) Y. Avishai and T. Mizutani, Nucl. Phys., A 326, (1979), 352,
   A 338, (1980), 377 and this conference

2ème PARTIE

QUELQUES ASPECTS DU ROLE DES PIONS VIRTUELS DANS LES NOYAUX

La description du noyau comme une collection de nucléons, protons
et neutrons, interagissant par des forces phénoménologiques dont on renonce au moins
provisoirement à expliciter l'origine a longtemps été la philosophie dominante des
physiciens nucléaires. Il est certain qu'elle a permis d'expliquer un grand nombre
de phénomènes et qu'elle a connu des succès éclatants comme le modèle des couches
pour ne citer qu'un exemple. Cette philosophie a cependant ses limites car on sait
depuis Yukawa qu'une théorie plus microscopique peut expliquer les interactions
au moyen d'échanges mésoniques et que tout particulièrement les forces dues à l'é-
change d'un pion doivent jouer un rôle important. La théorie du noyau comme une
collection de nucléons n'est donc valable que jusqu'à un certain point et en sé-
lectionnant judicieusement les observables on doit pouvoir mettre en évidence le
rôle des degrés de liberté mésoniques éludés dans l'approche classique. Inévita -
blement associés à ces degrés de liberté, les excitations nucléoniques (surtout
l'isobare Δ) que le pion peut engendrer doivent se manifester également.

Un exemple célèbre de manifestation du pion est l'électrodésinté-
gration du deuton au seuil[1,2]. A grand transfert de moment la section efficace
correspondante[2] dévie considérablement de celle calculée à partir des seuls
nucléons mais est très bien décrite au contraire lorsque l'on tient compte égale-
ment du pion échangé entre le proton et le neutron[1].

Plus généralement, il est naturel de penser que le pion se manifes-
te plus volontiers dans les observables qui dépendent du spin et de l'isospin des
nucléons. En effet il est bien connu que le pion lui-même se couple au spin et à
l'isospin nucléonique. Le canal de spin-isospin est donc un canal de choix pour
l'étude des degrés de liberté pioniques et des excitations de l'isobare Δ . Ce
domaine a connu un développement considérable dans les dernières années (on peut
en trouver une revue en ref.3 et on peut consulter la réf.4 pour des développe-
ments plus récents).

Le groupe de Lyon a développé une approche originale de ces pro-
blèmes[5,6] basée sur la notion de polarisabilité axiale. Dans cette optique les
excitations nucléoniques comme le Δ ne sont pas introduites explicitement mais
elles sont naturellement contenues dans le coefficient de polarisabilité axiale
du nucléon qui définit la réponse nucléonique à l'excitation de spin-isospin
Le milieu nucléaire devient donc analogue à un milieu diélectrique et l'on peut
alors définir un vecteur densité de polarisation. Cette approche a permis de pré-
voir dès 1973 l'existence d'une renormalisation de la constante de couplage axial

g_A de la désintégration β [5]. Celle-ci est réduite par les effets de polarization :
l'origine physique de cette réduction est semblable à celle de l'effet Lorentz-Lo-
renz dans les diélectriques. Un vide se crée autour d'un nucléon par suite des corré-
lations répulsives de courte portée. Le spin nucléonique polarisant le milieu nuclé-
aire, des charges(axiales) apparaissent à la surface du trou de corrélation provo-
quant la renormalisation en question.

Dans un langage plus familier en physique nucléaire, ce phénomène de
polarisation apparaît comme une excitation de configurations isobare-trou (Δ -h)
très semblable si ce n'est l'énergie d'excitation à la polarisation ordinaire
nucléon-trou (N-h) (fig.1). Le rôle des correlations à courte portée se traduit
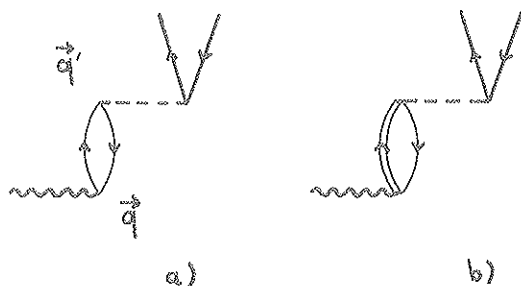

Fig.1 : Polarisation a) nucléon-trou
b) delta-trou

dans l'interaction entre ces différentes excitations. Elle est généralement sché-
matisée à l'aide d'un paramètre de Landau-Migdal faiblement dépendant du moment.
Dans le canal de spin-isospin, cette interaction est dénotée $g'\vec{\sigma}_1 \cdot \vec{\sigma}_2 \vec{\tau}_1 \cdot \vec{\tau}_2$ et
des formes analogues pour Nh- Δh et Δh- Δh avec les matrices de Pauli remplacées
par les matrices appropriées à la transition 1/2-3/2 ou 3/2-3/2 (voir par exemple
la réf.7). Elle introduit donc (par exemple dans une description RPA) des compo-
santes Δ -trou dans la fonction d'onde nucléaire à côté des composantes plus fa-
milières nucléon-trou et ces composantes interfèrent destructivement avec les con-
figurations principales impliquées dans la transition [8,9]. Il est cependant
difficile de mettre en évidence cette suppression dans les transitions β de Gamow-
Teller. Celles-ci sont en général périphériques ; il apparait alors des charges
axiales à la surface du noyau lui même qui tendent à masquer l'effet de réduction[6].

Une nouvelle voie s'est ouverte avec l'utilisation des réactions (p,n)pour l'étude
de la force Gamow-Teller, ce qui a permis l'importante découverte de la résonance Gamow- Teller
géante [10]. Avec de telles réactions tous les états finals sont énergétiquement
accessibles alors que seuls ceux de plus basse énergie sont excités dans la désin-
tégration β . Cette nouvelle technique fournit la force totale

$$S_{\beta^-} = g_A^2 \Sigma_n \ |<0 \ | \ \Sigma_i \vec{\sigma}_i \tau_i^+ | \ n >|^2$$

que l'on peut comparer à la règle de somme Gamow Teller

$$S = S_{\beta^-} - S_{\beta^+} = 3 \cdot (N-Z) \cdot g_A^2 \qquad\qquad (1)$$

cette dernière valeur impliquant que l'on s'est restreint aux degrés de liberté du nucléon. Les résultats des mesures de S_{β^-} [13] font apparaître un déficit important (35 à 50 %) par rapport à la limite inférieure donnée par la règle de somme.

Dans notre méthode, l'effet de la polarisation du milieu par excitations virtuelle de l'isobare Λ revient à remplacer g_A par

$$\tilde{g}_A = g_A/(1 + g' \, \alpha(x)) \tag{2}$$

où la polarisabilité nucléaire α est proportionnelle à la densité nucléaire et à la polarisabilité du nucléon. De manière simplifiée, la nouvelle règle de somme revient à moyenner $(\tilde{g}_A)^2$ sur la densité isovectorielle (neutrons moins protons) du noyau ce qui permet de définir un $(g_A)_{eff} < g_A$. Cette méthode est résumée dans l'article (II.1). La figure 1 de cet article montre que pour des valeurs de g' comprises dans la gamme présentement en faveur $0,7 \pm 0,1$ [11,12] on obtient des atténuations de la règle de somme entre 35 et 50 % en accord avec l'expérience.

On notera que l'effet Lorentz-Lorenz classique donne $g'=1/3$; d'autres mécanismes que l'échange du pion sont donc nécessaires mais c'est un sujet encore controversé [14]. On ne doit cependant pas dissimuler que les données expérimentales peuvent être révisées en hausse spécialement dans la partie de haute excitation et qu'il existe des mécanismes de réduction concurrents [15].

Nous n'avons jusqu'à présent considéré que les effets de la polarisation nucléaire à moment de transfert q pratiquement nul. On aura remarqué que l'interaction statique d'échange du pion :

$$V_{OPE} = - \frac{f_r^2}{m_\pi^2} \, \frac{\vec{\sigma}_1 \cdot \vec{q} \; \vec{\sigma}_2 \cdot \vec{q}}{\vec{q}^2 + m_\pi^2} \; \vec{\tau}_1 \cdot \vec{\tau}_2 \tag{3}$$

ne joue de rôle à $q=0$ qu'à cause de l'existence du trou de corrélation qui lui permet de contribuer à g'. Nous distinguerons successivement deux cas pour $|\vec{q}| \neq 0$:

i) $|\vec{q}|$ réel, V est attractif et peut contrebalancer g' si ce dernier n'est pas trop grand, conduisant ainsi à des renormalisations dans le sens de l'amplification (opalescence critique) [16].

ii) $|\vec{q}|$ imaginaire, V est répulsif et son effet s'ajoute à l'atténuation du type Lorentz-Lorenz. On n'a de contact avec l'expérience qu'à la limite $|\vec{q}| = im_\pi$ qui correspond au pole du champ du pion : le résidu qui est par définition la constante de couplage pion-noyau $f_{\pi N}$ détermine la valeur du champ asymptotique du méson π où $f_{\pi N}$ est différent de la constante f_r pion-nucléon ($f_r^2/4\pi = 0.08$)

Cas ou $|\vec{q}|$ est réel :

Dans la version la plus simple de notre modèle, le champ de pion créé par une source $\vec{\sigma}\vec{\tau}$ dans la matière nucléaire infinie devient : [6]

$$\varphi(q) = \frac{i\sqrt{2} \, f_r}{(1+g'\,\alpha)} \; \frac{\vec{\sigma} \cdot \vec{q} \; \vec{\tau}}{\left[1 - \dfrac{\alpha}{1+g'\,\alpha}\right] q^2 + m_\pi^2} = \frac{i\sqrt{2} \, f_r \, \vec{\sigma} \cdot \vec{q} \; \vec{\tau}}{(|\vec{q}^2| + m_\pi^2)(1 + \alpha(g' - \dfrac{q^2}{q^2 + m_\pi^2}))} \tag{4}$$

Dans cette expression l'effet Lorentz-Lorenz a été explicité dans la première égalité, la seconde laissant apparaître l'interaction particule-trou au dénominateur. Déjà avec la seule polarisabilité due au Δ $(\alpha \approx 0,9)$ le champ de pion est proche d'une singularité qui serait obtenue à $q^2 = \dfrac{m_\pi^2}{\dfrac{\alpha}{1+g'\alpha}-1}$ pour $\alpha > 1/(1-g')$. Mais une partie de la polarisabilité provient des simples excitations nucléons-trous qui à $q=0$ donnent par exemple trois fois la contribution du Δ et sembleraient conduire à une situation critique (transition de phase de condensation des pions) à la densité de la matière nucléaire pour les valeurs habituelles de g' [17]. En fait il faut tenir compte de la taille des sources nucléoniques (facteurs de forme) qui coupent la polarisabilité quand $|\vec{q}|^2$ croît pour déterminer le moment et la densité critique q_c et ρ_c. La transition de phase est alors rejetée au delà de la matière nucléaire ordinaire. Cependant pour $q=q_c$, le champ de pion présente un maximum qui est un précurseur de la condensation : c'est le phénomène d'opalescence critique [16].

Dans un langage plus habituel de la physique nucléaire, plus précisément celui de la R.P.A., cela signifie que l'interaction particule-trou est assez forte pour produire des effets collectifs de type attractif caractéristiques de l'échange du pion (à $q=0$ on a un effet collectif répulsif dû à g', c'est à dire la résonance Gamow-Teller géante). Si g' n'est pas trop grand, des états de parité non naturelle portant les nombres quantiques du pion ($T=1$, $J^\pi = 0^-$, 1^+, ...) descendent vers le fondamental et leurs champs pioniques, c'est à dire leurs facteurs de forme de type "spin longitudinal", i.e. $<\vec{\sigma}.\hat{q}\,\tau>$ présentent de fortes augmentations dans la région $q = 2 - 3\ m_\pi$ du moment critique [11]. Si g' est dans la zone $0,7 \pm 0,1$, l'amplification restera modérée (un facteur deux par exemple) et les niveaux pioniques bougeront peu. La dénomination de phénomènes critiques peut alors se discuter et l'on parlera tout aussi bien de polarisation de coeur pour l'effet de la polarisabilité nucléon-trou et de mélange de configurations d'isobares ou de courant d'échange pour la partie Δ-trou.

Dans le cas d'un système fini le formalisme est beaucoup plus complexe. Le moment q n'est pas conservé le long de la chaine des particules-trous : la polarisabilité devient non locale en q, $\alpha(\vec{q},\vec{q'})$ (fig.1). Il est décrit dans les articles II.2 et 3) comment la renormalisation des éléments de matrice de spin longitudinal $<\vec{\sigma}.\hat{q}>$ et transverse $<\vec{\sigma}\times\hat{q}>$ peut être calculée à l'aide d'un système d'équations intégrales couplées (voir aussi la réf.18).

Au point de vue expérimental, on disposait au début de cette étude de données précises sur $<\vec{\sigma}\times\hat{q}>$ (à une contribution de moment orbital près) grâce à la diffusion magnétique d'électrons sur les noyaux [19]. En particulier la célèbre transition M1(T=1) à 15,11 MeV dans le carbone 12 montrait précisément dans la région 2 à 3 m_π un second maximum très supérieur aux calculs théoriques [20] utilisant les fonctions d'onde classiques de Cohen et Kürath [21]. Nous avons donc appliqué nos techniques à ce cas précis et en variant le paramètre phénoménologique g' nous avons pu rendre compte de l'augmentation observée du facteur de forme magnétique. Toutefois la valeur de g' trouvée était à une proximité surprenante de la criticité (qui aurait été atteinte dans la matière nucléaire) et impliquait

une amplification de $<\vec{\sigma}.\hat{q}>$ et donc du champ pionique nucléaire par un facteur 10 dans la région critique (article II.2).

Nous remarquions cependant que $<\vec{\sigma}\times\hat{q}>$ n'est que modérément couplé à $<\vec{\sigma}.\hat{q}>$ et donc peu sensible à l'échange du pion. Au contraire on attend une plus grande influence du méson ρ , autre particule bien établie se couplant au spin et à l'isospin du nucléon, mais ce couplage est transverse et non longitudinal suivant l'interaction V_{ORE} :

$$V_{ORE} = - \frac{f_\rho^2}{m_\rho^2} \frac{(\vec{\sigma}_1 \times \vec{q}).(\ \vec{\sigma}_2 \times \vec{q})}{q^2 + m_\rho^2} \tag{5}$$

En incluant ce dernier dans notre interaction, nous avons constaté que l'essentiel de l'amplification du facteur de forme du carbone 12 pouvait être attribuée au ρ , le pion jouant un rôle secondaire (voir également la réf.22). Nos résultats impliquaient cependant une valeur basse g' (0,4) et encore une amplification du champ pionique par un facteur 4 (article II.3).

Des mesures directes de $<\vec{\sigma}.\hat{q}>$ ont plus récemment écarté cette possibilité, montrant que l'amplification est au plus d'un facteur 2, soit g' > 0,6.[23] Même si l'effet est plus faible qu'on ne l'avait initialement espéré, il demeure très intéressant de le mettre en évidence en exploitant le contraste entre les comportements des fonctions réponses des noyaux aux excitations $\vec{\sigma}.\hat{q}$ et $\vec{\sigma}\times\hat{q}$ dans le domaine quasi-élastique[24].

Cas où $|\vec{q}|$ est imaginaire pur et égal à im_π

Cette valeur du moment n'est pas physique. Elle permet cependant de définir la ou les constantes de couplage pion-noyau qui sont reliées à une quantité physique, l'amplitude du champ pionique loin du noyau (champ asymptotique avec une forme à la Yukawa). La renormalisation de ces constantes de couplage est calculée à partir de la source pionique, i.e. $<\vec{\sigma}.\hat{q}>$ obtenue comme précédemment par solution des équations couplées décrites en (II.2 et 3). On a simplement à effectuer un prolongement analytique pour la valeur $|\vec{q}| = im_\pi$ qui correspond au pole du pion.

Les applications ont été réalisées pour des transitions de noyaux légers, A=3,6,12 pour lesquelles existent des déterminations extrapolées au pôle de pion[25] à partir de données expérimentales de réactions d'échange de charge, par exemple des réactions (p,n) . Nous trouvons essentiellement une réduction par effet Lorentz-Lorenz, l'influence de l'échange du pion étant masquée par des effets de surface comme dans le cas de la désintégration β (article II.4,1ère partie). Les chiffres calculés d'après notre modèle sont toujours très supérieurs aux résultats des extrapolations. Il ne semble pas qu'il faille incriminer la validité de nos méthodes mais plutôt la fiabilité des déterminations "expérimentales".

Heureusement, comme dans la situation à q=0, l'étude de règles de somme est plus fructueuse que celle des transitions particulières. A $|\vec{q}| = im_\pi$

il existe une règle de somme $S^-(im_\pi) - S^+(im_\pi)$ dite du "pole effectif" analogue à la règle de somme de Gamow-Teller. Si on se limite aux degrés de liberté des nucléons, on trouve [26]:

$$S^-(im_\pi) - S^+(im_\pi) = 2.(N-Z).f_r^2 \qquad (6)$$

analogue à l'éq.(1). Le facteur 2 provient de ce que la constante de couplage des pions chargés est $f_r\sqrt{2}$ et on n'a pas le facteur 3 de (1) parce que le couplage ne fait intervenir que la seule direction $\vec{\sigma}.\hat{q}$. Pour tenir compte des degrés de liberté des Δ, nous avons utilisé la méthode de polarisation de la réf.(6) à laquelle nous avons déjà fait appel lors de la discussion sur l'effet Lorentz-Lorenz (article II. 4. 2ème partie). Cette méthode est une approximation de la méthode des équations intégrales. Le calcul de la règle de somme permet de définir $(f_r^2)_{eff}$. On trouve une réduction qui suit la loi exponentielle

$$(f_r^2)_{eff}/f_r^2 \approx e^{-\beta R} \qquad (7)$$

où R est le rayon du noyau $r_0 A^{1/3}$. L'effet Lorentz-Lorenz joue un rôle secondaire. En effet pour $g' \approx 0,7$, il ne donne qu'une atténuation d'un facteur 2 alors que l'échange du pion est responsable de la plus grande partie de la réduction drastique de la règle de somme. Ceci apparaît clairement sur la figure (2) tirée de
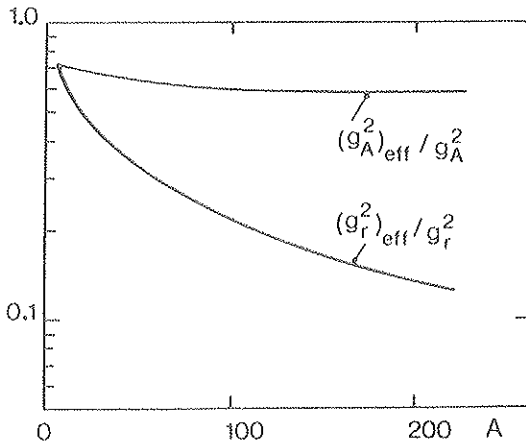

Fig .2: Renormalisation des constantes de couplage axiale et pion-noyau en fonction du nombre de masse

la réf.27 où sont comparées les variations avec A de $(g_A^2)_{eff}/g_A^2$ où l'atténuation Lorentz-Lorenz est dominante et de $(f_r^2)_{eff}/f_r^2$ où l'échange du pion devenu répulsif renforce considérablement la décroissance de la courbe avec A.

La détermination expérimentale de $(f_r^2)_{eff}$ se fait au moyen de relations de dispersion pour l'amplitude de diffusion $\pi^\pm$-noyau au seuil [26]. Les ingrédients sont les différences pour les π^+ et les π^- des sections efficaces et longueurs de diffusion pion-noyau. Ces données n'existent que pour de rares noyaux légers [28] (problème de l'extraction de l'effet coulombien) où les renormalisations sont peu prononcées. Pour notre part, nous avons évalué les quantités "expérimentales" nécessaires par des calculs de potentiel optique qui reproduisent bien les données pion-noyau [29]. Nous avons retrouvé la loi exponentielle en $e^{-\beta R}$ confirmant ainsi

la cohérence de nos modèles de polarisation avec l'"expérience".

Ainsi nous espérons avoir montré sur des problèmes physiques appropriés l'importance de degrés de liberté ignorés par la physique nucléaire traditionnelle. Nous n'avons pas caché toutefois que leurs manifestations ne sont pas toujours sans ambiguïtés et que d'autres mécanismes peuvent être à l'oeuvre. Ceci montre la nécessité d'une étude unifiée prenant en compte aussi bien l'"ancienne" que la "nouvelle" physique nucléaire.

REFERENCES

1) J.Hockert, D.O.Riska, M. Gari and A.Huffman, Nucl.Phys. A217 (1973) 14
   W.Fabian and H.Arenhövel, Nucl.Phys. A314 (1979) 253.

2) G.G.Simon et al.Phys.Rev.Lett. 37 (1976) 739
   M.Bernheim et al. Phys.Rev.Lett 46 (1981) 402

3) Mesons in Nuclei ed.M.Rho and D.H.Wilkinson
   (North Holland-Amsterdam, 1979)

4) 9th International Conference On High Energy Physics And Nuclear Structure.
   Versailles 1981 - Nucl.Phys. A 374 (1982)

5) M.Ericson, A.Figureau and C.Thevenet, Phys.Lett. 45B (1973) 19

6) J.Delorme, M.Ericson, A.Figureau and C.Thevenet, Ann.Phys. (N.Y.)102(1976)273

7) G.E.Brown and W.Weise, Phys.Rep.22 (1975) 279

8) M.Rho, Nucl.Phys. A231(1974) 493

9) K.Ohta and M. Wakamatzu , Phys.Lett.B51 (1974) 325

10) R.R.Doering, A.Galonsky, D.M.Patterson and G.F.Bertsch
    Phys.Rev.Lett. 35 (1975) 1691.
    G.Gaarde et al. Nucl.Phys. A 369 (1981) 258

11) J.Meyer-ter-Vehn, Phys.Rep.74 (1981) 323

12) J.Speth, V.Klempt, J.Wambach and G.E.Brown
    Nucl.Phys. A343 (1980) 382.
    G.E.Brown and M.Rho, Nucl.Phys. A372 (1981) 397

13) G.Gaarde a paraître dans Proceedings of the International Conference on Spin
    Excitations (Telluride, 1982) ed. F.Petrovich (Plenum, New York)

14) G.Baym and G.E.Brown, Nucl.Phys. A 247 (1975) 395.
    M.Rho, à paraître dans Proceedings of the I.U.C.F. Workshop on "The Interac-
    tion between Medium Energy Nucleons in Nuclei". (Bloomington, 1982).
    W.Weise, Phys.lett. 117B (1982) 150.
    W.H. Dickhoff, Nucl.Phys. A 399 (1983) 287

15) K.Shimizu, M.Ichimura and A.Arima, Nucl.Phys. A 226 (1974) 282
    B.Desplanques. ILL preprint 1983.
    G.F.Bertsch and I.Hamamoto, Phys.Rev. C26 (1982) 1323.

16) M.Ericson and J.Delorme, Phys.Lett. 76B (1978) 182
    M.Gyulassi et W.Greiner, Ann.Phys.(N.Y.)109 (1977) 485

17) A.B.Migdal, Z.h.ETF 61 (1971) 2210.

18) H.Toki and W.Weise, Phys.Rev.Lett. 42 (1979) 1034

19) J.B.Flanz et al. Phys.Rev. Lett 43 (1979) 1922

20) J.Dubach and W.C.Haxton Phys.Rev.Lett. 41 (1978) 1453

21) S.Cohen and D.Kurath, Nucl.Phys. 73 (1965) 1.

22) H.Toki and W.Weise 92B (1980) 265.

23) M.Haji-Saeid et al, Phys.Rev.Lett. 45 (1980) 880.
    J.L.Escudié et al. Phys.Rev. C24 (1981) 792.
    P.Truöl -à paraître dans Proceedings of the International Conference on Spin
    Excitations (Telluride, 1982) ed.Petrovich (Plenum, New York).

24) W.M.Alberico, M.Ericson and A.Molinari, Phys.Lett. 92 B (1980) 153.

25) O.Dumbrajs, Ann.of Phys. 118 (1979) 249 ; Phys.Rev. C22 (1980) 2151.

26) T.E.O.Ericson and M.P.Locher, Nucl.Phys. A 148 (1970) 1.

27) J.Delorme, A.Figureau and N.Giraud, Proceedings of the International Conference
    On Nuclear Structure(Amsterdam, 1982), ed. A.Van der Woude and B.J.Verhaar,p.216.

28) C.Wilkin et al., Nucl.Phys. B62 (1973) 61.
    G.T.A.Squier et al.Phys.Rev.Lett. 31 (1973) 389

29) K.Stricker, H.Mc Manus and J.A.Carr, Phys.Rev. C19 (1979) 929.

Article II-1

LORENTZ-LORENZ QUENCHING FOR THE GAMOW-TELLER SUM RULES[*]

J.Delorme, M.Ericson, A.Figureau and N.Giraud

Institut de Physique Nucléaire
Université Claude Bernard, Lyon I, 43 Bvd du 11 Novembre
69622 Villeurbanne Cedex, France.

One of the most striking aspects of the recent detailed exploration of the Gamow-Teller resonances[1] is the systematic observation that the summed axial vector strength is appreciably lower than that expected from the Gamow-Teller sum rule. The latter is obtained under the assumption of additivity of the free nucleon coupling $g_A \vec{\sigma}.\vec{\tau}$ (with $g_A = 1.25$) to the axial current ; indeed simple Pauli matrix algebra gives then :

$$\sum_n \left\{ \left| \langle n | \sum_i g_A \sigma_i^z \tau_i^+ | 0 \rangle \right|^2 - \left| \langle n | \sum_i g_A \sigma_i^z \tau_i^- | 0 \rangle \right|^2 \right\} = (N-Z) g_A^2 \qquad (1)$$

In principle, both the positively and negatively charged branches have to be measured ; in a nucleus with positive neutron excess however, equation (1) gives already a lower limit for the $\sigma \tau^+$ strength which is the quantity accessible through (p,n) reactions and Pauli blocking rapidly suppresses the τ^- branch as (N-Z) increases. Thus, if one assumes that no part of the strength has escaped detection, a reduction such as that observed in a wide range of nuclei is strongly suggestive of the intervention of new degrees of freedom.

An attractive mechanism is the now popular Lorentz-Lorenz effect which was once proposed to explain the reduction of axial β decay rates (For a survey, see refs. (2) and (3)). It arises from the coupling between nucleon and Δ isobar degrees of freedom through a short range spin-isospin dependent force. We present here some results of a calculation in which the coupling is described in a Δ-hole polarizability picture ; the model we use is the same as that introduced some years ago[4] to treat the modifications of the pion field in the nuclear medium. This is in principle practically equivalent to currently developped R.P.A. treatments of Δ-hole propagation, the only difference being the use of the static limit and of closure approxi-

mation on the Δ states (the Δ-hole polarizability becomes then local in configuration space). In our previous works it was shown that the coupling to Δ-hole excitations through a contact spin-isospin interaction characterized by the Landau-Migdal parameter g' induces a local renormalization of the axial (or pion) vertex (Lorentz-Lorenz effect) :

$$A^\pm(x) = g_A \sum_i \vec{\sigma}_i \tau_i^\pm \delta(x - x_i) \longrightarrow g_A / (1 + g'\alpha(x)) \sum_i \vec{\sigma}_i \tau_i^\pm \delta(x - x_i) \qquad (2)$$

The axial polarizability $\alpha(x)$ is proportionnal to the nuclear density $\alpha(x) = 8 \left(f^{*2} / 9 m_\pi^2 \omega_\Delta \right) \rho(x)$, ω_Δ and f^* being the excitation energy of the Δ resonance and the $\pi N\Delta$ coupling constant. The sum rule (1) is then simply modified to the following ground state expectation value, defining an effective axial coupling constant :

$$\sum_n \left\{ |\langle n|A_z^+(q=0)|0\rangle|^2 - |\langle n|A_z^-(q=0)|0\rangle|^2 \right\} = -\langle 0| \left[g_A / (1 + g'\alpha(x)) \right]^2 \sum_i \tau_i^3 |0\rangle$$

$$= g_A^2 \int d^3x \left[\rho_n(x) - \rho_p(x) \right] / (1 + g'\alpha(x))^2 = (N-Z) (g_A^{eff})^2 \qquad (3)$$

Actually the spin-isospin interaction is somewhat more complicated that the simple Landau-Migdal ansatz : in particular it comprises a one pion exchange part which, however, can be expected a priori to play little role here because it vanishes at zero momentum transfer (strictly speaking, it can have some influence for finite nuclear size, specially in the lightest nuclei). In this more general case, the derivation of the sum rule requires the knowledge of the full renormalization of the pion propagator. From P.C.A.C., one gets at fixed q :

$$\sum_n \left\{ |\langle n|A_z^+(q)|0\rangle|^2 - |\langle n|A_z^-(q)|0\rangle|^2 \right\} = \frac{g_A^2}{2 f^2} (q^2 + m_\pi^2)^2 \frac{m_\pi^2}{q^2} \langle 0|[\varphi(q), \varphi^+(q)]|0\rangle \qquad (4)$$

One checks easily that in a description limited to nucleon degrees of freedom $\varphi(q) = \frac{f\sqrt{2}}{m_\pi} \sum_i \vec{\sigma}_i \cdot \vec{q} / (q^2 + m_\pi^2) \cdot \tau_i^\pm$, and the right hand side of equ.(4) becomes $(N-Z) g_A^2$, independent of q, so that one recovers the primitive sum rule (1).

Using methods developped elsewhere[5], we have computed the right hand side of (4) at q=0, which differs from the simplified sum rule (3) by the inclusion of pion propagation effects. As for the case of equ.(3), we need the neutron and proton densities, which are chosen with a Fermi profile for a series of nuclei covering the whole range of atomic numbers (a modified Gaussian shape is preferred for the lightest case, $A=14$). The ratio $(g_A^{eff}/g_A)^2$ is represented in fig.(1), for values of g' in the now favoured range 0.7 ± 0.1. The calculated quenching increases slowly with the mass number, following the average nuclear density (characteristic of a contact interaction). We have found, as expected, that the Lorentz-Lorenz quenching (equ.(3)) is only slightly altered by the consideration of pion propagation effects (these produce only a reduction of the effect ranging from 2.6 to 5.6 % as the atomic number decreases). The smallness of the pion contribution is typical of the zero momentum limit ; it greatly contrasts with the situation which prevails e.g. at the
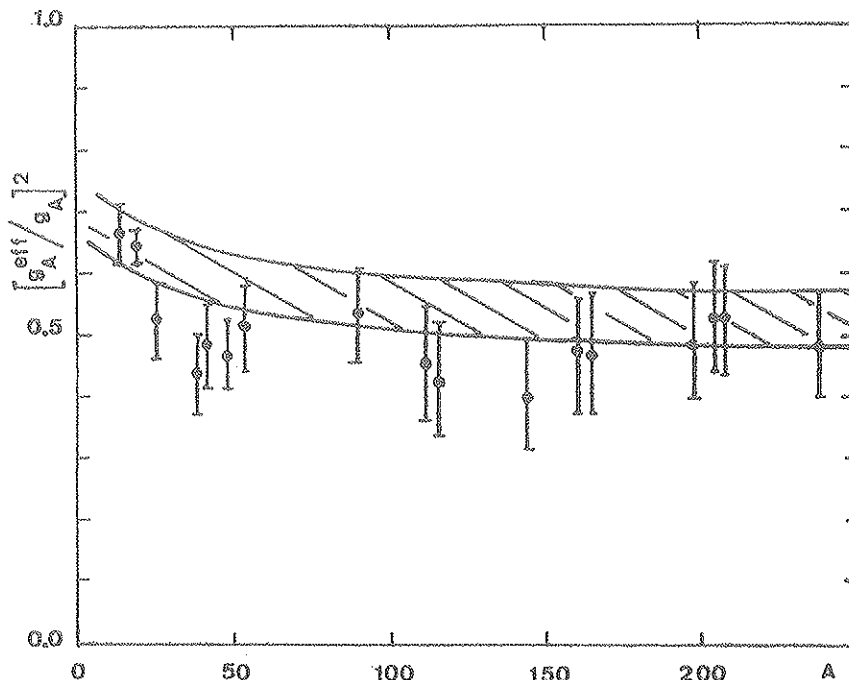
Fig. 1 : The reduction factor of the (squared) effective axial vector coupling constant with respect to the G-T sum rule value (1). The shaded area corresponds to values of g' between 0.6 (upper curve) and 0.8 (lower curve). The experimental points are taken from ref.(6).

pion pole (q→i m_π) where the sum rule (4) defines an effective on-shell pion-nucleus coupling constant, a quantity of interest for π-nucleus dispersion relations : our previous works [4,5] show that besides the universal Lorentz-Lorenz quenching, a considerable decrease of the π-nucleus coupling constant is to be attributed to the pion propagation.

Here the quenching is less dramatic, being essentially due to the Lorentz-Lorenz effect : Though the reduction is moderate in very light nuclei, it attains a factor 2 in the heaviest ones ; the experimental data [6] follow approximately the same trend (see fig.(1)).It is then very satisfying that a simple mechanism like the Lorentz-Lorenz effect can explain the existing results. The value g' = 0.8 seems to be favoured ; one should add however two remarks concerning the validity of such an interpretation. First the relevant parameter is the product of g' by the polarizability. Our curves have been obtained with a ratio of πNΔ to πNN coupling constants f^{*2}/f^2 = 4.5 taken from the Chew-Low model with recoil terms. Furthermore, the axial polarizability is not saturated by the Δ alone [7], which means that other N* isobars can contribute, but we do not know whether their short-range interaction with the nucleons can be described by a universal value of g'. There is in fact no compelling proof (see

refs.(3,9)) that the same g' applies even to the (N-hole)-(Δ-hole) and the (Δ-hole)-(Δ-hole) interactions as was implicitely assumed in equ.(2) ; the vertex renormalization should read more precisely $\left(1-g'_{N\Delta}\,\alpha/(1+g'_{\Delta\Delta}\,\alpha)\right)$ instead of $(1 + g'\alpha)^{-1}$. The second remark is that the interpretation of all the missing G.T.strength by a Lorentz-Lorenz quenching relies on the hypothesis that no strength can have been pushed at high excitation without appealing to the Δ isobar, as for instance in the second order core polarization mechanism through a tensor force once suggested by the Arima group [8] .

1. C.Gaarde, J.Rapaport, T.N.Taddeucci, C.D.Goodman, C.C.Foster, D.E.Bainum, C.A.Goulding, M.B.Greenfield, D.J.Horen and E.Sugarbaker : Nucl.Phys. A 369 (1981) 258.
   C.D.Goodman : Proc. of 9-Icohepans, Versailles 1981, Nucl. Phys. A 374 (1982) 241 C.
2. M.Ericson, this Conference.
3. M.Rho, this Conference.
4. J.Delorme, M.Ericson, A.Figureau and C.Thévenet : Annals of Physics 102 (1976) 273.
5. J.Delorme and A.Figureau : in 4ème Session d'Etudes Biennales de Physique Nucléaire, Report LYCEN 7702 (1977) p.C.7.1.
   J.Delorme, A.Figureau and N.Giraud:preprint LYCEN 8212(1982)
6. C.Gaarde, this Conference.
7. M.Ericson and A.Figureau. J.Phys.G : Nucl.Phys.7(1981)1197.
8. K.Shimizu, M.Ichimura and A.Arima : Nucl.Phys. A 226(1974)282.
9. J.Speth, this conference.

Article II-2

CRITICAL OPALESCENCE OF THE NUCLEAR PION FIELD:
A POSSIBLE EVIDENCE IN THE M1 (15.11 MeV) FORM FACTOR OF ^{12}C

J. DELORME, M. ERICSON[1], A. FIGUREAU and N. GIRAUD

*Institut de Physique Nucléaire de Lyon, Université Claude Bernard, Lyon I and IN2P3,
69621 Villeurbanne, France*

We have computed the nuclear pion field for the transition to the 15.11 MeV (1^+, $T = 1$) state of ^{12}C, evaluating the nuclear polarization with a large basis of nucleon- and isobar-hole excitations. The field shows an enhancement (or critical opalescence) in the momentum region beyond 1.5 m_π which leads to a substantial increase of the second maximum of the M1 form factor. Agreement with experiment can be obtained if the ^{12}C nucleus is much closer to the pion condensation threshold than currently expected.

We have recently suggested that the proximity of pion condensation, a phase transition generally accepted to occur at nuclear densities higher than the normal ones, should produce critical opalescence effects in ordinary nuclei [1] [1]. These manifest themselves as an enhancement of the (quasi)static pion field near the critical momentum which reflects a short-range ordering of the nucleonic spins, precursor of the long-range one.

Thus although pion condensation is not realized in the usual conditions, there are critical phenomena which influence the propagation of static pions in the nuclear medium. As static pions exist only as virtual particles they have to be produced by some external source. The ideal choice is a weak or electromagnetic source which does not suffer from the distortion problems which could mask the critical phenomena. As weak probes do not yet cover the interesting momentum range, one has to resort to an electromagnetic one, i.e. the photon as obtained from (e, e') reactions exciting states of unnatural parity. However, the variety of nuclei that could reveal critical opalescence is limited to the light ones for reasons to be explained below. Strongly interacting probes which do not present this drawback have also been suggested as the (p, p') or (γ, π) reactions [3,4]. As the photon is nevertheless the cleanest source of static virtual pions we have investigated in this work the problem of (e, e') isovector magnetic scattering (i.e. transitions which have the pion quantum numbers) with special emphasis on the M1 transition to the 15.11 MeV state of ^{12}C.

In the nucleus a photon converts into a pion via the polarization of the medium, the creation of nucleon- and Δ-holes (fig. 1; this is a particular case of core polarization). The same transformation occurs for the weak axial current and there we showed that its inclusion amounts to the replacement of the spin—isospin transition density $\sigma(x)$ [2] by the quantity $\Sigma(x) = \sigma(x) - P(x)/f_\pi\sqrt{2}$, where $P(x)$ is the axial polarization vector density for the investigated transition and f_π the π—N coupling constant [5]. The same replacement holds for the electromagnetic current. In a simple local approximation the vector P can be written:

$$P(x) = -f_\pi\sqrt{2}\, g'\tilde{\alpha}(x)\sigma(x) + \tilde{\alpha}(x)\nabla\varphi(x), \tag{1}$$

---

[1] Also at CERN, Geneva, Switzerland.
[1] Critical effects were also proposed by Gyulassi and Greiner in the context of heavy-ion collisions [2].
[2] Isospin indices will be omitted and formulae will refer to the charged case.
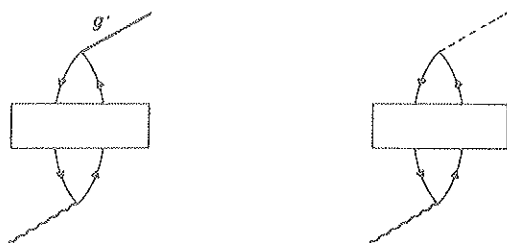
Fig. 1. The two contributions to the polarization (eq. (1)).
The square box represents the effective polarizability.

where $\varphi(x)$ is the pion field for the transition and $\tilde{\alpha}(x)$ the effective polarizability per unit volume. The first term represents a vertex renormalization governed by the Lorentz–Lorenz parameter g'. More important for our purpose is the term in $\nabla\varphi$ through which critical opalescence influences the spin density. However, the magnetization current is proportional to $\nabla\times\Sigma(x)$ so that, in an infinite homogeneous system where $\tilde{\alpha}$ is a constant, $\nabla\times(\tilde{\alpha}\nabla\varphi)$ vanishes. Translated in momentum space, this result reflects the fact that, in infinite matter, the particle–hole pairs transmit the external momentum unchanged to the pion and then transversality prohibits any contribution to the magnetic transition. This is not true in a small system where a momentum transfer of the order of the inverse nuclear size is allowed. For that reason we have focused our attention on light nuclei and especially the M1 transition in ^{12}C which has been subject to extensive experimental investigation.

It is known that calculations in the impulse approximation fail to reproduce the second maximum of the form factor by an order of magnitude (a recent study can be found in ref. [6]). The inclusion of standard one-pion exchange currents does not improve appreciably the situation since their contribution passes through zero at practically the position of that maximum [7]. Our consideration of the polarization term amounts first to enlarging the model space up to very high excitations whereas most calculations use ^{12}C wave functions restricted to the 1p shell, and second to incorporating the effects of the Δ excitation of the nucleon. These two aspects are treated nonperturbatively in a cooperative way. Thus this method is not in principle reducible to a traditional nuclear physics treatment supplemented with meson exchange even in an extended basis. The other components of the pion exchange current, i.e. the pair term and the pionic current, have to be added separately.

The polarizability α is in general a nonlocal quantity $\alpha(x, x')$, i.e., in momentum space it is a function $\alpha(q, q')$ of the incoming and outgoing momenta q and q'. As pointed out in ref. [5] it is actually a tensor in spin space with the multipole expansion:

$$\alpha_{\mu\mu'}(q, q') = \sum_{J,L,L',M} (-)^\mu \alpha_{LL'}^J(q, q') C(L1J; M - \mu, \mu) C(L'1J; M + \mu', -\mu') Y_{L,\mu-M}(\hat{q}) Y^*_{L',-\mu'-M}(\hat{q}'). \quad (2)$$

Its contraction with the momenta q and q' gives the pion self-energy, the expression of which has been given by Toki and Weise in the harmonic oscillator basis [3]. We have performed the calculation in the static case (i.e. zero pion frequency) up to 25 $\hbar\omega$ particle excitations though saturation in the interesting momentum range is practically attained at 15 $\hbar\omega$. The multipoles $\alpha_{LL'}^J$ contain at each vertex pion–baryon form factors $v(q) = (1 + q^2/\Lambda^2)^{-1}$ with $\Lambda = 1.2$ GeV. The (repulsive) short-range interaction between the baryons modifies the polarizabilities $\alpha_{LL'}^J$, into effective ones $\tilde{\alpha}_{LL'}^J$, which are solutions of the integral equations:

$$\tilde{\alpha}_{LL'}^J(q, q') = \alpha_{LL'}^J(q, q') + g' \int dk \frac{k^2}{(2\pi)^3} \sum_{L''} \alpha_{LL''}^J(q, k) \tilde{\alpha}_{L''L'}^J(k, q'), \quad (3)$$

where we have used a schematic interaction in the spin–isospin channel described by a momentum-independent Landau–Migdal parameter g' (note however that eq. (3) implies a cut off at high momenta since form factors are contained in the polarizabilities). A pure Lorentz–Lorenz effect would give $g' = 1/3$ [8] but larger values (ranging from 0.5 to 0.8) are currently accepted [9–12]. This equation implies a decrease of the pion self-energy and hence less-pronounced critical effects.

The pion field for a transition of multipolarity J can be obtained as the solution of the integral equation (in the static limit):

$$(q^2 + m_\pi^2)\varphi^J(q) = -i\sqrt{2} f_\pi q \sum_L C(J1L; 00)\left[o^{(L,J)}(q) + g' \int dq' \frac{q'^2}{(2\pi)^3} \sum_{L'} \tilde{\alpha}_{LL'}^J(q,q') o^{(L',J)}(q') \right]$$

$$- q \int dq' \frac{q'^3}{(2\pi)^3} \sum_{LL'} C(J1L; 00)C(J1L'; 00)\tilde{\alpha}_{LL'}^J(q,q')\varphi^J(q'). \tag{4}$$

The first term displays the Lorentz–Lorenz renormalization of the source multipoles $o^{(L,J)}$ which are defined as:

$$o^{(L,J)}(q) = i^L v(q)\langle f \| \tau^+ \sqrt{4\pi} j_L(qr)[Y_L \otimes o]^J \| i\rangle. \tag{5}$$

They have been computed with the Cohen–Kurath 8–16 2 BME interaction [13] and an oscillator parameter b = 1.65 fm, which reproduces well the elastic form factor of ^{12}C [14,15]. They are known to give a good description of spin-flip processes at low momentum transfer such as β decay, μ capture and M1 excitation. The polarizabilities have been evaluated with the same size parameter and it is clear that they should involve nucleon excitations only outside the 1p shell. Instead of solving eqs. (3) and (4), we have found it more convenient to derive and solve the equivalent coupled equations which are obeyed by the multipoles $A^{(L,J)}$ of the axial current (g_A = 1.25):

$$A^{(L,J)}(q) + \frac{q^2}{m_\pi^2} C(J1L; 00) \sum_{L'} C(J1L'; 00)A^{(L',J)}(q) = -g_A o^{(L,J)}(q) + g' \int dq' \frac{q'^2}{(2\pi)^3} \sum_{L'} \alpha_{LL'}^J(q,q')A^{(L',J)}(q')$$

$$- (1-g') \int dq' \frac{q'^4}{m_\pi^2(2\pi)^3} \sum_{L'} C(J1L'; 00)\alpha_{LL'}^J(q,q') \sum_{L''} C(J1L''; 00)A^{(L'',J)}(q'). \tag{6}$$

The pion field is obtained through PCAC from the longitudinal component of the current whereas the spin part of the magnetic form factor is given by the transverse component up to a form factor ratio.

Varying g' with all other parameters kept fixed we have looked at the evolution of the solutions. The strength of the pion field is shown on fig. 2. The decrease in the low-momentum region is due to the Lorentz–Lorenz renormalization. A more striking feature is the critical opalescence which is manifest in the large-momentum range q $> 1.5\, m_\pi$. The effects are particularly spectacular close to criticality (which is attained at g' = 0.335). Even in less favourable situations the enhancement remains appreciable (e.g. a factor 2 for g' = 0.6). The persistence in light systems of the critical effects that we had first predicted for infinitely large nuclei was expected from several works showing that the pion condensation threshold is not very different in small and infinite systems [16–18].

In the M1 form factor F_T the critical phenomena appear somewhat differently (fig. 3), reflecting the different behaviour of transverse and longitudinal components. The second maximum is also enhanced but in addition it is sizeably shifted towards small q values. Furthermore, at large q the squared form factor decreases sharply below the one-body value towards a second zero in contrast with the still large enhancement of the field: this behaviour arises from the vertex renormalization which at large momenta is the only surviving contribution to the transverse part of $P(x)$. The theoretical curves include also the effects of pair and pion currents that we have borrowed from the authors of refs. [7] and [19]. Their role is not crucial and amounts essentially to cancelling the Lorentz–Lorenz decrease in the region of the first maximum. As concerns experimental work, there exist a large amount of data concerning this transition. On fig. 3 we have plotted only the most recent ones according to the compilation of refs. [7] and [20]. One sees that the data are rather well reproduced in the region $q < 3m_\pi$ if we take g' = 0.375. In particular we get the right size and position of the second maximum together with the position of the minimum (at least as given by the recent Bates experiment [21]). At larger q instead, there is no sign for the existence of a second minimum. This discrepancy may indicate that an ingredient is still lacking in our model although it should perhaps not be taken too seriously, as a rather small contribution can easily fill the gap.

More intriguing is the fact that our favoured value of g' is definitely lower than the current ones. If we accept blindly the agreement obtained with experiment it would mean that one is very close to criticality. Indeed the cor-
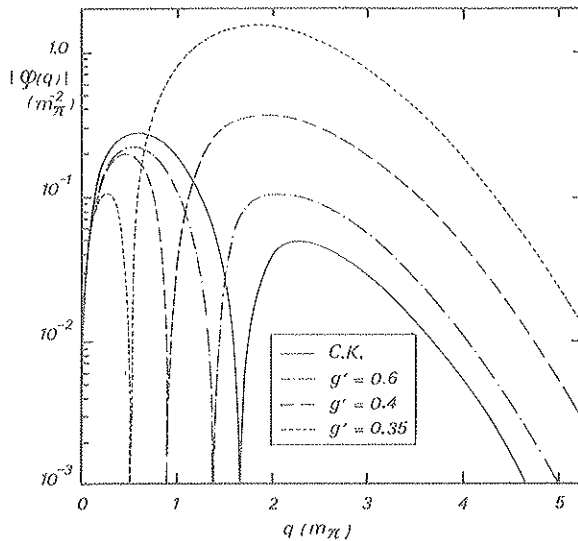
Fig. 2. The strength of the pion field for the transition to the 1^+ (15.11 MeV) state in ^{12}C. The curve labelled C.K. corresponds to the one-body calculation with Cohen—Kurath wave functions.
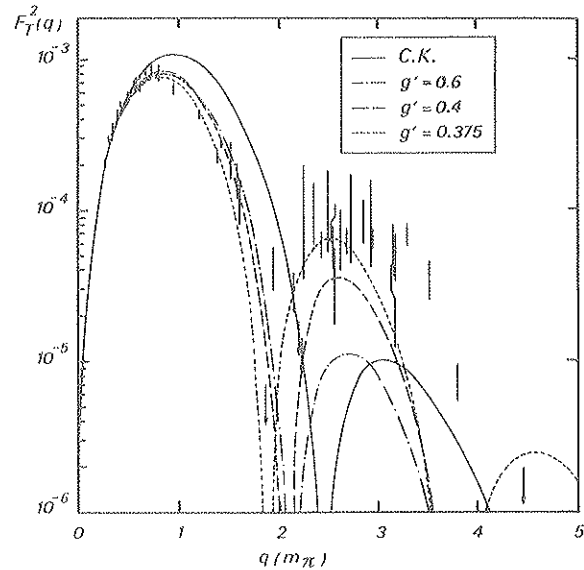

Fig. 3. The squared magnetic form factor (curves are labelled as in fig. 2).

responding pion field is enhanced by a factor 10 in the large-momentum region. It is then clear that the critical phenomena would be essential for reproducing the second maximum. The nuclear polarizability alone without the cooperative effects represented by the enhancement of the pion field would not produce a sufficient increase: using the *unrenormalized* field and maximizing the polarizability by taking $g' = 0$ we find only 50% enhancement of the one-body F_T^2 at the second maximum (this procedure is equivalent to a classical first-order core polarization calculation). Sensitivity of the critical opalescence to the size of the particle—hole basis has been explored. Limitation to 15 and $10\hbar\omega$ excitations would reduce the effects by 10 and 30%, respectively. We have also checked the importance of treating the isobars in a cooperative way with the nucleons. Suppression of the Δ contribution leads to a decrease of F_T^2 by a factor 4 as compared to our best fit (again at the second maximum).

We have selected the quantity g' as the parameter to be varied but it is not the only one which governs the importance of critical phenomena. These depend first of all on the bare polarizability and in addition on the range of the pion—nucleon interaction. The multipoles $\alpha_{LL'}^J$, have been calculated in the harmonic oscillator model. If their magnitude is underestimated the experiment would be accounted for with larger g'. This possibility cannot be excluded. As for the range of the π—N interaction, we get agreement with a larger g' when it is decreased (e.g. $g' = 0.43$ for $\Lambda = 2$ GeV). We can conclude that it changes the results moderately. Finally there remains the problem of the q dependence of the parameter g'. A priori the usual values which have been derived at low q do not necessarily apply in the opalescence region. Some decrease with the momentum is expected from microscopic calculations [22]. As remarked above this effect is partly simulated by a decrease of the repulsion at the rate of the squared π—N form factor. We have tried a more rapid variation of g' by imposing a momentum dependence governed by the mass of the ρ meson. A good fit to experiment is then obtained with the sensibly larger value $g' = 0.475$. This number is marginally consistent with current expectations. One would need a more drastic dependence to get reconciled with the average value. We consider that the problem is open.

To conclude this study, we have proposed an interpretation of the observed anomaly in the M1 form factor of ^{12}C. It lies in the strong nuclear axial polarizability which makes possible the conversion of the photon into a virtual pion and produces an opalescence phenomenon in the propagation of this pion. If the proposed interpretation

77.

is correct, it shows that nuclei are close to criticality, much closer than suspected. This is a surprising result. We are aware that one can question the validity of our simple linear model so near the phase transition where the fluctuations of the pion field become huge (recall that our result means enhancement by a factor 10). We consider anyway that one has to entertain seriously the idea that critical effects are displayed in the large-momentum behaviour of the M1 form factor, though it looks plausible that they could be less pronounced than in our simple description. We have still to explore possible extensions of our model like the conversion of a photon into a rho meson via the nuclear polarization which may help to fill the undesirable second maximum and enhance the form factor around the second minimum. One would need then less criticality to explain the data. We also have to exert some caution before concluding definitively in favour of opalescence effects. We cannot exclude that the anomaly in ^{12}C has another explanation in the traditional framework of nuclear physics, for instance by the deformation of this nucleus. After the present study had been completed, a new theoretical attempt has been published by Sagawa et al. [23] based essentially on an evaluation of first-order core polarization. The experimental data are not very well reproduced (in particular the positions of the minimum and second maximum, especially with the new data of ref. [21]) but a very interesting feature is the significant enhancement over the one-body form factor obtained at large transfers. This result is at variance with our estimate of first-order effects and the origin of the difference is not yet clear to us. A possible explanation might be the use of an effective interaction more attractive than our schematic one. It avoids in particular the occurrence of a second minimum but could cause problems with criticality. Clearing up this question might be the clue to a complete understanding of the data in the light of critical phenomena. We believe that these stand already as very good candidates to the final explanation. On the experimental side, precision measurements would be clearly helpful in the whole momentum range beyond the first maximum.

This first investigation of critical opalescence in nuclei is thus very encouraging. Due to the importance of the issue, namely the existence of a short-range order of the nucleon spins, it should be settled in a more definite fashion from additional cases; a single piece of evidence is not enough to be fully conclusive. The following developments are possible on the theoretical as well as on the experimental side. First, it would be interesting to explore the same transition with inelastic proton scattering. Such a study would serve as a test for the control of the distortion effects. It will detect directly the opalescence of the pion field in contrast with (e, e') reactions which have sensitivity only through conversion of transverse photons into pions. The field might thus be open to the heavy nuclei [3]. In addition we are presently investigating other spin-flip transitions in light systems and also the possibility of detecting the short-range order with another spin-sensitive electromagnetic probe, the photopion reactions. Critical opalescence is not a property of one particular nucleus. If the anomaly in ^{12}C indeed has its origin in critical phenomena we expect similar effects to occur in spin-flip transitions in other nuclei and to be detectable in a variety of ways.

References

[1] M. Ericson and J. Delorme, Phys. Lett. 76B (1978) 182.
[2] M. Gyulassi and W. Greiner, Ann. Phys. (NY) 109 (1977) 485.
[3] H. Toki and W. Weise, Phys. Rev. Lett. 42 (1979) 1034.
[4] M. Ericson, in: Mesons in nuclei, Vol. III, eds. M. Rho and D.H. Wilkinson (North-Holland, 1979) p. 905.
[5] J. Delorme, M. Ericson, A. Figureau and C. Thévenet, Ann. Phys. (NY) 102 (1976) 273.
[6] N.C. Mukhopadhyay and J. Martorell, Nucl. Phys. A296 (1978) 461.
[7] J. Dubach and W.C. Haxton, Phys. Rev. Lett. 41 (1978) 1453.
[8] M. Ericson and T.E.O. Ericson, Ann. Phys. (NY) 36 (1966) 323.
[9] G.E. Brown, S.O. Bäckman, E. Oset and W. Weise, Nucl. Phys. A286 (1977) 191.
[10] J. Speth, E. Werner and W. Wild, Phys. Rep. 33C (1977) 127.

[11] E. Oset and M. Rho, Phys. Rev. Lett. 42 (1979) 47.

[12] J. Meyer-ter-Vehn, to be published.

[13] S. Cohen and D. Kurath, Nucl. Phys. 73 (1965) 1.

[14] H. Crannell, Phys. Rev. 148 (1966) 1107.

[15] T.W. Donnelly and G.E. Walker, Phys. Rev. Lett. 22 (1969) 1121.

[16] S.A. Fayans, E.E. Saperstein and S.V. Tolokonnikov, J. Phys. G3 (1977) L51.

[17] J. Meyer-ter-Vehn, Z. Phys. A287 (1978) 241.

[18] H. Toki and W. Weise, to be published.

[19] P. Desgrolard and P. Guichon, Phys. Rev. C19 (1979) 120;
P. Guichon, private communication.

[20] W.C. Haxton, Phys. Lett. 76B (1978) 165.

[21] J.B. Flanz et al., Bull. Am. Phys. Soc. 23 (1978) 583.

[22] S.O. Bäckman and W. Weise, in: Mesons in nuclei, Vol. III, eds. M. Rho and D.H. Wilkinson (North-Holland, 1979) p. 1095.

[23] H. Sagawa, T. Suzuki, H. Hyuga and A. Arima, Nucl. Phys. A322 (1979) 361.

Article II-3

CRITICAL OPALESCENCE OF THE PION FIELD AND THE M1 FORM FACTOR OF ^{12}C:
AN INVESTIGATION OF THE ROLE OF THE RHO MESON

J. DELORME, A. FIGUREAU and N. GIRAUD
Institut de Physique Nucléaire and IN2P3, Université Claude Bernard, Lyon-1, 69622 Villeurbanne Cédex, France

It is shown that the inelastic M1 form factor of ^{12}C can be interpreted by nuclear polarization phenomena with inclusion of the rho meson in the polarizing interaction playing an essential role at large momenta. Whereas much of the observed anomaly can be attributed to standard core polarization effects, a large opalescence of the pion field (a factor 4.5 enhancement) would be needed to get full agreement with experiment.

We have recently proposed [1] an interpretation of the large momentum anomaly in the M1 form factor of ^{12}C in terms of the critical opalescence (or precondensation enhancement) of the nuclear pion field. We showed that such collective phenomena were able to explain most of the anomaly provided the ^{12}C nucleus is relatively close to condensation, in any case closer than currently expected. The experimental data were well reproduced except at large momenta where the calculated form factor had a too rapid drop. The aim of this letter is to show that the inclusion of the rho meson which was not considered in our previous study is able to cure most of this disease. The large influence of the rho meson on channels with pion quantum numbers has been emphasized by Baym and Brown [2]. Their calculation refers to nuclear matter where the conversion of the rho into a pion in the nuclear medium occurs only through correlations and is responsible for the major part of the Lorentz–Lorenz effect. In our previous work this effect was incorporated in the empirical Migdal parameter g'. In a finite system this is not the whole story since the conversion rho–pion is possible through the nuclear surface even in the absence of correlations. More important, we consider also the conversion of a photon into a rho meson via the polarization of the medium (fig. 1). In other words our improved treatment consists in allowing the replacement of any pion line by a rho meson line in the standard particle–hole (and Δ–hole) chain.

The baryon–baryon interaction $G(q)$ in the spin-flip isospin-flip channel is now modified so as to include rho meson exchange in addition to our previous consideration of one-pion exchange plus a short range Migdal interaction:

$$G(q) = \tau_1 \cdot \tau_2 \left[f^2 \left(g' \sigma_1 \cdot \sigma_2 - \frac{\sigma_1 \cdot q \, \sigma_2 \cdot q}{q^2 + m_\pi^2} \right) v_\pi^2(q) - f_\rho^2 \frac{(\sigma_1 \times q) \cdot (\sigma_2 \times q)}{q^2 + m_\rho^2} v_\rho^2(q) \right]. \tag{1}$$
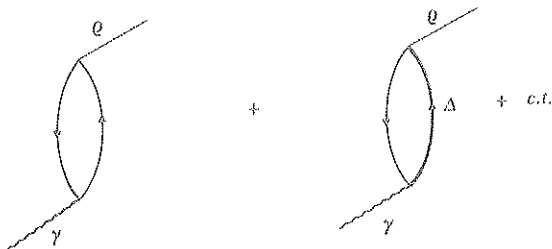

Fig. 1. Conversion of the photon into a rho meson through the nuclear polarization.

Here, $f(f_\rho)$ and v_π (v_ρ) are pion (rho)–nucleon coupling constants and form factors. The value of the ratio C_ρ $= f_\rho^2/f^2$ is taken as 2.18 which corresponds to the strong coupling deduced in the work of Höhler and Pietarinen [3] (the vector dominance model would give instead $C_\rho = 0.8$). We have chosen the form factors as $v(q) = (1 + q^2/\Lambda^2)^{-1}$ with $\Lambda = 1.2$ and 2.0 GeV for π and ρ, respectively. Our coupled integral equations for the multipoles $A^{(L,J)}$ of the axial current now become:

$$A^{(L,J)}(q) + \frac{q^2}{m_\pi^2} \, C(J1L;00) \sum_{L'} C(J1L';00) A^{(L',J)}(q)$$

$$= -g_A \, o^{(L,J)}(q) + \int dq' \, \frac{q'^2}{(2\pi)^3} \left(g' - C_\rho \, \frac{q'^2}{q'^2 + m_\rho^2} \frac{v_\rho^2}{v_\pi^2} \right) \sum_{L'} \alpha_{LL'}^J(q,q') A^{(L',J)}(q')$$

$$- \int dq' \, \frac{q'^4}{(2\pi)^3 m_\pi^2} \left(1 - g' - C_\rho \, \frac{m_\pi^2}{q'^2 + m_\rho^2} \frac{v_\rho^2}{v_\pi^2} \right) \sum_{L'} C(J1L';00) \alpha_{LL'}^J(q,q') \sum_{L''} C(J1L'';00) A^{(L'',J)}(q') \,, \tag{2}$$

where the polarizability (or self-energy) coefficients $\alpha_{LL'}^J$ are defined as in ref. [1] and the source multipoles $o^{(L,J)}$ are reduced matrix elements of the spin-flip isospin-flip operator.

It is instructive to convert the $A^{(L,J)}$ multipoles into transverse and longitudinal components $A_t^{(J)}$ and $A_\varrho^{(J)}$:

$$A_t^{(J)}(q) = \sqrt{2} \sum_L C(J1L;1,-1) A^{(L,J)}(q), \quad A_\varrho^{(J)}(q) = \sum_L C(J1L;00) A^{(L,J)}(q). \tag{3}$$

With convenient proportionality factors, these quantities yield, respectively, the intrinsic spin part of the magnetic form factor and the nuclear pion field (through PCAC) for the multipolarity J. Contracting in the same way the L indices of $\alpha_{LL'}^J$ with Clebsch–Gordan coefficients we can define the polarizabilities α_{tt}^J, $\alpha_{\varrho\varrho}^J$, $\alpha_{\varrho t}^J$ and $\alpha_{t\varrho}^J$. We get then a new version of eq. (2):

$$A_t^{(J)}(q) = -g_A \, o_t^{(J)}(q) + \int dq' \, \frac{q'^2}{(2\pi)^3} \left(g' - C_\rho \, \frac{q'^2}{q'^2 + m_\rho^2} \frac{v_\rho^2}{v_\pi^2} \right) \alpha_{tt}^J(q,q') A_t^{(J)}(q')$$

$$+ \int dq' \, \frac{q'^2}{(2\pi)^3 m_\pi^2} \, [g'(q'^2 + m_\pi^2) - q'^2] \alpha_{t\varrho}^J(q,q') A_\varrho^{(J)}(q') \,,$$

$$(1 + q^2/m_\pi^2) A_\varrho^{(J)}(q) = -g_A \, o_\varrho^{(J)}(q) + \int dq' \, \frac{q'^2}{(2\pi)^3 m_\pi^2} \, [g'(q'^2 + m_\pi^2) - q'^2] \alpha_{\varrho\varrho}^J(q,q') A_\varrho^{(J)}(q') \tag{4}$$

$$+ \int dq' \, \frac{q'^2}{(2\pi)^3} \left(g' - C_\rho \, \frac{q'^2}{q'^2 + m_\rho^2} \frac{v_\rho^2}{v_\pi^2} \right) \alpha_{\varrho t}^J(q,q') A_t^{(J)}(q') \,.$$

It is apparent that the rho and pion parts of the interaction are associated under the integrals with the transverse and longitudinal multipoles. Concentrating on the equation for the transverse form factor one can see that the rho meson induces an effective suppression of g' at large momenta (at $q = 3m_\pi$ the reduction amounts already to 0.58). Such a quenching of the Lorentz–Lorenz effect is precisely the ingredient that was needed in our previous work to suppress the rapid drop of the M1 form factor at large transfers. As for the longitudinal part, i.e. the pion field, it is not affected directly by the rho meson but only through its coupling to A_t. There is no simple way to predict how it will be modified. However in the nuclear matter limit $\alpha_{LL'}^J \sim \delta_{LL'} \delta(q - q')$, the nondiagonal polarizabilities $\alpha_{\varrho t}$ and $\alpha_{t\varrho}$ vanish and the two equations decouple. The rho meson does not influence any longer the pion propagation (except for the effects incorporated into g'). Conversely the pion field disappears from the equation

of the transverse form factor which does not therefore offer a detector for critical opalescence in the limit of large nuclei.

We have solved eqs. (2) in the particular case of the M1 transition to the 15.11 MeV ($T = 1$) state of ^{12}C. The solutions for the pion field are practically unchanged compared to our previous study. In particular the critical value of g' stays at 0.265 [+] (for the same oscillator length $b = 1.65$ fm). On the other hand the transverse form factor is more strongly affected as is apparent in fig. 2 where the curves with (solid curve) and without (long dashed curve) rho meson are presented for $g' = 0.39$, the value which reproduces best the recent precision data obtained at Mainz [4] and MIT [5] (the pair and pion exchange currents have been added as in ref. [1]). The two curves differ appreciably in the whole region of the second maximum. Especially striking is the difference in the behaviour at large momenta. The agreement of our new description with experiment is quite good in the entire range of momentum transfer except for some underestimation at large momenta (note also that on the low momentum side we find a width of 32.6 eV to be compared with the measured 37 ± 1.1 [6]). Our number for g' is not far from our previous best fit but the difference in the pion field enhancement is significant (a factor 4.5 compared to 10 in ref. [1]). One needs now less pronounced critical effects to explain experiments but nevertheless our favoured value of g' remains outside the accepted range (let us recall for instance that microscopic calculations [7,8] in nuclear matter show that a "strong" rho coupling leads to values of g' in the range 0.6 to 0.8). For comparison we have also plotted in fig. 3 the curve for $g' = 0.5$, a value marginally consistent with expectations. It certainly fails to fit the data though it represents a strong improvement over the Cohen–Kurath description.

In order to give a feeling for the need of the field enhancement we have suppressed the opalescence phenomena in the solution of the system (2) by imposing a bare pion propagator. This procedure amounts practically to a cal-

[+] Due to a change in the Δ coupling constant, one should not compare directly the present numbers with the values of g' given in ref. [1] (for instance the critical g' was 0.335).
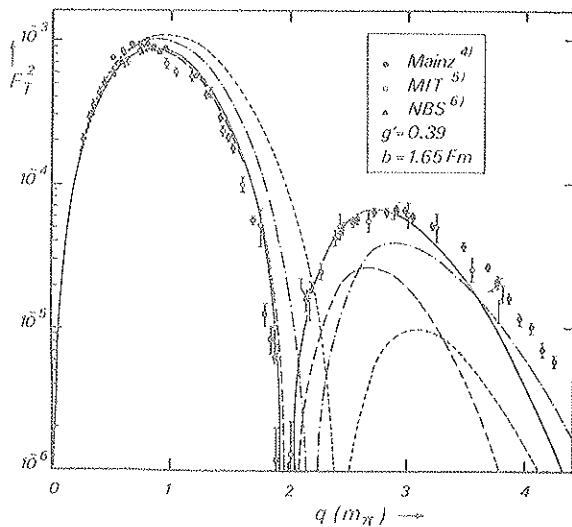

Fig. 2. The square of the M1 form factor of the 15.1 MeV ($T = 1$) state of ^{12}C. The various curves have been defined in the text except the short dashed one which represents a one-body calculation with the 8–16 2 BME Cohen–Kurath interaction. Note that the Mainz data are preliminary and correspond to a q_{eff} plot so that distortion effects may explain the slight discrepancy at low momentum with the MIT data (older data are shown in ref. [1]).
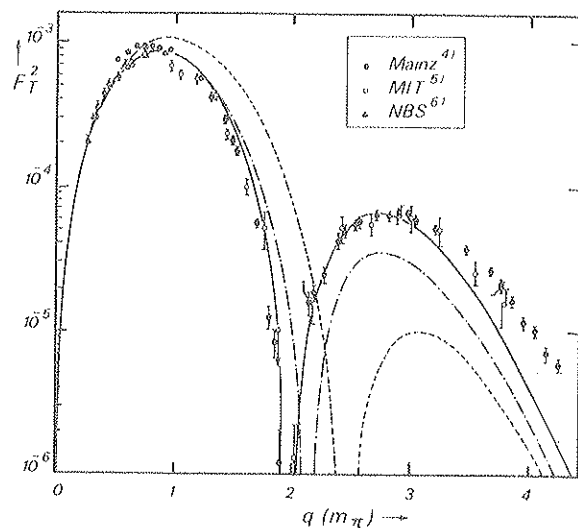

Fig. 3. The square of the M1 form factor for $g' = 0.39$ (solid curve) and $g' = 0.50$ (dot–dashed). The same one-body calculations as in fig. 2 (short dashed) are also shown for reference.

culation of core polarization on a large particle–hole and Δ–hole basis. The results are plotted in fig. 2 again for g' = 0.39 (dot–dashed curve). The large effect obtained at high momenta, in contrast with our previous work, exhibits the crucial role of the γ–rho conversion (fig. 1). The curve is very similar to that obtained in the recent work of Sagawa et al. [9] who used a mixture of Rosenfeld and Hamada–Johnston interactions as the polarizing potential. It shows considerable improvement over the Cohen–Kurath one but cannot fit the experiments, especially in the region of the form factor minimum. The collective opalescence phenomena appear clearly as a bump over the core polarization and displace the diffraction minimum to lower momenta. They are needed to reproduce both the size of the second maximum and the position of the minimum. As g' increases the field enhancement becomes less pronounced, the opalescence effects are less and less marked: at g' = 0.5 they cause only slight deviations from the core polarization curve.

The present investigation shows that the polarization of the nuclear medium is a good candidate to explain the anomaly observed in ^{12}C. In order to reproduce the detailed behaviour of the measured form factor, in particular near the diffraction minimum and the secondary maximum, a large opalescence of the pion field would be needed i.e. a factor 4.5 enhancement. We insist however that we do not consider that the M1 form factor shows firm and definite evidence for critical phenomena. The low value of the Migdal parameter g' remains very intriguing and it is important to check that the resulting effective interaction is not in conflict with the observed position of pion-like levels. We also have to prove the validity of our simple model for other transitions. Such investigations are in progress. Moreover it is not excluded that the final explanation of the ^{12}C anomaly resides in less exotic nuclear physics refinements.

Finally we would like to comment on an important result of our study which survives even if one renounces to interpret the M1 data in terms of critical opalescence. We have shown that the critical behaviour of the pion field has an observable influence on the transverse form factor of ^{12}C only if g' is smaller than 0.5. However the longitudinal multipoles, i.e. those of the field itself still present large enhancements at g' = 0.5 or 0.6 (factors 3 or 2, respectively, in the critical region) which should be detectable with other spin-sensitive probes.

References

[1] J. Delorme, M. Ericson, A. Figureau and N. Giraud, preprint LYCEN 7953 (1979).
[2] G. Baym and G.E. Brown, Nucl. Phys. A247 (1975) 395.
[3] G. Höhler and E. Pietarinen, Nucl. Phys. B95 (1975) 210.
[4] R. Neuhausen, private communication.
[5] J.B. Flanz, private communication to J.P. Deutsch.
[6] B.T. Chertok, C. Sheffield, J.W. Lightbody, S. Penner and D. Blum, Phys. Rev. C8 (1973) 23.
[7] G.E. Brown, S.O. Bäckman, E. Oset and W. Weise, Nucl. Phys. A286 (1977) 191.
[8] S.O. Bäckman and W. Weise, in: Mesons in nuclei, Vol. III, eds. M. Rho and D.H. Wilkinson (North-Holland, Amsterdam, 1979) p. 1095.
[9] H. Sagawa, T. Suzuki, H. Hyuga and A. Arima, Nucl. Phys. A322 (1979) 361.

Article II-4

PION COUPLING CONSTANTS IN NUCLEI
AND THE ISOBAR-HOLE MODEL

J. DELORME, A. FIGUREAU and N. GIRAUD

Institut de Physique Nucléaire (et IN2P3), Université Claude Bernard Lyon-I,
43, Bd du 11 Novembre 1918, 69622 Villeurbanne Cedex, France

Abstract: We discuss the relevance of the on-shell pion–nucleus coupling constants to modern theories of pion and isobar degrees of freedom in nuclei. The excitation of specific transitions is first considered and the on-shell coupling constant is shown to carry other information than the familiar Gamow–Teller constant measured in β-decay; we present a critical discussion of the scarce existing determinations which are at considerable variance with our theoretical expectations. Next, the sum rule for the "effective" pion–nucleus coupling constant is calculated and predicted to be drastically reduced by Δ-hole renormalization of the pion propagator besides the Lorentz–Lorenz effect. Dispersion relations strongly favour the validity of the model.

1. Introduction

The study of spin degrees of freedom is one of the most exciting problems of modern day nuclear physics. Among the prominent results of the last few years is the discovery of giant Gamow–Teller resonances in medium to heavy nuclei [1], the long-searched-for collective manifestation of the nuclear force in the spin–isospin channel [2,3] ($\Delta S = 1, \Delta T = 1$). The experiments point to a strong repulsive component of the interaction at low momenta $g'\sigma_1 \cdot \sigma_2\tau_1 \cdot \tau_2$ ($g' \sim 0.6$–0.7) which would moreover explain the non-observation of a large fraction of the spin strength through a coupling to the Δ-resonance [4-14] (Lorentz–Lorenz effect). In contradistinction a careful examination of the properties of unnatural-parity transitions revealed no track of collectivity at larger momenta ($q > m_\pi$) where the one-pion exchange attraction overbalances the g' repulsion [15,16]. The overall force remains indeed too weak to produce those collective features characteristic of attraction which would be the precursors to pion condensation. As a consequence the pion component manifests itself only indirectly by the suppression of the repulsive component of the force.

The purpose of this paper is to point out the relevance of the on-shell pion–nucleus coupling constant to direct manifestations of pion exchange. It is an extension of an already published work [7,17] on the role of the axial polarizability of the nuclear medium (more precisely its Δ-isobar part) where it was signaled that besides the familiar Lorentz–Lorenz quenching, the effective pion-nucleus coupling constant undergoes an extra reduction from the pion propagation itself. There is moreover a great need for clarification due to a number of misleading or even inexact

510   J. Delorme et al. / Pion coupling constants

statements which have been published on this relatively unexplored subject. As the pion pole does not lie in the physical region, the on-shell coupling constants are accessible through extrapolation of measured quantities or dispersion relations [18,19]. The first possibility has recently been exploited with conformal mapping techniques [20] which have allowed the extraction of values relevant to several transitions in light nuclei from precise charge exchange experiments. As for dispersion relations they have been limited up to now to a couple of very light nuclei [see e.g. ref. [21]; a complete review is given in ref. [19])] due to the difficulty of subtracting Coulomb effects from the measured π-nucleus total cross sections and scattering lengths. One can however reasonably hope that progress in the understanding of π-nucleus interaction will permit soon the exploitation of the measurements which are available in a number of nuclei.

The paper is organized as follows. Pion-nucleus vertices are introduced in sect. 2 and define the coupling constants. Expressions are given under the hypothesis of additivity of the nucleon contributions (impulse approximation). Sect. 3 is devoted to the estimation of the modifications brought in by the nuclear polarizability for specific transitions in ^{12}C and ^{6}Li with particular emphasis on the Δ-isobar component which can be viewed as a part of the meson exchange renormalization. The results are compared to the numbers recently obtained by extrapolation. A critical discussion follows. The sum rule for the effective pion pole which is needed in dispersion relations is derived in sect. 4 and predicted to be strongly reduced in heavy nuclei. A comparison with available information is then presented.

2. The pion–nucleon vertices

The pion–nucleus vertex function (fig. 1) $(q, \omega \equiv P' - P, E' - E)j_\pi(q, \omega) \equiv \langle P'|j_\pi|P\rangle = (q^2 - \omega^2 + m_\pi^2)\langle P'|\phi_\pi|P\rangle$ is usually defined on a cartesian basis in the "elementary particle" description [22,23] where the nuclear states are simply characterized by their spins and momenta in analogy with the expression appropriate to nucleons:

$$j_\pi^\pm(q, \omega) = -\frac{f_r\sqrt{2}}{m_\pi} v(q^2 - \omega^2) i\bar{u}'(P')\gamma_\mu\gamma_5\tau^\pm u(P)q_\mu. \tag{1}$$

Here $f_r^2/4\pi = 0.08$; $v(q^2 - \omega^2)$ is a form factor normalized at the pion pole $(v(-m_\pi^2) = 1)$ and the factor $\sqrt{2}$ is relevant to the case of charged pions. Such a
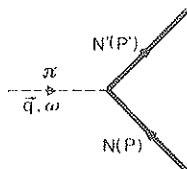

Fig. 1. The π-nucleus vertex.

basis has however a non-unique character except for the simplest cases $(\frac{1}{2}-\frac{1}{2}$; $0^+ - 1^+; \ldots)$. We prefer the use of an universal multipole expansion which is more transparent for comparison to nuclear models. It takes the following form for a transition between nuclear states with spins j, j' and z-axis projections m, m':

$$j_\pi(q, \omega) = \sum_J (-)^{m'-m} C(jJj'; m, m'-m) \sqrt{\frac{4\pi}{2j'+1}} Y_{J,m-m'}(\hat{q})(iq)^J \left[\frac{f_{\pi NN'}^{(J)}}{m_\pi}(q, \omega)\right].$$

(2)

The kinematic factor $(iq)^J$ has been extracted so that the coupling constants $f_{\pi NN'}^{(J)}$ remain finite at $q = 0$ and obey the usual reality conditions under time reversal. The values of J are limited to unnatural parity (i.e. magnetic) multipoles $(0^-, 1^+, 2^-, \ldots)$ corresponding to pion-like transitions. In this formalism it is quite easy to compute the coupling constants in the impulse approximation, i.e. under the assumption that the vertex is composed with the addition of nucleon contributions. Taking for the non-relativistic limit of eq. (1) $-i\bar{u}'\gamma_\mu\gamma_5 u q_\mu \approx \boldsymbol{\sigma} \cdot \boldsymbol{q}$ which is generally valid for transitions of low excitation (this approximation can break near $q = 0$ for the special case $J = 0$, see below), one finds:

$$[f_{\pi NN'}^{(J)}(q, \omega)]_{IA} \approx f_\pi\sqrt{2}v(q, \omega)\left[\sqrt{\frac{J}{2J+1}}\sigma^{(J-1,J)}(q) + \sqrt{\frac{J+1}{2J+1}}\sigma^{(J+1,J)}(q)\right]\Big/q^{J-1},$$

(3)

where the reduced matrix elements of the spin operator $\sigma^{(L,J)}$ are as usual:

$$\sigma^{(L,J)}(q) = \left\langle j' \left\|\sum_i \tau_i^\pm j_L(qx_i)\sqrt{4\pi}[Y_L(\hat{x}_i)\otimes\sigma_i]^J\right\| j\right\rangle.$$

(4)

Note that at $q = 0$, the $J = 0$ form factor is no longer determined by eq. (3) but rather by the multipoles of $\boldsymbol{\sigma} \cdot \boldsymbol{p}/2m_p$ which are characteristic of the time component of the axial current (m_p, p = nucleon mass and momentum). From the axial vector matrix elements we define further Gamow–Teller multipoles $f_{ANN'}^{(L,J)}$ which in the impulse approximation reduce to $g_A\sigma^{(L,J)}/q^L$. Using PCAC and neglecting the small (except for $J = 0$) time component, one gets a Goldberger–Treiman relation:

$$f_{\pi NN'}^{(J)}(q = 0) = \frac{m_\pi}{f_\pi}\sqrt{\frac{J}{2J+1}}f_{ANN'}^{(J-1,J)}(q = 0) \qquad J \neq 0,$$

(5)

with f_π (pion decay constant) $= 0.944m_\pi$. Therefore β-decay measurements when available are informative on π-nucleus vertices at zero momentum. The on-shell coupling constants $f_{\pi NN'}^{(J)} \equiv f_{\pi NN'}^{(J)}(q^2 - \omega^2 = -m_\pi^2)$ which are our present concern correspond to the pion pole $q^2 - \omega^2 = -m_\pi^2$, i.e. to a non-physical imaginary value of the momentum transfer $q = i\sqrt{m_\pi^2 - \omega^2} \approx im_\pi$ for low-lying transitions (static limit). The question then arises: which sort of variation should one expect between $f_{\pi NN'}^{(J)}$ and $f_{\pi NN'}^{(J)}(q = 0)$? In the case of nucleons an extrapolation distance of m_π^2

is rather small compared to the usual hadronic scales and there is not much difference between the two points. This is not true for nuclei due to their larger size. To illustrate this point, let us consider the transition $0^+ - 1^+(\Delta T = 1)$ between the ground states of ^{12}C and ^{12}B (or ^{12}N) that we assume for this specific purpose to have a simple $(p_{3/2})^{-1}p_{1/2}$ particle–hole structure. In the impulse approximation and with harmonic oscillator wave functions, one gets:

$$f_{\pi^{12}C^{12}B}^{(J=1)}(q, \omega \approx 0.1 m_\pi) = \tfrac{4}{3}f_r\sqrt{2}v(q, \omega)(1 - \tfrac{1}{4}q^2b^2)\,e^{-q^2b^2/4} \tag{6}$$

(corrections for centre-of-mass motion have been neglected). The ratio between the pole and β-decay points is thus in this model:

$$\frac{f_{\pi^{12}C^{12}B}}{f_{\pi^{12}C^{12}B}(0)} = (1 + \tfrac{1}{4}m_\pi^2b^2)\frac{e^{m_\pi^2b^2/4}}{v(0)}, \tag{7}$$

which is ~ 1.91 for $b = 1.65$ fm and a cut-off mass of 1.2 GeV in a monopole form-factor at the pion–nucleon vertex.

The origin of this rather large factor is easily understood. For imaginary arguments, the Bessel functions in eqs. (3) and (4) turn from circular to hyperbolic functions which grow monotonically, thus producing the sensible increase of the on-shell constant over the Goldberger–Treiman value. Equivalently, one can consider that for a pion source located at a point x_i, the decrease of the field is governed by the Yukawa function $Y(x, x_i) = e^{-m_\pi|x-x_i|}/|x - x_i|$. Only the asymptotic behaviour is needed to compute the residue at the pole since the rest of the function drops more rapidly than $e^{-m_\pi x}$ and does not give rise to a singularity at $q^2 = -m_\pi^2$: $Y(x \to \infty, x_i) = (e^{-m_\pi x}/x)\,e^{m_\pi x_i \cdot \hat{x}}$. Hence after suitable angular average, the standard factor $e^{-m_\pi x}/x$ gets multiplied by an exponentially rising function of x_i which integrated over the spin–isospin transition density gives the searched-for residue. The resulting enhancement of $f_{\pi NN'}^{(J)}$ is thus a trivial size (or nuclear form factor) effect. It is especially dramatic in heavy nuclei where the spin density peaks at large distances from the centre [this phenomenon is the analog of the size enhancement discussed in ref. [18] for potential scattering].

In view of this exponential weighting of the transition density, one can *a priori* wonder whether the tail of the wave functions plays a more important role than at real momentum transfer and question the use of the harmonic oscillator for the present purpose [cf. eq. (6)]. This problem is connected to the deeper criticism that gaussian form factors do not possess the correct analytic structure, in particular the logarithmic singularity of the triangle graph. Indeed, according to general arguments, the nearest singularity (anomalous threshold) of the pion–nucleus form factor is a branching point at $q_A^2 = -2m_p(\varepsilon^{1/2} + \varepsilon'^{1/2})^2$, ε and ε' being the binding energies of the last nucleon in the initial and final states. It turns out that a right asymptotic behaviour of the nuclear wave functions which is essential to produce the logarithmic singularity at q_A^2 is not yet crucial at the transfer $q^2 = -m_\pi^2$. Coming back to our previous example of the transition ^{12}C–^{12}B, we have replaced the

single-particle wave functions of the harmonic oscillator by those of a square well reproducing the binding energies $\varepsilon = 15.96$ MeV and $\varepsilon' = 3.37$ MeV. The size parameter has been adjusted so as to yield the same rms radius. We have found that the variation between $q^2 = 0$ and $-m_\pi^2$ is slightly more pronounced (by 2%) for the more realistic wave functions. This calculation shows that the anomalous threshold $q_A^2 = -3.28 m_\pi^2$ lies too far from the pole for its singularity structure to influence appreciably the on-shell coupling constant (remember that the variation is only logarithmic near the singularity). More appreciable deviations can however occur for more loosely bound nuclear states which have a branching point closer to $-m_\pi^2$. This is indeed the case for the analog transition between ^{12}C and ^{12}N where the threshold is located at $-2.73 m_\pi^2$: the coupling constant becomes 8% larger for the square-well wave functions.

3. Nuclear polarization effects

Only a limited number of on-shell pion-nucleus coupling constants is presently available [19,20]. They have been determined by extrapolation to the pion pole of angular distributions of charge exchange reactions for some $\frac{1}{2}^+ \to \frac{1}{2}^+$ ($\pi\,^3$H^{3}He) and $0^+ \rightleftarrows 1^+$ ($\pi\,^6$Li^{6}Be, $\pi\,^{12}$C^{12}N, $\pi\,^{14}$N^{14}O) transitions. Indeed, measurements of nuclear reactions which can proceed through pion exchange do not probe the time-like region. They can be informative on pion-nucleus vertices at various space-like transfers but it is necessary to perform an *extrapolation* to get the relevant residue or on-shell coupling constant. As an example, the $q^2 = 0$ point can be extracted through PCAC from forward-angle charge exchange but it lies too far from the pole to give *alone* a precise idea of the magnitude of the residue for reasons connected with the large size effect discussed in sect. 2. This warning applies *a fortiori* to the $q^2 = +m_\pi^2$ point attained by pion photoproduction at threshold [24].

We will not give consideration here to the results of the $A = 14$ nuclei because of the difficulty for reproducing the practically complete cancellation of the multipole $\sigma^{(0,1)}$ at $q = 0$. We treat mainly the $A = 12$ system and give some comments relative to $A = 3$ and 6. In order to facilitate the comparison with the most recent works which use a cartesian basis with different normalizations, it is useful to make the correspondence with our multipole coupling constants (only the multipolarity $J = 1$ is relevant for the spin values considered here):

$$\text{for } \tfrac{1}{2}^+ - \tfrac{1}{2}^+ \quad \frac{[f^{(J=1)}_{\pi\,^3\text{He}^3\text{H}}]^2}{4\pi} = 2m_\pi^2 \frac{[f_{\pi\,^3\text{He}^3\text{H}}]^2_{\text{Primakoff}[25]}}{4\pi} = 4[f_{\pi\,^3\text{He}^3\text{H}}]^2_{\text{Dumbrajs}[20]}$$

$$\text{for } 0^+ - 1^+ \quad \frac{[f^{(J=1)}_{\pi\text{NN}'}]^2}{4\pi} = 2m_\pi^2 \frac{[f_{\pi\text{NN}'}]^2_{\text{Primakoff}[25]}}{4\pi} = 4[f_{\pi\text{NN}'}]^2_{\text{Dumbrajs}[20]}$$

$$= 4\left[\frac{g^2_{\pi\text{NN}'}}{4\pi}\frac{m_\pi^2}{4MM'}\right]_{\text{Moake et al.}[26]}, \tag{8}$$

where in the last expression M and M' stand for the nuclear masses. It is rather trivial to note that the magnitude of these constants has no direct relation to the value 0.16 ($= 2f_\pi^2/4\pi$) relevant to nucleons. Any estimation has to go through the standard arsenal of nuclear physics so that even in the simplest models, nuclear structure effects and size enhancement render meaningless any comparison to the nucleon value. This is no longer true in the case of sum rules as will be discussed in sect. 4.

The multipoles for the 1p shell nuclei $A = 6$ and 12 have been obtained in the one-body approximation through eq. (3) where the spin matrix elements have been evaluated with Cohen–Kurath wave functions (8–16 2BME) and harmonic oscillator

TABLE 1

The squared on-shell pion coupling constants for $A = 12, 6, 3$

	IA	IA + polarization	EP	Conformal mapping
$[f_{\pi^{12}C^{12}N}^{(J=1)}]^2/4\pi$	0.182	0.176	$0.300^{+0.200\,a}_{-0.150}$	0.016 ± 0.004
$[f_{\pi^6Li^6Be}^{(J=1)}]^2/4\pi$	1.30	1.27		0.280 ± 0.024
$[f_{\pi^3He^3H}^{(J=1)}]^2/4\pi$	0.516		0.413 ± 0.042	0.22 ± 0.08

The columns labelled IA, IA + polarization, EP refer respectively to calculations in the impulse approximation without and with polarization corrections (present work) and in the elementary particle treatment [25] [the superscript ^{a}) indicates that the quoted number applies to the analog $\pi^{12}C^{12}B$ transitions]. The last column presents the results obtained by extrapolation of measured cross sections [20].

orbitals. The results are given in table 1 (1st column) and compared to the extrapolated numbers of Dumbrajs (4th column) converted into our notations via the relations (8). We have added an estimate for $A = 3$ using only space-symmetric S-state wave functions with a gaussian form. In all the three cases there is a striking disagreement which attains an order of magnitude for $A = 12$. The difference is so large that a change of wave functions would not much improve the situation. In any case one should realize that our present description already does fairly well at zero transfer: the β-decay rates are overestimated by only 8.5, 8.1 and 5.7% for $A = 12, 6$ (in the case of the analog $^6He \to ^6Li$ transition) and 3 respectively. Variation of the length parameters would not cure the discrepancy either. To take the example of ^{12}C, we have tried two different length parameters adjusted from Hartree–Fock calculations in order to simulate the different radial behaviour of the $p_{3/2}$ and $p_{1/2}$ orbitals [27]. The result is an increase of at most 10% of the squared constant! We can also recall that as shown in the preceding section, orbitals with a correct asymptotic behaviour are expected to modify only slightly the calculated numbers and again in the upward direction.

Remarking that the discrepancy factor increases (linearly) with A, one could tentatively invoke nuclear medium effects breaking the impulse approximation. It is however unlikely that factors as huge as those needed to reconcile the first and

last columns of table 1 can be produced by phenomena such as meson exchange or core polarization. For instance in the case of β-decay the modifications to the one body estimates for the considered nuclei are at the level of 10% or less [28]) and no spectacular increase is to be expected at $q^2 = -m_\pi^2$ since the one-body form factors for these transitions have no zero in the time-like region. This guess is borne out by the calculations presented below.

We treat here the medium effects generated by the nuclear polarizability in a particle–hole approximation. One accounts in this way for core polarization and Δ-isobar components in the nucleus by a RPA-like iterated procedure, a formalism which has been developed for the study of precursors to pion condensation (critical opalescence) and that we recall briefly [29]). Standard first-order calculations would however be good approximations under the normal density conditions which are now believed to be far from critical. It was shown that the high-lying (and Δ-isobar) components admixed into the nuclear wave functions by the spin–isospin forces could be taken into account via a renormalization of the spin matrix elements (4). The two renormalized spin multipoles for a given J were obtained in the static limit (i.e. $\omega = 0$) as solutions of coupled integral equations with the one-body expression (4) as source terms and kernels constructed from the polarizability and the interaction in the $\sigma_1 \cdot \sigma_2 \tau_1 \cdot \tau_2$ channel. It is convenient to introduce the following orthogonal combinations of L indices which are appropriate to the matrix elements of spin projections on axes which are longitudinal $(\sigma \cdot \hat{q})$ or transverse $(\sigma \wedge \hat{q})$ with respect to the momentum:

$$\sigma_l^J(q) = \sqrt{\frac{J}{2J+1}}\,\sigma^{(J-1,J)} + \sqrt{\frac{J+1}{2J+1}}\,\sigma^{(J+1,J)},$$

$$\sigma_t^J(q) = \sqrt{\frac{J+1}{2J+1}}\,\sigma^{(J-1,J)} - \sqrt{\frac{J}{2J+1}}\,\sigma^{(J+1,J)}. \tag{9}$$

One has similar expressions for the renormalized multipoles that we denote Σ_l^J and Σ_t^J.

Polarization (particle–hole as well as Δ-hole) insertions $\alpha_{\mu\mu'}(q, q')$ with spin operators σ_μ and $\sigma_{\mu'}$ at the vertices (fig. 2) define multipoles $\alpha_{LL'}^J(q, q')$:

$$\alpha_{\mu\mu'}(q, q') = \sum_{LL'Jm} (-)^\mu C(L1J; m-\mu, \mu) C(L'1J; m+\mu', -\mu')$$

$$\times Y_{L,\mu-m}(\hat{q}) Y_{L',-\mu'-m}^*(\hat{q}')\alpha_{LL'}^J(q, q'). \tag{10}$$

Fig. 2. The polarization insertions (nucleon–hole and Δ-hole).

Playing the same game as before with each of the two L indices, one obtains the longitudinal polarizability $\alpha^J_{\ell\ell}(q, q') = \sum_{LL'} C(J1L; 00)C(J1L'; 00)\alpha^J_{LL'}(q, q')$ and the transverse one $\alpha^J_{tt}(q, q') = 2 \sum_{LL'} C(J1L; +1, -1)C(J1L'; +1, -1)\alpha^J_{LL'}(q, q')$ as well as mixed multipoles $\alpha_{\ell t}$ and $\alpha_{t\ell}$. Finally the particle–hole interaction in the spin–isospin channel is decomposed into longitudinal and transverse parts:

$$V_{\sigma\tau}(q) = [V_\ell(q)\sigma_1 \cdot \hat{q}\sigma_2 \cdot \hat{q} + V_t(q)(\sigma_1 \wedge \hat{q}) \cdot (\sigma_2 \wedge \hat{q})]\tau_1 \cdot \tau_2, \qquad (11)$$

so that a schematic form comprising a short-range Landau–Migdal interaction in addition to the prominent π- and ρ-meson exchanges gives:

$$V_\ell(q) = \frac{f_r^2}{m_\pi^2}\left(g' - \frac{q^2}{q^2 + m_\pi^2}\right)v^2(q), \qquad V_t(q) = \frac{f_r^2}{m_\pi^2}\left(g' - C_\rho(q)\frac{q^2}{q^2 + m_\rho^2}\right)v^2(q), \qquad (12)$$

where C_ρ is the ratio $f_r^2 m_\rho^2 v^2(q)/f_\rho^2 m_\pi^2 v_\rho^2(q)$ between the ρ- and π-nucleon vertex factors.

The fundamental equations are then put into the form:

$$\Sigma^J_\ell(q) = \sigma^J_\ell(q) + (2\pi)^{-3}\int dq'q'^2[\alpha^J_{\ell\ell}(q, q')V_\ell(q')\Sigma^J_\ell(q') + \alpha^J_{\ell t}(q, q')V_t(q')\Sigma^J_t(q')],$$

$$\Sigma^J_t(q) = \sigma^J_t(q) + (2\pi)^{-3}\int dq'q'^2[\alpha^J_{tt}(q, q')V_t(q')\Sigma^J_t(q') + \alpha^J_{t\ell}(q, q')V_\ell(q')\Sigma^J_\ell(q')]$$

$$(13)$$

[note a slight difference with respect to our previous works [29]: for convenience $v(q)$ form factors have been taken out from the α- and Σ-multipoles]. The renormalized pion–nucleus multipoles $f^{(J)}_{\pi NN'}(q)$ are readily obtained from the analog of the one-body expression (3):

$$f^{(J)}_{\pi NN'}(q) = f_r\sqrt{2}v(q)\Sigma^J_\ell(q)/q^{J-1}, \qquad J \neq 0. \qquad (14)$$

As for the transverse partners Σ^J_t, they are associated with e.g. the multipoles $f^{(J)}_{\rho NN'}$ of the rho-nucleus vertex. The coupling between the longitudinal and transverse spin modes is however generally weak because the mixed polarizabilities $\alpha_{\ell t}$ and $\alpha_{t\ell}$ are typically one order of magnitude smaller than $\alpha_{\ell\ell}$ and α_{tt}. The equations (13) practically reduce to separate equations for the pion- and rho-nucleus vertices. This approximation will be used in the next section for an application to the effective pole sum rule.

For the present purpose, the equations (13) are first solved for any space-like value of the momentum q. The residues $f^{(J)}_{\pi NN'}$ are then obtained by analytical continuation of the first equation in the complex q-plane till $q = im_\pi$. The calculations have been performed with the values $g' = 0.6$ and 0.7 which are in the range favoured nowadays [16]. We have excluded the three-body system which is too light to justify the use of the present methods and deserves a more accurate treatment.

TABLE 2

The squared on-shell pion coupling constants for $A = 12$ and 6 as a function of the parameter g' characteristic of the short-range repulsion

	$f^2(q^2 = -m_\pi^2)/4\pi$	
	$g' = 0.6$	$g' = 0.7$
$A = 12$	0.176 (0.134)	0.164 (0.129)
$A = 16$	1.27 (1.17)	1.24 (1.16)

The numbers inside parentheses correspond to the case where polarization effects are limited to the Lorentz–Lorenz quenching.

Among the 1p shell nuclei $A = 6$ and 12, the last case is the most significant in view of the difficulties in a pure shell-model description of $A = 6$. The results are given in table 2 and repeated in the second column of table 1 for $g' = 0.6$. The renormalization appears to be weak in agreement with our previous expectations. We observe a cancellation between the nucleon and Δ-components of the polarization corrections. In order to give an idea of their individual size, we have kept only the Δ-contribution with an interaction reduced to the repulsive g' term. One isolates in this way the famous Lorentz–Lorenz quenching[4-14]) which has recently been pushed forward as an attractive candidate to explain the observed reduction of both the magnetic[10]) and Gamow–Teller[1]) strengths in medium to heavy nuclei. The numbers are given inside parentheses in table 2 for each value of g'. The effect is rather sizeable for $A = 12$ where the quenching attains 26% (29%) for $g' = 0.6$ (0.7). The moderate 10% reduction for $A = 6$ is to be attributed to the diffuseness of this nucleus, the Lorentz–Lorenz phenomena producing a local, density-dependent renormalization.

For comparison we display in table 3 the percentages of renormalization calculated at the pole and at zero transfer. One remarks that the overall quenching is much more pronounced in the second case though the Lorentz–Lorenz effect (given

TABLE 3

Comparison between the relative renormalization of the squared coupling constants on the mass-shell $(q^2 = -m_\pi^2)$ and at zero transfer $(q^2 = 0)$

	$(\Delta f^2/f^2)\|_{q^2 = -m_\pi^2}$		$(\Delta f^2/f^2)\|_{q^2 = 0}$	
	$g' = 0.6$	$g' = 0.7$	$g' = 0.6$	$g' = 0.7$
$A = 12$	−3.3% (−26%)	−10% (−29%)	−22% (−31%)	−25% (−34%)
$A = 6$	−2.3% (−10%)	−4.6% (−11%)	−11% (−13%)	−12% (−14%)

The parentheses refer as before to the Lorentz–Lorenz effect.

as before inside parentheses) has not changed much. This is due to the disappearance of the nucleon contribution or in other words the trivial vanishing of the core polarization at $q^2 = 0$. Hence there is a new information carried by the pion coupling constant at the pole: most of the Lorentz–Lorenz quenching is cancelled between the β-decay point and $q^2 = -m_\pi^2$ due to core polarization effects. An experimental observation of this predicted behaviour would be of importance for the validity of modern models for pion propagation in the nuclear medium.

However, as can be seen in tables 1 and 2, the size of any part of the polarization modifications is by far insufficient to explain the disagreement with the extrapolated coupling constants. One can argue that we have considered only a specific part among the possible mesonic corrections and wave function admixtures. Our belief is that none of the usually considered meson contributions can produce the needed tremendous decrease. It is important to realize that one would need a physical effect rapidly varying with the transfer, since it should be small at zero momentum to retain agreement with β-decay. Even more so, comparison with the latter reveals that the extrapolation methods assign to the squared π-nucleus form factors values which are lower on-shell than at $q = 0$ in the cases $A = 12$ (by a factor 3!) and $A = 3$, the two numbers staying about equal for $A = 6$. This behaviour is in complete opposition to all standard computations which predict a monotonic increase in the time-like region. This increase which should stop at the anomalous threshold singularity is the natural continuation of the decrease calculated and observed in the space-like or physical region (with however one zero in the 1p shell case). Actually one should note that comparison to experiment is not so easy even at $q^2 > 0$, because the longitudinal spin form factors Σ_ℓ^I are only occasionally accessible in contrast with the transverse ones which are commonly explored by electron scattering. The information available from (p, n) [26] or the analog (p, p') [30] reactions shows that they follow the predicted shape with rather moderate deviations at transfers $q^2 > 2m_\pi^2$. The transverse partners are also reasonably well reproduced at $q^2 \lesssim m_\pi^2$ with more sensible discrepancies at larger transfers [31]. In our opinion, one can therefore be confident that the same theory should be rather successful till $q^2 = -m_\pi^2$ since a major accident is practically excluded on such a small momentum range. We can also mention that our results are roughly in agreement with semiphenomenological estimates [25] following the "elementary particle approach" (see 3rd column of table 1).

It should be clear however that we do not claim that a π-nucleus form factor $f_{\pi NN'}(q)$ cannot decrease in the time-like region. Actually, there exist nuclear transitions which have this property. Again in the 1p shell, a pure $p_{1/2} \to p_{1/2}$ transition has a form factor which in the one body approximation varies as $v(q)(1 + \frac{1}{2}q^2 b^2) e^{-q^2 b^2/4}$ to be compared to $v(q)(1 - \frac{1}{4}q^2 b^2) e^{-q^2 b^2/4}$ which is appropriate to $p_{3/2} \to p_{1/2}$, a structure which is dominant for $A = 12$. In the first case, the form factor decreases (at $q^2 < 0$) till a zero which is in the region of the pion pole. One can thus expect a very small on-shell coupling constant for e.g. $^{13}C \to$

^{13}N(g.s.) (however meson corrections are likely to be relatively more important than in our present estimations). It is evident however that this sort of behaviour is characteristic of a particular structure which is certainly not relevant to the nuclei considered in the present paper.

All we can conclude is that within our present knowledge of nuclear structure one cannot understand the findings of extrapolation methods, especially the huge discrepancy for $A = 6$ and 12. If the numbers are to be taken seriously, the explanation should lie in a completely unexpected mechanism with strange momentum transfer properties, a possibility which we find unlikely. Though we do not feel fully competent to criticize the techniques of ref.[20]), we suggest that the precision on the determined coupling constants might have been considerably overestimated. Indeed the nuclear (p, n) cross sections used there have generally a rapid variation with momentum transfer so that an extrapolation distance of m_π^2 might lead to important errors especially when one realizes that the one-pion exchange contribution never dominates in the physical region and even vanishes at $q^2 = 0$†.

It is likely that an improvement of the experimental precision and maybe the extension of the covered angular range may be required to keep the uncertainty inside reasonable limits. We believe that efforts beyond the first attempts are still to be made before useful information on the on-shell pion coupling constants can be obtained with extrapolation techniques.

In view of these difficulties, one could think of direct determinations using peripheral reactions which are sensitive to the asymptotic nuclear pion field. This yet unexplored approach might be the most promising source of information about this elusive quantity.

4. The effective pion–nucleus coupling constant

As emphasized previously, dispersion relations provide a most powerful tool for the determination of the π-nucleus coupling constants in a region which is not directly attainable experimentally. Relatively few cases have been treated, however, due to the difficulties in extracting correctly Coulomb effects. The general method is well understood, and its developments for the pion–nucleus elastic scattering amplitude have been described with great details in the literature [18]). We will therefore skip all general considerations and attach our attention to the particular

---

† Actually, we have computed the (p, n) cross section on ^{12}C from an effective nucleon–nucleon interaction [32]) with good agreement with experiment [26]). It turns out that due to a much more rapid variation in the time-like region a quadratic extrapolation of the quantity $(q^2 + m_\pi^2)^2 (d\sigma/d\Omega)$ similar to that practised by Dumbrajs leads to considerable underestimation of the residue at the pole (with practically the same value as that found in his work). This model strongly suggests that a realistic extrapolation necessitates a higher polynomial expansion which was rejected in ref.[20]) in view of its low confidence level.

relation obtained for the spin–isospin antisymmetric π-nucleus scattering length, defined as the difference $(N-Z)a^{-} = \frac{1}{2}[a_{\pi^+} - a_{\pi^-}]$:

$$(N-Z)a^{-} = \frac{1}{4\pi m_\pi (2j+1)} \sum_{N'J} \frac{(\omega_{N'}^2 - m_\pi^2)^J [f_{\pi^+ NN'}^{(J)2} - f_{\pi^- NN'}^{(J)2}]}{\omega_{N'}^2 - m_\pi^2}$$

$$+ \frac{m_\pi}{4\pi^2} P \int_{\omega_0}^{\infty} d\omega \frac{q[\sigma_{\pi^+}(\omega) - \sigma_{\pi^-}(\omega)]}{\omega^2 - m_\pi^2}, \tag{15}$$

where $a_{\pi^\pm}$ and $\sigma_{\pi^\pm}$ are respectively the $\pi^\pm$-nucleus scattering lengths and total cross sections. The sum over N' runs over the pole terms (fig. 3) which correspond to the nuclear excited states lying below the pion threshold; these poles are located at $\omega_{N'} = \pm(\varepsilon_{N'} - m_\pi^2/2M)$, $\varepsilon_{N'}$ being the excitation energy of the state N' counted from the ground state N. It is especially important to note that the remaining sum over the possible multipolarities J is alternate ($\omega_{N'} \leqslant m_\pi$), according to the parity of the transition (since pionic transitions have unnatural parity, odd and even multipolarities occur with respectively positive and negative signs in eqs. (15) and (16)).
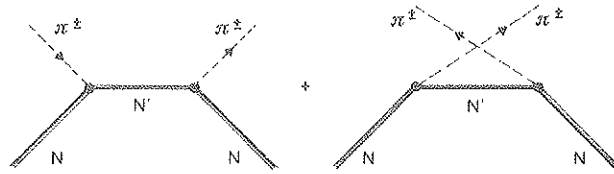

Fig. 3. The pole terms in the dispersion relation (15).

The individual contributions of the various poles would be difficult to resolve and it is customary to absorb them in an effective pole:

$$\frac{1}{2j+1} \sum_{N'J} (\omega_{N'}^2 - m_\pi^2)^{J-1} [f_{\pi^+ NN'}^{(J)2} - f_{\pi^- NN'}^{(J)2}] \equiv 2f_{\text{eff}}^2, \tag{16}$$

where f_{eff} defines the effective pion-nucleus coupling constant. The dispersion relation writes then:

$$(N-Z)a^{-} = \frac{2f_{\text{eff}}^2}{4\pi m_\pi} + \frac{m_\pi}{4\pi^2} P \int_{\omega_0}^{\infty} \frac{d\omega}{q} [\sigma_{\pi^+}(\omega) - \sigma_{\pi^-}(\omega)]. \tag{17}$$

The quantity f_{eff}^2 is of great interest as was shown long ago since one finds in a simple approximation that it is directly connected to the pion–nucleon constant f_r^2, independent of the nuclear structure [18]). This universal result, obtained through a sum rule, is valid as long as many-body contributions to the pion source function are not considered (impulse approximation).

Let us sketch briefly the derivation of the sum rule, following the treatment of Ericson and Locher [18]). The exact expression for f_{eff}^2 is:

$$f_{\text{eff}}^2 = \tfrac{1}{2} \sum_{N'} \frac{m^2}{\omega_{N'}^2 - m_\pi^2} \lim_{q \to q_{N'}} [|\langle N'(P+q)|j_\pi^+|N(P)\rangle|^2 - |\langle N'(P+q)|j_\pi^-|N(P)\rangle|^2] , \quad (18)$$

with $q_{N'}^2 = \omega_{N'}^2 - m_\pi^2$. In the impulse approximation, the matrix elements of the pion source are

$$\langle N'|j_\pi^+|N\rangle = \frac{f_r\sqrt{2}}{m_\pi} \left\langle N' \left| \sum_{i=1}^{A} \sigma_i \cdot q\tau_i^+ \, e^{iq\cdot x_i} \right| N \right\rangle v(q^2 - \omega^2) .$$

If one assumes that the nuclear excitations which contribute most are sufficiently low compared to the pion mass, we can approximate $q_N \approx im_\pi$ and apply closure on the intermediate states. Hence we obtain the sum rule:

$$f_{\text{eff}}^2 = -\frac{f_r^2}{m_\pi^2} \lim_{q \to im_\pi} \langle N| \left[\sum_j \sigma_j \cdot q\tau_j^-, \sum_i \sigma_i \cdot q\tau_i^+ \right] |N\rangle$$

$$= -f_r^2 \langle N| \sum_i \tau_i^3 |N\rangle = f_r^2 (N - Z) . \quad (19)$$

In this form, this expression can easily be seen as the equivalent at $q = im_\pi$ of the Gamow–Teller sum rule [1,33]) which involves the spin–isospin matrix elements at zero momentum transfer: $(g_A^{\text{eff}})^2 = (N - Z)g_A^2$. Actually, this similarity stems from our neglect of the nuclear excitation energy in $q_{N'}$. A priori, this seems amply justified in light nuclei where low multipoles are expected to give the bulk of the contributions. In heavier nuclei however, this approximation can be questioned. So we have estimated the sum in eq. (18) for harmonic oscillator states, keeping the energy dependence. We have found that the difference with eq. (19) is surprisingly small (less than 0.5%), even for nuclei with the highest masses.

Therefore, with a very good accuracy, the effective pole term is simply given by the coherent pole sum. In contradistinction with the case of individual transitions studied in sects. 2 and 3, the π-nucleon coupling constant gives then a scale for the effective nuclear coupling constant, apart from the factor $N - Z$. The universality of this result, which is independent in particular of the nuclear size, is to be attributed to the fact that the source operators and their commutator in (18) are local quantities in the impulse approximation: the nuclear size is washed out by the sum rule. On the contrary, when many-body effects are considered, the effective coupling constant will depend on the particular nucleus, reflecting the non-locality of this commutator. The detection of a deviation from the universal value (19) would then constitute a direct evidence for non-nucleonic degrees of freedom in nuclei.

Here the many-body contributions will be treated in the same spirit as in sect. 3, i.e. within the polarizability picture. In analogy with our previous eq. (13) one

can write integral equations for the matrix elements of the commutator of the pion sources $[j_\pi^+(q), j_\pi^-(q)]$ needed in the estimations of the effective constant [eq. (18)]. The expressions become very cumbersome, essentially because the solutions have to be found in the two variables q and q', which necessitates a huge numerical work that we have not undertaken. We prefer to use here an approximation scheme described in the appendix which leads to a Klein–Gordon equation in x-space obeyed by the nuclear matrix elements $\varphi(x)$ of the static pion field in the nuclear medium:

$$(-\nabla^2 + m_\pi^2)\varphi(x) = -\frac{f_r\sqrt{2}}{m_\pi}\nabla \cdot [(1 + g'\alpha(x))\sigma(x)] + \nabla\alpha(x) \cdot \nabla\varphi(x). \tag{20}$$

This equation has been already obtained and extensively studied in previous works [4,7,17]. In this expression $\sigma(x)$ is the matrix element of the spin–isospin operator in the impulse approximation:

$$\sigma^\pm(x) = \langle N' | \sum_i \sigma_i \tau_i^\pm \delta(x - x_i) | N \rangle \tag{21}$$

(its space integral is simply the Gamow–Teller matrix element). The many-body effects are introduced via the effective axial polarizability $\alpha(x)$ which leads to vertex (Lorentz–Lorenz) and propagator renormalizations [respectively 1st and 2nd terms in the right-hand side of eq. (20)].

As shown in the appendix, this quantity is related to the Δ-hole part α_0 of the static polarizability:

$$\alpha = \frac{\alpha_0}{1 - g'\alpha_0} \quad \text{with} \dagger \ \alpha_0(x) = -\frac{32}{9}\frac{f_r^2}{m_\pi^2\omega_\Delta}\rho(x), \tag{22}$$

ω_Δ and $\rho(x)$ being respectively the Δ excitation energy and the nuclear density. As for the nucleon–hole part of α considered in the previous section, it is not amenable to a local approximation. However, we need not take explicitly its role into account: indeed it represents a core polarization phenomenon and could be described equivalently by a modification of the wave functions. Since a sum rule over all transitions is our present concern, only a ground-state expectation value where the nucleon–hole polarizability is implicitly contained has to be considered. It will even turn out that no detailed description of the ground-state properties is required for the sum rule.

The solution of the inhomogeneous equation (20) is most easily constructed from the Green functions $\phi^\pm(x, x_i)$:

$$\varphi^\pm(x) = \langle N' | \sum_i (1 + g'\alpha(x_i))\varphi^\pm(x, x_i) | N \rangle. \tag{23}$$

---

† This expression is obtained under the assumption that the $\pi N\Delta$ and πNN coupling constants are in the ratio given by the Chew–Low model $f_r^{*2}/f_r^2 = 4$.

where $\varphi^*(x, x_i)$ obeys

$$[-\nabla(1 + \alpha(x)) \cdot \nabla + m_\pi^2]\varphi^*(x, x_i) = -\frac{f_r\sqrt{2}}{m_\pi}\tau_i^{\pm}\sigma_i \cdot \nabla\delta(x - x_i). \qquad (24)$$

This equation describes the propagation of the pionic field $\varphi(x, x_i)$ generated by a single point source located at x_i. A computational form is then derived by developing the Green function into a multipole expansion† (this is strictly valid for the case of a spherical symmetric density):

$$\varphi^*(x, x_i) = \frac{f_r\sqrt{2}}{m_\pi}\sum_{L,J} f_{LJ}(x, x_i)\sum_m Y^*_{Jm}(\hat{x})[Y_L(\hat{x}_i)\otimes\sigma_i]^J_m. \qquad (25)$$

This formula allows the link with the multipole coupling constants $f^J_{\pi NN'}$ defined in sect. 3, once a Fourier transform is made [compare with eqs. (3) and (4)]:

$$f^J_{\pi NN'}(q) = f_r\sqrt{2}\sum_{L=J\pm 1}\sqrt{\frac{2L+1}{2J+1}}\langle N'\|\sum_i \tau_i^{\pm}\left\{(1 + g'\alpha(x_i))\int_0^\infty dx\, x^2 j_J(qx)f_{LJ}(x, x_i)\right\}$$

$$\times\sqrt{4\pi}[Y_L(\hat{x}_i)\otimes\sigma_i]^J\|N\rangle m_\pi(q^2 + m_\pi^2)/q^J. \qquad (26)$$

We are then left with the differential equation in the x-variable:

$$(x(1 + \alpha(x))^{1/2}f_{LJ}(x))'' = \left[\frac{J(J+1)}{x^2} + \frac{1}{1+\alpha(x)}\left(m_\pi^2 + \frac{\alpha'(x)}{x} + \frac{\alpha''(x)}{2} - \frac{\alpha'(x)^2}{4(1+\alpha(x))}\right)\right]$$

$$\times x(1 + \alpha(x))^{1/2}f_{LJ}(x). \qquad (27)$$

So the general solution for f_{LJ} is

$$f_{LJ}(x, x_i) = C_{LJ}(x_i)Y^{ext}_J(x)\theta(x - x_i) + D_{LJ}(x_i)Y^{int}_J(x)\theta(x_i - x), \qquad (28)$$

where we have separated the field into an external and an internal part, since it presents a discontinuity at the location x_i of the source; Y^{int}_J and Y^{ext}_J are two independent solutions of eq. (27), subject to the boundary conditions:

$$Y^{ext}_J(x) \sim e^{-m_\pi x}/x \qquad \text{if } x \to \infty,$$

$$Y^{int}_J(x) \sim x^J \qquad \text{if } x \to 0.$$

Finally, the coefficients C_{LJ} and D_{LJ} are determined by the discontinuity of the source, whose strength is that of a free nucleon. We remark that C_{LJ} fixes the amplitude of the asymptotic pion field.

Let us note here that an analytic solution is known when the polarizability effects are turned off:

$$\varphi(x, x_i) = -\frac{f_r\sqrt{2}}{m_\pi}\sigma_i \cdot \nabla\frac{e^{-m_\pi|x-x_i|}}{|x - x_i|} \qquad (29)$$

† From now on, we omit for simplicity the isospin indices.

and there exists a multipole expansion of the type (25) in terms of spherical Bessel and Hankel functions; in particular the coefficient for the asymptotic field is:

$$C_{LJ}^{(0)}(x_i) = C(L1J; 00)(-i)^L j_L(im_\pi x_i) \,. \tag{30}$$

The summation of this rather complicated series gives the simple Yukawa field (29) because of the spherical symmetry of the vacuum around the nucleon. When the source is embedded in a nucleus ($\alpha \neq 0$), this symmetry no longer exists in general and all multipoles are renormalized differently, according to eq. (27). In particular the pion coupling constants $f^J_{\pi NN'}$ will not present a universal renormalization for all transitions. They are obtained from eq. (26) at the limit $q^2 = -m_\pi^2$

$$f^J_{\pi NN'} = f_r \sqrt{2} \sum_L \sqrt{\frac{2L+1}{2J+1}} \, \langle N' \| \sum_i \tau_i^\pm (1 + g'\alpha(x_i))$$

$$\times C_{LJ}(x_i)\sqrt{4\pi}[\, Y_L(\hat{x}_i) \otimes \sigma_i]^J \| N\rangle / m_\pi^{J-1} \,. \tag{31}$$

However in this section we are interested in the search of general properties displayed by the sum rule over all accessible states, and we expect that the fluctuating behaviour of particular transitions will be averaged out.

According to eqs. (16) and (26), the expression for the sum rule is (assuming again $\omega_{N'}^2 \ll m_\pi^2$):

$$f^2_{\text{eff}} = f_r^2 \lim_{q \to im_\pi} (q^2 + m_\pi^2)^2 \langle N | \sum_i \tau_i^3 (1 + g'\alpha(x_i))^2 \sum_{J,L} (2L+1)$$

$$\times \left\{ \int_0^\infty dx\, x^2 j_J(qx) f_{LJ}(x, x_i) \right\}^2 | N\rangle \,, \tag{32}$$

where use has been made of the commutation relations for the $\sigma\tau$ operators, as in eq. (19). The relation between the residue of the pole and the asymptotic behaviour of the pion field is clearly revealed in this formula because of the exponential increase of the Bessel function with imaginary argument. In fact, only the singular part of the integrals will contribute to the effective pole, which is then determined by the asymptotic fields.

$$f_{LJ}(x, x_i) \xrightarrow[x \to \infty]{} \frac{1}{x} C_{LJ}(x_i) e^{-m_\pi x} \,.$$

The effective coupling constant is then:

$$f^2_{\text{eff}} = -f_r^2 \int dx\, \tau^3(x)(1 + g'\alpha(x))^2 \left\{ \sum_{L,J} (-1)^L (2L+1) C^2_{LJ}(x) \right\} \,, \tag{33}$$

an expression in which we have introduced the isospin density

$$\tau^3(x) \equiv \langle N | \sum_i \tau_i^3 \delta(x - x_i) | N\rangle = \rho_p(x) - \rho_n(x)$$

(Note that J and L must differ by one unit only.) One checks easily, using expression (30) and summing the Bessel functions $\sum_L (2L+1)j_L^2(z) = 1$, that we get back to the sum rule (19) when the polarizability effects are suppressed. Hence the latter will show up as a deviation of the sum $[1 + g'\alpha(x)]^2 \sum_{LJ} (-1)^L (2L+1) C_{LJ}^2(x)$ from unity.

We have calculated the sum (33) for a wide range of nuclei, the dependence on the nucleon number being implicitly introduced through the axial polarizability α_0. The density $\rho(x)$ has been chosen to be of Fermi type, so as to give a sufficiently realistic description of nuclei while particular features are not considered:

$$\rho(x) = \rho_F/(1 + e^{(x-c)/a}),$$

$$\rho_F = 0.16 \ \mathrm{fm}^{-3}, \tag{34}$$

$$a = 0.566 \ \mathrm{fm},$$

and the size parameter c is related to the atomic number A by the normalization condition. For the smallest nuclei, this description becomes less accurate and we have preferred a modified gaussian density: the renormalizations found in these cases are compatible with the general trend obtained from the Fermi profile. Finally, the isospin density $\tau_3(x) = \rho_p(x) - \rho_n(x)$ was given the same radial dependence as $\rho(x)$ in (34), reflecting the great similarity between proton and neutron densities. It can be argued that only valence nucleons should be taken into account in order to eliminate interference with Coulomb isospin-breaking effects, but we have checked that the results of our calculations are only moderately sensitive to the shape of $\tau_3(x)$, as long as its gross features are sufficiently realistic. So we do not need to complicate our scheme, avoiding at the same time a spoiling of the transparency of our calculations.

The renormalization factor f_{eff}^2/f_r^2 computed for a neutron excess of 1 is plotted in fig. 4 (full curve) as a function of $A^{1/3}$ for $g' = 0.6$. The individual points correspond to nuclei with atomic numbers 9, 13 and 17 (with gaussian density). This result exhibits a surprisingly simple behaviour of the renormalizations: it shows that the effective coupling constant (squared) is quenched, the more the heavier the nucleus. The law of variation is $\exp(-kA^{1/3})$ ($k \sim 0.41$, depending relatively little on the exact value of g') to a very high accuracy, which means that huge effects would be observed in heavy nuclei. Even for medium weight nuclei, such as calcium, the quenching already attains a factor of 3. Such an exponential decrease is not unexpected since in a simplified picture [7] one can find that the asymptotic field behaves as $\exp(-m'_\pi R)$ where R is the nuclear radius and $m'_\pi = m_\pi(1 + \alpha)^{-1/2}$ is the effective mass characterizing the pion propagation in the medium.

A part only of this effect can be attributed to the vertex renormalization $(1 + g'\alpha)^2$ (Lorentz–Lorenz effect), which is slowly varying over the whole range of atomic number (see the dotted line in fig. 4). Most of the reduction arises in fact from pion propagation. This feature is at considerable variance with the situation at
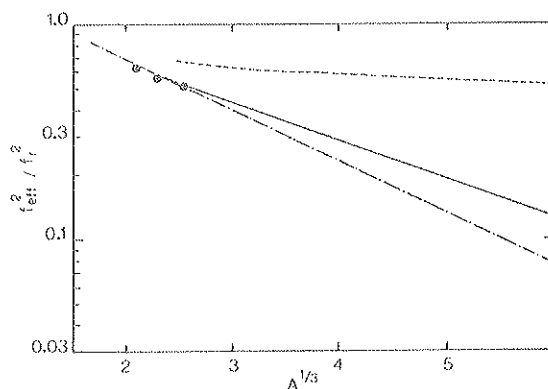
Fig. 4. The renormalization of the effective pion–nucleus coupling constant as a function of the atomic number. Full curve refers to our calculation in the Δ-hole polarization model (the dotted curve presents the Lorentz–Lorenz quenching alone). The dot-dashed curve represents our estimation by dispersion relations.

space-like momentum, where the pion produces an enhancement opposed to the Lorentz–Lorenz effect. Loosely speaking, this can be seen as a manifestation of the change of sign of the one-pion exchange potential which becomes repulsive in the time-like region, acting then constructively with the momentum-independent interaction g'.

The general reduction of the effective coupling constant is to be contrasted with our findings for an individual transition (sect. 3); there is no reason *a priori*, however, to expect a relation between the two results: the alternation of the series for the effective pole precludes any attempt in this direction to succeed. We have checked in the particular case of oxygen that no single multipolarity can be attributed the essential part of the renormalization. As expected, the most important contributions to the sum rule have lower multipolarity for lighter nuclei, but many of them (up to $L = 3$ in oxygen), with different signs, were necessary to saturate the sum. It is remarkable also that a vast majority among them were enhanced rather than quenched by the many-body effects induced by pion propagation. So the physical effect which leads to the quenching of the effective coupling constant cannot be reduced easily to those governing each of its contributions.

The confrontation of our model with experiment can be attempted through the dispersion relation (17) since f_{eff}^2 is the sum of the scattering length $(N - Z)a_-$ and of an integral over the difference $\sigma_\pi - \sigma_{\pi^-} = \Delta\sigma$. It is clear that at least the second quantity will show an A-dependent quenching with respect to the case of free nucleons, due to shadow effects. In fact it is well known that the pion-nucleus total cross sections exhibit a strong dependence on atomic number since they scale with the mass number as $A^{0.62}$ in the energy range covering the 3–3 resonance [34]). This black-sphere behaviour is understood as the consequence of shadowing of the interaction by the surrounding nucleons, due to the large imaginary part of the

pion-nucleon amplitude in the A_{33} region. It is then interesting to check through the dispersion relation that a consequence is the quenching of the effective pole as predicted by our model.

Experimental data cannot be entered directly in the dispersion integral (17) since the Coulomb effects are important in the $\pi^+ - \pi^-$ difference and render the extraction of the purely nuclear cross sections difficult and uncertain. Only light nuclei have been considered up to now [35]), which do not provide the most favourable test for our model since the Lorentz–Lorenz effect constitutes the largest part of the renormalization. The various determinations of the effective coupling constant for ^{7}Li and ^{9}Be have been discussed in a recent review† [19]): a reduction is observed for both nuclei, which seems less important for the first, lighter, one. Its absolute value (0.75–0.87 for ^{7}Li, 0.50–0.75 for ^{9}Be) is also consistent with our general prediction, and with our more exact result 0.63 obtained for ^{9}Be by considering density distributions with a modified gaussian profile. This concordance is encouraging, but we must emphasize that the propagation effects are very small in these nuclei, the Lorentz–Lorenz effect providing already a quenching factor 0.69: a more significant test can only come from heavier nuclei. Analyses of the existing data including Coulomb subtractions are then eagerly awaited. This task does not seem to be insuperable up to $A = 40$.

In the absence of such results, we have made a simulation which should, at least qualitatively, confirm our prediction. This calculation was made with an optical potential similar to that developed by Stricker, McManus and Carr [37]). Our parameters are slightly different since our input for πN phase shifts consists in the analytic best fit [38]) to all modern data. This fit provides a smooth interpolation in energy up to 400 MeV. Our results are practically identical to those presented in ref. [37]), and are in a fair agreement with published total cross-sections for nuclei ranging from ^{12}C to ^{208}Pb, and energies up to 400 MeV. We feel then reasonably confident that the same model should not be too unrealistic to predict the $\pi^+ - \pi^-$ differences.

The $\pi^\pm$ total cross sections in the absence of a Coulomb potential were then calculated for a whole series of fictitious nuclei with unit neutron excess, the energy varying between threshold and 450 MeV, and this difference was integrated over this range‡ as in eq. (17). Indeed, we have assumed that the integrand for $\Delta\sigma$ is dominated by the 3–3 resonance region as was found experimentally in the lightest nuclei [35]). Remarkably enough, we obtain for the dispersion integral essentially an exponential behaviour very similar to that found for the effective pole, the exponent being now $-0.494A^{1/3}$. This contrasts strongly with the more direct effect of

---

† The case of ^{3}He has also been considered [36]), and the coupling constant has been found to be strongly enhanced (50%) though with very large uncertainties. Such a light nucleus is quite out of the scope of our model.

‡ The integral over the unphysical pion absorption cut contributes little [18]): its contribution to the coupling constant should not exceed 10%.

shadowing. For each charge state of the pion, the cross sections behave as a power of the atomic number: $\sigma_{\pi^+} + \sigma_{\pi^-} \sim A^{0.63}$ practically equal to the experimental variation and to the expectation for scattering on a black sphere. The exponential behaviour can then be reasonably viewed as reflecting the attenuation of the pion wave inside the medium. Let us remark here that this quenching is in agreement with the experimental data on ^{7}Li and ^{9}Be [ref. [35]] (however a distinction between power and exponential variations is clearly impossible in these cases).

The second ingredient needed in the dispersion relation, i.e. the isospin antisymmetric scattering length, can also be computed with the optical potential. We recall that here also a reduction is expected, which is interpreted as due to the distortion of the pion wave function by the repulsive s-wave nuclear potential. We find that this prediction is fulfilled, the dependence with A being again exponential: $a_- \sim \exp(-0.588 A^{1/3})$. As with the integrals, this behaviour is at variance with the individual variations of $a(\pi^+)$ and $a(\pi^-)$, which grow as $A^{0.66}$ (implying a scaling law $A^{-1/3}$ when normalized to 1 nucleon). We have checked these results with an optical potential more appropriate to such a calculation, i.e. fitted entirely on π-mesic atom data [39]), and found no qualitative difference. Combining then the numbers found for the dispersion integrals and the scattering lengths which turn out to make about equally important contributions, we obtain for the renormalization of the effective pole f_{eff}^2/f_r^2 the dot–dashed curve of fig. 4. One finds a perfectly straight line in the logarithmic plot with a slope equal to -0.535, to be compared with -0.41 previously obtained with the polarization model (full curve).

The agreement is good at the qualitative level, since the variation laws are very similar; at the quantitative level, the difference between the two curves attains at most 35%, for the heaviest nuclei. Furthermore, even this rather small deviation cannot be considered significant, since we have not paid much attention to the consistency between the p-wave parameters of the optical potential at physical energies and their extrapolation at zero energy which enters the polarizability α_0: actually increasing this polarizability by 27% as found in the extrapolation model of Adler [40]), one finds a nearly perfect agreement between the two curves. A further source of uncertainty lies in the fact already mentioned that we have integrated the cross-sections only from the threshold to the tail of the 3–3 resonance, neglecting both the high energy region and the absorption below threshold. The validity of this assumption remains to be explored. Work is in progress in this direction.

So the very strong quenching of the effective coupling appears to be associated through the dispersion relation with shadow effects, on the one hand, and with the reduction of the antisymmetric scattering length due to s-wave distortion effects, on the other hand. These two different many-body phenomena combine coherently, and with approximately the same strengths, to produce a suppression of the effective coupling constant in agreement with the conclusion of the polarization model. We

find thus a gratifying consistency between the descriptions used for the interactions of real and virtual pions with nuclei.

To conclude, we have shown in this paper that the pion-nucleus coupling constants present, besides the Lorentz–Lorenz quenching, renormalization effects generated by pion-induced polarization of the nuclear medium. A spectacular suppression should be observed especially in heavy nuclei for the effective pion-nucleus constant, the largest part of which arises from Δ-hole modifications of the pion propagator. An experimental confirmation would be taken as new evidence for pionic degrees of freedom in nuclei. Already our optical model calculations strongly support the existence of this effect.

Our work has natural implications for the problem of the renormalization of the Gamow–Teller strength. As we already mentioned, the sum rule (19) obtained for f_{eff}^2 in the one-body approximation is the translation at $q^2 = -m_\pi^2$ of the Gamow–Teller sum rule for g_A^2. The same equivalence persists for the exact sum rules, which include the many-body effects. Indeed, extrapolation of the dispersion relation (15), (17) from real to soft pions (i.e. $q^2 = 0$) leads to the Adler–Weisberger relation in nuclei [42]. As compared to the situation that we have just studied, it can be expected that the shadowing of the cross sections persists for soft pions in the 3–3 resonance region. On the other hand, the scattering lengths no longer suffer a reduction since s-wave distortion disappears for zero mass pions. As a consequence, the AW relation predicts that in large nuclei the quenching of g_A^2 tends to a limit $(g_A^{\text{eff}})^2/g_A^2 \approx 0.60$, in contrast with the effective pole which follows an exponential decrease. This feature is borne out by the polarization model, which predicts that $[g_A^{\text{eff}}]^2$ is essentially reduced by the Lorentz–Lorenz quenching (≈ 0.50). However the exact connection between the shadow and the short-range repulsion at the origin of the Lorentz–Lorenz effect is yet to be established.

Appendix

We give here a sketch of the successive approximations which lead from the integral equations (13) for the spin multipoles to the Klein–Gordon equation (20) in x-space obeyed by the pion field matrix elements. We first drop for simplicity the coupling terms between transverse and longitudinal degrees of freedom which become anyway negligible in large nuclei (without this approximation, one would obtain coupled equations describing the propagation of π- and ρ-mesons). We remark that if one separates the longitudinal interaction V_ℓ (eq. 12) into its contact

(g') and pion exchange components, (13) can be replaced by

$$\Sigma_\ell^J(q) = \sigma_\ell^J(q) + g' \frac{f_r^2}{m_\pi^2} (2\pi)^{-3} \int dq' q'^2 \tilde{\alpha}_{\ell\ell}^J(q, q') v^2(q') \sigma_\ell^J(q')$$

$$- \frac{f_r^2}{m_\pi^2} (2\pi)^{-3} \int dq' q'^2 \tilde{\alpha}_{\ell\ell}^J(q, q') \frac{q'^2}{q'^2 + m_\pi^2} v^2(q') \Sigma_\ell^J(q') \qquad \text{(A.1)}$$

with the effective polarizabilities $\tilde{\alpha}_{\ell\ell}^J(q, q')$ defined by

$$\tilde{\alpha}_{\ell\ell}^J(q, q') = \alpha_{\ell\ell}^J(q, q') + g' \frac{f_r^2}{m_\pi^2} (2\pi)^{-3} \int dq'' q''^2 \alpha_{\ell\ell}^J(q, q'') v^2(q'') \tilde{\alpha}_{\ell\ell}^J(q'', q') .$$

$$\text{(A.2)}$$

Introducing pion field multipoles according to the definition

$$\phi^J(q) = \frac{f_r \sqrt{2}}{m_\pi} v(q) \frac{q \Sigma_\ell^J(q)}{q^2 + m_\pi^2} , \qquad \text{(A.3)}$$

one finds the equation

$$(q^2 + m_\pi^2) \phi^J(q) = \frac{f_r \sqrt{2}}{m_\pi} q v(q) \left\{ \sigma_\ell^J(q) \right.$$

$$\left. + g' \frac{f_r^2}{m_\pi^2} (2\pi)^{-3} \int dq' q'^2 \tilde{\alpha}_{\ell\ell}^J(q, q') v^2(q') \sigma_\ell^J(q') \right\}$$

$$- \frac{f_r^2}{m_\pi^2} v(q) q (2\pi)^{-3} \int dq' q'^2 \tilde{\alpha}_{\ell\ell}^J(q, q') v(q') q' \phi^J(q') . \qquad \text{(A.4)}$$

If one now drops the form factors $v(q)$, which should be rather innocuous when the involved momenta are small compared to $\Lambda \approx 1.2$ GeV, one gets a simple equation in x-space:

$$(-\nabla^2 + m_\pi^2) \phi(x) = -\frac{f_r \sqrt{2}}{2m_\pi} \nabla \cdot \left\{ \sigma(x) + g' \frac{f_r^2}{m_\pi^2} \int dx' \tilde{\alpha}_{\ell\ell}(x, x') \sigma(x') \right\}$$

$$+ \frac{f_r^2}{m_\pi^2} \nabla \cdot \int dx' \tilde{\alpha}_{\ell\ell}(x, x') \nabla \phi(x') . \qquad \text{(A.5)}$$

The last step leading to eq. (20) is accomplished if one assumes that the polarizability is local in x-space:

$$\frac{f_r^2}{m_\pi^2} \alpha_{\ell\ell}(x, x') = \alpha_0 \delta(x - x') , \qquad \frac{f_r^2}{m_\pi^2} \tilde{\alpha}_{\ell\ell}(x, x') = \frac{\alpha_0}{1 - g' \alpha_0} \delta(x - x') . \qquad \text{(A.6)}$$

One can show easily that such an approximation is legitimate for the Δ-hole part of the static polarizability. Indeed the latter is defined as:

$$\frac{f_r^2}{m_\pi^2} \alpha_{\ell\ell}(x, x') = -\frac{4f_r^2}{m_\pi^2} \sum_{\Delta h} \left\{ \frac{\langle 0|\Sigma_z T^\alpha \delta(x'-r)|\Delta h\rangle\langle \Delta h|\Sigma_z T^\alpha \delta(x-r)|0\rangle}{\varepsilon_{\Delta h} - \omega} \right.$$
$$\left. + c.t. (\omega \to -\omega) \right\}_{\omega=0} , \qquad (A.7)$$

where r is the integration coordinate and Σ, T spin and isospin operators making the transition between $\frac{1}{2}$ and $\frac{3}{2}$ states. Assuming an average Δ-hole energy $\varepsilon_{\Delta h} \approx \omega_\Delta$, one can perform closure on the Δ-states, the remaining sum on the hole states simply giving the nuclear density:

$$\frac{f_r^2}{m_\pi^2} \alpha_{\ell\ell}(x, x') = -\frac{32}{9} \frac{f_r^2}{m_\pi^2 \omega_\Delta} \rho(x)\delta(x-x') . \qquad (A.8)$$

References

1) C. Gaarde, J. Rapaport, T.N. Taddeucci, C.D. Goodman, C.C. Foster, D.E. Bainum, C.A. Goulding, M.B. Greenfield, D.J. Horen and E. Sugarbaker, Nucl. Phys. A369 (1981) 258
2) K. Ikeda, S. Fujii and J.I. Fujita, Phys. Lett. 3 (1963) 271
3) J. Speth, Lecture notes in physics, vol. 108, ed. H. Arenhövel and D. Drechsel (Springer, 1979) p. 266
4) M. Ericson, A. Figureau and C. Thévenet, Phys. Lett. 45B (1973) 19
5) M. Rho, Nucl. Phys. A231 (1974) 493
6) K. Ohta and M. Wakamatsu, Nucl. Phys. A234 (1974) 445
7) J. Delorme, M. Ericson, A. Figureau and C. Thévenet, Ann. of Phys. 102 (1976) 273
8) E. Oset and M. Rho, Phys. Rev. Lett. 42 (1979) 47
9) I.S. Towner and F.C. Khanna, Phys. Rev. Lett. 42 (1979) 51
10) W. Knüpfer, M. Dillig and A. Richter, Phys. Lett. 95B (1980) 349
11) N.C. Mukhopadhyay, H. Toki and W. Weise, Phys. Lett. 84B (1979) 35
12) A. Bohr and B. Mottelson, Phys. Lett. 100B (1981) 10
13) G.E. Brown and M. Rho, Nucl. Phys. A372 (1981) 397
14) T. Suzuki, S. Krewald and J. Speth, Phys. Lett. 107B (1981) 9
15) J. Meyer-Ter-Vehn, Phys. Reports 74 (1981) 323
16) J. Speth, V. Klemt, J. Wambach and G.E. Brown, Nucl. Phys. A343 (1980) 382
17) J. Delorme and A. Figureau, 4ème Session d'Etudes Biennale de Physique Nucléaire, 1977, tome 1, p. C. 7-1 (unpublished report)
18) T.E.O. Ericson and M.P. Locher, Nucl. Phys. A148 (1970)1
19) M.P. Locher and T. Mizutani, Phys. Reports 46 (1978) 43
20) O. Dumbrajs, Ann. of Phys. 118 (1979) 249;
    O. Dumbrajs, Phys. Rev. C22 (1980) 2151
21) M. Ericson and M. Krell, Nucl. Phys. A241 (1975) 487
22) C.W. Kim and H. Primakoff, in Mesons in nuclei, ed. M. Rho and D.H. Wilkinson, vol. I (North-Holland, Amsterdam, 1979) 67
23) J. Delorme, in Mesons in nuclei, ed. M. Rho and D.H. Wilkinson, vol. I (North-Holland, Amsterdam, 1979) 107
24) M. Moreno, J. Pestieau and J. Urias, Phys. Rev. C12 (1975) 514
25) H. Primakoff, Nucl. Phys. A317 (1979) 279

532   *J. Delorme et al. / Pion coupling constants*

26) G.L. Moake, L.J. Gutay, R.P. Scharenberg, P.T. Debevec and P.A. Quin, Phys. Rev. C21 (1980) 2211;
   J. Rapaport, T. Taddeucci, C. Gaarde, C.D. Goodman, C.C. Foster, C.A. Goulding, D. Horen, E. Sugarbaker, T.G. Masterson and D. Lind, Phys. Rev. C24 (1981) 335
27) Ph. Quentin, private communication
28) P. Desgrolard and P. Guichon, Phys. Rev. C19 (1979) 120;
   P. Guichon and C. Samour, Nucl. Phys. A382 (1982) 461
29) J. Delorme, M. Ericson, A. Figureau and N. Giraud, Phys. Lett. 89B (1980) 327
30) J.L. Escudié, S.M. Austin, A. Boudard, G. Bruge, A. Chaumeaux, L. Farvacque, D. Legrand, J.C. Lugol, B. Mayer, P. Belery, P.T. Debevec, T. Delbar, J. Deutsch, G. Grégoire, R. Prieels, J.M. Cameron, C. Glashausser and C.A. Whitten, Phys. Rev. C24 (1981) 792;
   M. Haji-Saeid, C. Glashausser, G. Igo, W. Cornelius, M. Gazzaly, F. Irom, J. McClelland, J.M. Moss, G. Pauletta, H.A. Thiessen and C.A. Whitten Jr., Phys. Rev. Lett. 45 (1980) 880
31) J.B. Flanz, R.S. Hicks, R.A. Lindgren, G.A. Peterson, J. Dubach and W.C. Haxton, Phys. Rev. Lett. 43 (1979) 1922;
   J.C. Bergstrom, Phys. Rev. C21 (1980) 2496
32) W.G. Love and M.A. Francy, Phys. Rev. C24 (1981) 1073
33) J. Delorme, M. Ericson and P. Guichon, to be published
34) D. Ashery, I. Navon, G. Azuelos, H. Walter, H. Pfeiffer and F. Schlepütz, Phys. Rev. C23 (1981) 2173
35) C. Wilkin, C.R. Cox, J.J. Domingo, K. Gabathuler, E. Pedroni, J. Rohlin, P. Schwaller and N.W. Tanner, Nucl. Phys. B62 (1973) 61;
   G.T.A. Squier, M.E. Cage, G.J. Pyle, A.S. Clough, G.K. Turner, B.W. Allardyce, C.J. Batty, D.J. Baugh, W.J. McDonald, R.A.J. Riddle and L.H. Watson, Phys. Rev. Lett. 31 (1973) 389
36) F. Nichitiu, and M.G. Sapozhnikov, J. of Phys. G4 (1978) 805
37) K. Stricker, H. McManus and J.A. Carr, Phys. Rev. C19 (1979) 929
38) G. Rowe, M. Salomon and R.H. Landau, Phys. Rev. C18 (1978) 584
39) M. Krell and T.E.O. Ericson, Nucl. Phys. B11 (1969) 521
40) S.L. Adler, Ann. of Phys. 50 (1968) 189
41) C. Bastard, private communication
42) M. Ericson, Ann. of Phys. 63 (1971) 562

TABLE DES MATIERES

THÈSE de L'UNIVERSITÉ DE LYON I (SCIENCES)

NOM : GIRAUD

(avec précision du nom de jeune fille, le cas échéant)

Prénoms : Noël Alain

DATE de SOUTENANCE

24 février 1983

TITRE : PIONS RÉELS ET VIRTUELS DANS LES NOYAUX

NATURE :

Numéro d'ordre :

DOCT. d'UNIV.	DOCTEUR-INGENIEUR	DOCTORAT D'ETAT	DOCTORAT de 3e CYCLE
☐	☐	☒	☐

Spécialité :

Cote B.I.U. - Lyon : T 50/210/19 / et bis   CLASSE :

RÉSUMÉ :

La première partie de la thèse porte sur l'interaction des pions physiques avec le deuton étudiée dans le cadre d'une théorie à trois corps. Nous avons déduit la section efficace élastique dans le domaine d'énergie au voisinage de la résonance (3-3), en tenant compte de l'absorption virtuelle du pion.

La deuxième partie concerne les pions virtuels dans les noyaux. En particulier nous avons étudié le nuage de pions virtuels autour du noyau et déduit la constante de couplage effective pion noyau. Celle-ci est fortement réduite par les effets de polarisation du milieu nucléaire (essentiellement par excitation virtuelle de l'isobare Δ) par rapport à sa valeur pour une collection de nucléons libres. Nous avons également étudié dans le cadre du même modèle de polarisation le champ pionique à l'intérieur du noyau. A petit transfert de moment ce champ est diminué. A grand moment il est augmenté. Ce dernier phénomène correspond aux effets d'opalescence critique liés à la transition de phase de la condensation du pion. Nous avons effectué une étude détaillée de ce phénomène pour les facteurs de forme magnétiques dans les isotopes du carbone.

MOTS-CLES : problème à 3 corps. diffusion pion-deuton. champ de pion nucléaire. constante de couplage pion-noyaux. transitions Gamow-Teller

Laboratoire (s) de recherches :

Physique théorique. Institut de Physique Nucléaire

Directeur de recherches : M.Jean DELORME, Maître de Recherche au CNRS.

Président de jury : Mme M.ERICSON

Composition du jury : MM.J.DELORME, C.FAYARD, G.H.LAMOT, P.QUENTIN

CET IMPRIME DOIT FIGURER EN DERNIERE PAGE DE CHAQUE THESE (ne pas compléter la Cote B.I.U. et CLASSE)